This is to certify that the
dissertation entitled

NOREPINEPHRINE TRANSPORTER IN THE AUTONOMIC INNERVATION OF THE HEART AND ITS ROLE IN HYPERTENSION

presented by

Erica Ariece-Dorothy Wehrwein

has been accepted towards fulfillment
of the requirements for the

Ph.D. degree in Physiology

David J. Kreulen
Major Professor's Signature

4/21/08
Date

NOREPINEPHRINE TRANSPORTER IN THE AUTONOMIC INNERVATION OF THE HEART AND ITS ROLE IN HYPERTENSION

By

Erica Ariece-Dorothy Wehrwein

A DISSERTATION

Submitted to
Michigan State University
in partial fulfillment of the requirements
for the degree of

DOCTOR OF PHILOSOPHY

Department of Physiology

2008

ABSTRACT

ELUCIDATING A ROLE FOR CARDIAC NOREPINEPHRINE TRANSPORTER IN HYPERTENSION

By

Erica Ariece-Dorothy Wehrwein

Norepinephrine (NE) is cleared from the neuroeffector junction by NE transporter (NET). NET function is reduced in the hypertensive heart; however, there is limited information about the cause of the decrease in function. **The goal of this thesis was to evaluate NET in the heart of normal animals (Aims 1 & 2) and to assess the basis for reduced reuptake function with hypertension (Aim 3).**

Aim 1: Characterization and cellular localization of NET mRNA and protein expression in stellate ganglia and heart from normal animals. A) This study revealed for the first time the presence of NET mRNA in heart homogenate with the atria expressing more than the ventricles. Sympathetic denervation with did not deplete NET mRNA content in the heart so the source of this mRNA is not sympathetic nerve terminals. Since NET mRNA was not in nerve terminals, there are alternative cellular sources of NET mRNA, and thus NET protein, aside from sympathetic neurons. B) Substantial NET protein was observed in the sympathetically denervated heart supporting the notion that there are alternative sources of NET protein in the heart. NET immunoreactivity was present in

cardiac-associated sensory ganglia and parasympathetic intrinsic cardiac ganglia.

Aim 2: Correlation of NET protein to chamber NE content. It was expected that NET protein would positively correlate to tissue NE content since NET is present in NE-containing sympathetic nerves where it functions to clear released NE from the neuroeffector junction. However, NET protein was inversely correlated to chamber NE content. There was a high level of NET protein in the ventricles where NE is low, and a low amount of NET protein in the atria where NE is the highest.

Aim 3: Changes in NET mRNA and protein in hypertension. NET mRNA in the right and left stellate ganglia were unchanged in hypertension; however, the left stellate ganglia displays an increase NET protein suggesting a post-transcriptional mechanism of NET protein upregulation. In the heart of hypertensive rats, NET protein was increased in the right atria while left atrial NET was reduced. There is no change in the ventricle.

In conclusion, there are regional differences in NET mRNA and protein between the right and left stellate ganglia as well as between heart chambers. Chamber-specific differences in NET protein and function must be considered in normal heart function as well as the pathology of the NE reuptake system in hypertension and other cardiovascular disorders.

DEDICATION

To my Grandmother, role model, and friend,
Dorothy Madeline Wehrwein
September 29, 1917-April 25, 2008

ACKNOWLEDGEMENTS

There are rarely any accomplishments that occur without the guidance and assistance of others. This is no exception. Many people have influenced me along my path the earning a Ph.D. in physiology. I will always be grateful to those who have been a part of my maturation as a person and scientist.

I would like to thank my research advisor Dr. David L Kreulen. For many reasons, it has been a great pleasure to work with such a wonderful person. He is an example of a well balanced person who finds time to take pleasure in all aspects of life, both personal and professional. I admire his honesty and humor. He has been a role model in many ways. I have learned lab management skills, honed my decisiveness, strengthened my independence as a scientist, and learned many life lessons about working in academia. His friendship and mentorship has been there when needed, even on personal matters, and are greatly appreciated. His hospitality, kindness, sense of humor, balanced life, and thoughtfulness will always be with me. It was especially helpful to have his encouragement to apply for grants and awards and meet deadlines that I thought impossible. Furthermore, he has been supportive to my desires to teach and gain experience with committee work even when it took me away from the lab. He has been very generous in support of me for awards, meetings, and travel.

My mother was exceptionally important in taking every effort to ensure that my life has been full of love and opportunity. She made exceptional efforts to provide me a strong foundation, loving home, learning opportunities, intellectual development, many opportunities that others did not have such as visiting museums, home schooling at an early age, teaching me about many areas of life and science, and has provided wonderful support, love and pride. She is a natural teacher who has been a strong influence in my life and career development with both encouragement to achieve by providing me a solid foundation in curiosity and learning. It is touching to see her share stories of my successes with friends, family, and strangers, and to keep up with my accomplishments so faithfully. Thank you, Mom.

My family, including my Grandmother, Uncles, Aunts, and Cousins, has always been extremely supportive in all aspects of my life and during my continuing education process. My Grandmother was crucial in supporting me both emotionally and financially though many years of schooling. Within my family, there is a strong interest and curiosity with the wonders of the natural world. I recall learning much about the world and science from interactions with my family. As I understand it, this largely had to do with teachings from my Grandfather to my family that con tinues today. Due to these strong family influences, many of us have been very successful and I want to congratulate my cousins Renae Maggetti and Dr. Dan Wehrwein from also completing their graduate studies. Having such a wonderful family is something that I am very

proud of and it was a very moving emotional experience to look up and see my family cheering for me at graduation. I love you all!

Much credit is given to the influence of Mr. Bud Ellis who has been a teacher, mentor, role model, partner, and friend. Mr. Ellis was my high school biology teacher and so much more. I still remember things that I learned from him in high school. It was under his tutelage that I was first exposed to scientific research and methods. I would not be where I am today without his influence on my life. I learned basic research skills, learned how to write a scientific paper, analyze data, give successful presentations, and keep good laboratory records. These skills are the foundation of my success in the sciences. In addition, he has been a role model and has taught me many life lessons through conversations on many different topics. Each time we talk I feel that I learn something. His ability and passion for teaching and mentoring have been well recognized but it is still vital to mention just how difference one person can make. We continue to work together in teaching a summer science program. I hope to have his positive influence in my life in years to come. I have learned so very much from him and no doubt will continue to do so in the future.

Friendships are a wonderful and necessary part of a full life and I have been blessed to have many close friendships with some of the best people that you would ever wish to meet. I especially recognize my friend throughout my graduate work at MSU, Ted Towse. From the first day of orientation at MSU,

Ted has been a consistent friend, study partner, role model, scientific colleague, partner, companion, and friendly competitor. My life would not be the same without him as a part of it in the past several years and my life has been forever changed by my interactions with him. Other partners in school at MSU include Jesse Hollanbaugh, Jill Slade, and Jennifer Bomberger, These people have been though many late nights of studying with me, helped my prepare for talks and presentations, listened to many frustrations on research, discussed data, rejoiced with my successes and helped me though many hard and challenging times. Their friendships and support will always be treasured. Special thanks also to Julie Ruterbusch, Barb Czapski, Berta Remimbas-Cohen, and Ken Cohen. Although, they were not at MSU with me they were close to my heart and also provided much support over the years.

I could never distinguish my lab mates from my friends as they are the same people. I have been so fortunately to have a great team of friends to be my co-workers over the years. My desk-mate Xian Cao has been my dear friend, my stress relief, my scientific colleague, and the other half of my brain on many occasions. We have shared many laughs, tears, celebrations, frustrations, wonderful data discussions, experimental planning, and late nights through the years (What would I do without you?). Also, I have relied heavily on our lab technicians Anna Wright and Lindsay Parker. Not only did they provide my solid experimental support on all levels from animals to data analysis, but have gone above and beyond to help me personally more times than I can explain. Both

have taken time to help me directly even with many other obligations in the lab. Anna has continued to be a thoughtful friend even after leaving the lab. Lindsay has been great fun and provided a lab "soundtrack" for the ups and downs of experiments (Hallelujah!). It has been a great pleasure to work with Mohammad Esfahanian as my reliable and organized right-hand man thorough the most challenging set of experiments and data that I could imagine. It was fun to share good music and friendship during our confusion. There is much camaraderie among other lab members as well: Xiaohong Wang, Carmen Affonso, Ian Behr, Arun Nagaraju, Josh Mastenbrook, and Amy Albin. Josh also spent many hours helping with tissue processing and Amy has been brilliant with confocal imaging of heart. Thanks everyone!

My dissertation committee members were Dr. Stephen DiCarlo, Dr. William Spielman, Dr. Ronald Meyer, and Dr. Gregory Fink. While I am appreciative to all members for their assistance, I particularly recognize Drs. DiCarlo and Fink who have made efforts far above and beyond the call of duty. Dr. DiCarlo has influence my career in many ways including spending significant time to help with advice on grant writing, educational research, mentorship style, and career. He is responsible for nominating me for APS committees which has been an extremely important step in my career development that I have really enjoyed and will continue to participate in. In addition has helped me learn how to review papers and been a mentor for many years. Dr. Fink has been a second research advisor and mentor. He has taken time to meet with me many times and have

many data discussions over email. He is very knowledgeable in this research area and has helped me think though confusing data with a new perspective. I really admire him for his successes and his lab management style, and I feel fortunate to have his input and support. Every time we talk I realize that I should be talking to him more often because I learn so much each time.

It has been my great pleasure and privilege to have the opportunity to meet and work with many collaborators. It is a wonderful experience to interact with scientists with similar interests and to solve problems together. I have had collaborators on this project who have been co-authors on papers and will continue to be friends and colleagues. I would like to recognize Drs. John Osborn, Misa Yoshimoto, Beth Habecker, Don Hoover, Ming Huang, Greg Swain, Martin Novonty, Veronika Mocko, Dasa Babankova, and John Spitsbergen.

The MSU histology lab crew (Amy, Kathy, and Rick) has been a competent, efficient, and fun part of my doctoral research. The office staff has been very helpful. Thanks Michelle, Kelli, Kim, Barb, Diane, Linda, and Richard.

There are a couple of other people who although not directly associated with my research project have had great influence. Dr. JR Haywood has reached out and helped me many times and has been a selfless mentor. Through his influence I was introduced to Drs. Mike Joyner and NIsha Charkoudian who will be my post-

doctoral mentors at Mayo Clinic. He has met with me during difficult times of deciding on my future plans and has offered me the opportunity to learn to review manuscripts. By witnessing his interactions with others and he has been an inspiration and role model. Dr. Stephanie Watts was my lab rotation advisor and introduced me to a new manner of lab managing that I have learned much from that I can incorporate into my own style of managing in the future. She has continued to be a supporter and positive influence on my career. She has reached out with advice many times and graciously stepped in to help me with maintaining animal protocols during the past several years.

TABLE OF CONTENTS

LIST OF TABLES

LIST OF FIGURES

CHAPTER 5

CHAPTER 6

KEY TO SYMBOLS AND ABBREVIATIONS

[^{3}H]	tritiated
6-OHDA	6-hydroxydopamine
BLAST	basic local alignment and search tool
Bmax	binding maximum for nisoxetine
CBB	Coomassie brilliant blue
cDNA	complementary DNA
CE-EC	capillary electrophoresis with electrochemical detection
CG	celiac ganglia
CGRP	calcitonin gene related peptide
ChAT	choline acetyl transferase
Cl	chloride
Ct	cycle threshold
Ctrl	control
DEPC	diethylpyrocarbonate
DHPG	dihydroxyphenoglycol
DMSO	dimethylsulfoxide
DNA	deoxyribonucleic acid
DOCA	deoxycorticosterone acetate
DRG	dorsal root ganglia
EDTA	ethylenediaminetetraacetic acid
GAPDH	glyceraldehyde phosphate dehydrogenase

HEPES	4-(2-hydroxyethyl) piperazine-1 ethanesulfonic acid
HRP	horseradish peroxidase
HT	hypertensive
i.p.	intraperitoneal
ICA	intrinsic cardiac adrenergic cells
IgG	immunoglobin G
IP	immunoprecipitation
IR	immunoreactivity
Kd	kilo Dalton
KO	knockout mouse
LA	left atrium
LST	left stellate ganglion
LV	left ventricle
MA	mesenteric artery
mRNA	messenger ribonucleic acid
MV	mesenteric vein
Na	sodium
NaCl	sodium chloride
NCBI	national center for biotechnology information
NE	norepinephrine
NET	norepinephrine transporter
NGF	nerve growth factor
no RT	no reverse transcriptase control

NT	normotensive
NTC	no template control
PAGE	polyacrylamide gel electrophoresis
PBS	phosphate-buffered saline
PCR	polymerase chain reaction
PMSF	phenol methane sulfanyl fluoride
PVDF	polyvinylidene Fluoride
qPCR	quantitative real time polymerase chain reaction
RA	right atrium
REST	relative expression software tool
RNA	ribonucleic acid
RST	right stellate ganglion
RT-PCR	reverse transcription polymerase chain reaction
RV	right ventricle
SDS	sodium dodecyl sulfate
SGX	stellate ganglionectomy
SPE	solid phase extraction
TAE buffer	tris-glacial acetic acid-EDTA buffer
TEMED	tetramethylethylenediamine
TH	tyrosine hydroxylase
VMAT2	vesiscular monoamine transporter 2
VS	ventricular septal wall
WT	wild type mouse

CHAPTER 1: INTRODUCTION

Approximately 65 million American adults are classified as hypertensive and the prevalence is increasing. Hypertension is a known risk factor for heart disease, myocardial infarction, and stroke. It is often a multifactorial disease that results from the interaction of many factors including obesity, genetics, diet, environmental factors, physical inactivity, stress, and **elevated activity of the sympathetic nervous system**.

The primary neurotransmitter of the sympathetic nervous system is norepinephrine (NE). Normally, released NE is rapidly removed from the cardiac neuroeffector junction by the neuronal NE transporter (NET) located in sympathetic nerve endings. If clearance by NET is reduced, NE remains in the cardiac neuroeffector junction leading to enhanced adrenergic receptor activation associated with **elevated heart rate and cardiac output**. Eventually the excess NE enters into the plasma via venous effluent as NE "spillover". Elevated levels of plasma NE spillover can arise from a combination of increased release from nerve terminals by increased nerve firing and reduced clearance of NE from the neuroeffector junction (1; 9). In many forms of hypertension, there is an elevation of plasma NE (3) indicating that there is a role of the sympathetic nervous system in the disease.

Cardiac sympathetic nerve activity is increased in hypertension (2; 7) and, in order to prevent excess junctional NE and a corresponding elevation of plasma NE, an increase in the function of cardiac NE reuptake mechanisms must also occur. A reduction in expression or function of NET below what is needed to

compensate for released NE results in an elevation of plasma NE levels, such as is seen in hypertension, due to a reduced ability to clear NE from the junction.

The NE reuptake capacity of the heart is functionally diminished in hypertension. Isolated hearts and heart slices from deoxycorticosterone-acetate salt (DOCA-salt) and spontaneously hypertensive animals have reduced NE uptake (4; 6; 8). Impaired NE uptake has also been demonstrated in DOCA-salt animals *in vivo* (5). The *molecular and biochemical* basis for the observed *functional* decrease is not known. This reduction in function is presumably occurring at local reuptake sites in the cardiac sympathetic nerve terminal varicosities within the heart; however, it is important to analyze both the nerve terminals and the cell bodies of the sympathetic neurons that innervate the heart, stellate ganglion neurons, to determine where the loss of function is regulated.

The overall goal of this project is to evaluate a possible role of cardiac NET downregulation in hypertension by analyzing stellate ganglion neurons and myocardial sympathetic nerve terminals from normotensive and hypertensive animals. Since there is little known about the molecular and biochemical nature of NET mRNA and protein *in vivo* or about the distribution of NET in native cardiac tissue, it is first important to fully analyze NET in stellate ganglion neurons and cardiac sympathetic nerve terminals.

Reference List

1. **de Champlain J, Krakoff LR and Axelrod J**. A reduction in the accumulation of H3-norepinephrine in experimental hypertension. *Life Sci* 5: 2283-2291, 1966.

2. **Ferrier C, Cox H and Esler MD**. Elevated total body noradrenaline spillover in normotensive members of hypertensive families. *Clin Sci (Colch)* 84: 225-230, 1993.

3. **Goldstein DS**. Plasma catecholamines and essential hypertension. An analytical review. *Hypertension* 5: 86-99, 1983.

4. **Gudeska S, Glavas E, Stojanova D, Petrov S, Trajkov T and Nikodijevic B**. Alteration in the uptake and storage of cardiac noradrenaline in spontaneously hypertensive rats. *Biomedicine* 25: 157-159, 1976.

5. **Kazda S, Pohlova I, Bibr B and Kockova J**. Norepinephrine content of tissues in Doca-hypertensive rats. *Am J Physiol* 216: 1472-1475, 1969.

6. **Krakoff LR, Ben Ishay D and Mekler J**. Reduced sympathetic neuronal uptake (uptake1) in a genetic model of desoxycorticosterone-NaCl hypertension. *Proc Soc Exp Biol Med* 178: 240-245, 1985.

7. **Oparil S, Zaman MA and Calhoun DA**. Pathogenesis of hypertension. *Ann Intern Med* 139: 761-776, 2003.

8. **Rascher W, Schomig A, Dietz R, Weber J and Gross F**. Plasma catecholamines, noradrenaline metabolism and vascular response in desoxycorticosterone acetate hypertension of rats. *Eur J Pharmacol* 75: 255-263, 1981.

9. **Schlaich MP, Lambert E, Kaye DM, Krozowski Z, Campbell DJ, Lambert G, Hastings J, Aggarwal A and Esler MD**. Sympathetic augmentation in hypertension: role of nerve firing, norepinephrine reuptake, and Angiotensin neuromodulation. *Hypertension* 43: 169-175, 2004.

CHAPTER 2: LITERATURE REVIEW AND RATIONALE

Hypertension Definition, Statistics, and Causes

Hypertension is characterized by elevated blood pressure persistently exceeding 140/90mmHg. According to the National Institutes of Health, approximately one-third of American adults (65 million people) are classified as hypertensive. In 90-95 percent of the cases of hypertension, there is no single identifiable cause of the disease (3; 33). These cases are classified as "essential" or "primary" hypertension. Essential hypertension is heterogeneous (i.e., different causal factors in different patients) and likely has many related contributing factors including, but not limited to, **elevated sympathetic nervous system activity**, dietary salt intake, obesity, insulin resistance, renin-angiotensin system activation, genetics, endothelial dysfunction, and altered nitric oxide (3; 5). **The focus of this thesis was to examine the role of elevated sympathetic nervous system activity, specifically, the altered expression and regulation of NET at the cardiac sympathetic neuroeffector junction.**

Role of the Sympathetic Nervous System in Hypertension

Sympathetic nervous system activation, in particular, altered norepinephrine (NE) handling, has been implicated in hypertension (15; 22; 39). Elevated NE can contribute directly to a hypertensive state (e.g., increased cardiac output, increased vascular resistance, modulation of renin release, altered renal blood flow, etc.). Generally used as a measure of sympathetic nerve activity, plasma

NE levels are elevated in hypertensive humans and animal models (11). Specifically, the sympathetic nervous system has been shown to play a role in the genesis of DOCA-salt and spontaneously hypertensive animal models, as well as human essential hypertension (2; 19; 40). NE released from the heart and kidney is elevated in hypertensive and borderline hypertensive patients (8; 37), suggesting that elevation of plasma NE may be an early event in the pathogenesis of hypertension (30). The effectiveness of pharmacologic blockade of the sympathetic nervous system as a therapy for hypertension is consistent with the above findings. Proposed mechanisms for increased spillover of NE include sympathetic hyperinnervation, epinephrine cotransmission, increased nerve firing rates, and *dysfunction of NE reuptake* (9). In fact, hypertensive patients have *both* increased nerve firing rates and *reduced neuronal reuptake of NE* (37).

Neuronal NE Reuptake via NET

As first described by Hertting and Axelrod (20), the actions of NE in the synapse are attenuated by reuptake of NE into nerve terminals. A majority (80-90 percent) of released NE is quickly cleared by a reuptake into the neuron; however, a small amount (10-20 percent) of NE is lost into the plasma as spillover. Subsequently, it was determined that this uptake process into nerve terminals occurred through a membrane transporter known as NET or "uptake-1". Clearance of NE from the synapse removes excess junctional NE, prevents adrenergic receptor desensitization, and reduces spillover of NE into the

circulation. NET mediated reuptake of NE increases when elevated nerve firing releases more NE into the synapse (7); however, if NET function does not proportionally increase with release, excess NE would accumulate in the synapse and spillover into the circulation. In fact, **NET deficient mice demonstrate significantly elevated plasma NE and an associated elevation of heart rate and mean arterial pressure** (24).

NET is a plasma membrane protein that contains twelve membrane spanning domains and belongs to the large gene family of Na^+/Cl^- dependent neurotransmitter transporters (Figure 1). Transporters in this family share significant sequence homology and are responsible for clearance of NE, dopamine, and serotonin from the neuroeffector junction (43). Neurotransmitter transport is dependent upon inward co-transport of Na^+ and Cl^- through the single subunit transporter (43). NET contains a large extracellular loop between transmembrane domain 3 and 4 along with long, intracellular N-terminal and C-terminal tails. The extracellular loop contains a variable number of glycosylation sites and the tails contain consensus sequences for phosphorylation (43). These modification sites indicate that NET transport function and subcellular distribution are regulated by phosphorylation (43). Acutely, NET is regulated by membrane potential, substrate exposure, pre-synaptic receptor manipulation, and second messenger systems such as protein kinase C. The acute regulation occurs quickly with a subcellular redistribution of transporter from insertion in the plasma membrane to intracellular sites, or by changing the transport efficiency while

inserted in the membrane (43). NE transport through NET is inhibited by cocaine, desiprimine, and nisoxetine (6).

Role of the Heart

Hypertensive subjects demonstrate an elevation of sympathetic stimulation to the heart as compared to normotensive subjects, supporting the idea that tissue-specific changes in sympathetic nervous system contribute to hypertension (10; 33). Historically, the heart has been considered in hypertension with the work of DeChamplian, and LeLorier in the mid-1960's (27). This early work, along with that of Iversen (21), demonstrated a mechanism for NE reuptake in the heart and a functional loss of NE reuptake in the hypertensive heart. *Functional* studies indicating a reduction in NE reuptake have recently been revisited by Esler and Robertson (13; 14; 38). The consensus is that the hypertensive heart demonstrates a *functional* decrease in NE clearance and an associated spillover of NE from the neuroeffector junction to the plasma; however, the *mechanism* by which this happens has yet to be identified. The cloning of NET allows a *mechanistic study to be performed in hypertensive subjects to address the molecular and biochemical basis of elevated plasma NE in hypertension.*

Importantly, the development of hypertension can be prevented in DOCA-salt hypertension by removal of cardiac sympathetic nerves, destruction of the sympathetic nervous system at birth, or inhibition of adrenergic receptors (4). **This demonstrates that hypertension development in the DOCA-salt model**

is dependent upon an intact cardiac sympathetic nervous system, lending credence to the importance of the heart in hypertension and to a strong neurogenic component to the disease. Furthermore, several groups have demonstrated a reduction in functional NE reuptake capacity in the DOCA-salt heart both *in vivo* and in isolated heart preparations (16; 23; 26; 35). Together, this evidence suggests that the *NET dysfunction could play a prominent role in neurogenic hypertension.*

The heart has a high sympathetic innervation, nerve activity, and a very efficient uptake system. There is a roughly 20:1 ratio of *released* NE to NE spillover in the heart. The ratio is much lower in other organs, such as the liver and kidney, which have ratios of 4:1 or 8:1, respectively (25). That is to say that the reuptake system in the heart can clear up to 5 times more *released* NE then it does in other organs. Also, the heart is exceptionally dependent on NET for clearance of *circulating* NE, such that while the heart clears nearly 70% of infused NE via NET, other organs clear only 4-14% of circulating NE by neuronal reuptake (12). It follows then, that if the cardiac NE reuptake system were to be impaired, there would be a substantial local accumulation of *released* NE in the neuroeffector junction and a reduction in clearance of *circulating* NE, ultimately resulting in elevated plasma levels of NE. In addition, since the nerve activity to the heart has been shown to increase in hypertension there would be a even greater chance of spillover of NE. The proposed studies focus on identifying a possible role of cardiac specific NET dysfunction in hypertension. **It is hypothesized that**

a defect in cardiac NET is partially responsible for the attenuation of functional NE reuptake in the heart. Previous work from the lab suggests that the protein level of NET correlates with tissue capacity to transport NE. Specifically, there has been shown to be an increase in *arterial* NE transport in hypertensive animals and humans (1; 44) and this was related to an increase in NET protein in the mesenteric artery (31). We propose an opposite situation in the heart, in which **the reduction in NE transport in the heart is due to a reduction in NET protein**.

Stellate Ganglion Innervation

The cardiac sympathetic axons and nerve terminals originate largely in the cell bodies of the bilateral stellate ganglia. The cardiac targets of stellate axons are the sinoatrial node, the conducting system, cardiomyocytes, and coronary vessels (42). Bilateral stellate ganglionectomy in the rat reduces cardiac NE content by 89-100% (34). In the rat, all heart chambers receive bilateral innervation from the right and left stellate ganglia; however, the majority of the rat right ventricular innervation arises in the left stellate ganglion and there is substantial ipsilateral innervation to the atrial appendages (34).

Sympathetic ganglia and adrenal gland have high expression of NET mRNA (17; 18; 28; 29; 32). Sympathetic ganglia contain the cell bodies of neurons whose axons project to end organs such as the heart. Adrenal medullary cells are "neuron-like" and therefore would also contain the genetic machinery necessary

for the production of NET mRNA and protein. It is unknown if NET protein expression is different in the right versus left stellate ganglia, but NET mRNA is expressed at higher levels in the right stellate ganglia (28). Several studies have demonstrated a lack of NET mRNA expression in the myocardium and in heart extracts so it is believed that the NET protein in the heart comes from the cell bodies in the stellate ganglia (28; 41) (36).

Summary

There is a prominent role for the sympathetic nervous system in both human essential hypertension and in numerous animal models of hypertension, including the DOCA-salt model. Essential hypertensive patients and the DOCA-salt model show elevated plasma NE associated with both elevated sympathetic nerve firing and diminished reuptake of NE, indicating a neurogenic component to the disease. The cardiac sympathetic innervation plays a crucial role in the development of DOCA-salt hypertension. Stellate ganglionectomy prevents the hypertension in animals administered DOCA-salt (4) indicating that a perturbation in the function or innervation pattern of the stellate ganglion neurons plays a role in the development and maintenance of high blood pressure in this animal model of neurogenic hypertension. The functional determination of reduced reuptake of NE has not been explained mechanistically.

A detailed examination on the localization and distribution of NET in cardiac tissues of normal animals must be undertaken in order to establish a framework

from which to evaluate changes in NET with disease. **The purpose of this thesis is to examine NET mRNA and protein in the normal cardiovascular system then determine the causes of reduced NE reuptake in hypertension by examining the molecular and biochemical nature of cardiac NET in DOCA-salt hypertension**.

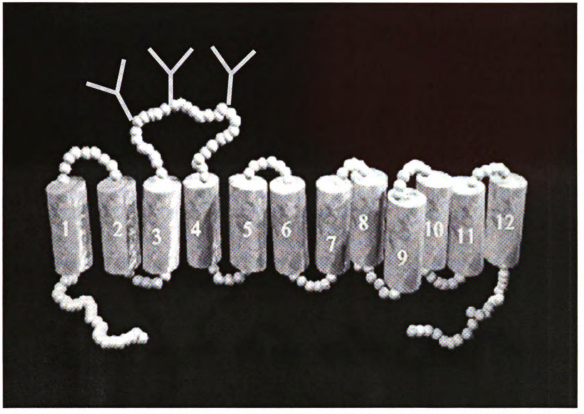

Figure 2.1: Structure of norepinephrine transporter (NET). The cartoon shows the proposed structure of NET with 12 transmembrane (TMD) domains, multiple glycosylation sites on the large extracellular loop between TMD 3 & 4, and long intracellular N-terminal and C-terminal tails. Three glycosylation sites on the large extracellular loop are noted.

Reference List

1. **Aalkjaer C, Heagerty AM, Petersen KK, Swales JD and Mulvany MJ**. Evidence for increased media thickness, increased neuronal amine uptake, and depressed excitation--contraction coupling in isolated resistance vessels from essential hypertensives. *Circ Res* 61: 181-186, 1987.

2. **Anderson EA, Sinkey CA, Lawton WJ and Mark AL**. Elevated sympathetic nerve activity in borderline hypertensive humans. Evidence from direct intraneural recordings. *Hypertension* 14: 177-183, 1989.

3. **Beevers G, Lip GY and O'Brien E**. ABC of hypertension: The pathophysiology of hypertension. *Br Med J* 322: 912-916, 2001.

4. **Bell C and McLachlan EM**. Dependence of deoxycorticosterone/salt hypertension in the rat on the activity of adrenergic cardiac nerves. *Clin Sci (Lond)* 57: 203-210, 1979.

5. **Carretero OA and Oparil S**. Essential hypertension. Part I: definition and etiology. *Circulation* 101: 329-335, 2000.

6. **Eisenhofer G**. The role of neuronal and extraneuronal plasma membrane transporters in the inactivation of peripheral catecholamines. *Pharmacol Ther* 91: 35-62, 2001.

7. **Eisenhofer G, Cox HS and Esler MD**. Parallel increases in noradrenaline reuptake and release into plasma during activation of the sympathetic nervous system in rabbits. *Naunyn Schmiedebergs Arch Pharmacol* 342: 328-335, 1990.

8. **Esler MD, Lambert G and Jennings G**. Regional norepinephrine turnover in human hypertension. *Clin Exp Hypertens A* 11 Suppl 1: 75-89, 1989.

9. **Esler MD, Rumantir M, Kaye DM, Jennings G, Hastings J, Socratous F and Lambert G**. Sympathetic nerve biology in essential hypertension. *Clin Exp Pharmacol Physiol* 28: 986-989, 2001.

10. **Ferrier C, Cox H and Esler MD**. Elevated total body noradrenaline spillover in normotensive members of hypertensive families. *Clin Sci (Colch)* 84: 225-230, 1993.

11. **Goldstein DS**. Plasma catecholamines and essential hypertension. An analytical review. *Hypertension* 5: 86-99, 1983.

12. **Goldstein DS, Brush JE, Jr., Eisenhofer G, Stull R and Esler M**. In vivo measurement of neuronal uptake of norepinephrine in the human heart. *Circulation* 78: 41-48, 1988.

13. **Goldstein DS, Robertson DM, Esler MD, Straus SE and Eisenhofer G**. Dysautonomias: clinical disorders of the autonomic nervous system. *Ann Intern Med* 137: 753-763, 2002.

14. **Grassi G and Esler MD**. How to assess sympathetic activity in humans. *J Hypertens* 17: 719-734, 1999.

15. **Grassi G and Mancia G**. Neurogenic hypertension: is the enigma of its origin near the solution? *Hypertension* 43: 154-155, 2004.

16. **Gudeska S, Glavas E, Stojanova D, Petrov S, Trajkov T and Nikodijevic B**. Alteration in the uptake and storage of cardiac noradrenaline in spontaneously hypertensive rats. *Biomedicine* 25: 157-159, 1976.

17. **Habecker BA, Grygielko ET, Huhtala TA, Foote B and Brooks VL**. Ganglionic tyrosine hydroxylase and norepinephrine transporter are decreased by increased sodium chloride in vivo and in vitro. *Auton Neurosci* 107: 85-98, 2003.

18. **Habecker BA, Klein MG, Cox BC and Packard BA**. Norepinephrine transporter expression in cholinergic sympathetic neurons: differential regulation of membrane and vesicular transporters. *Dev Biol* 220: 85-96, 2000.

19. **Hallback M and Weiss L**. Mechanisms of spontaneous hypertension in rats. *Med Clin North Am* 61: 593-609, 1977.

20. **Hertting G and Axelrod J**. Fate of tritiated noradrenaline at the sympathetic nerve-endings. *Nature* 192: 172-173, 1961.

21. **Iversen LL**. The uptake of noradrenaline by isolated perfused rat heart. *Br J Pharmacol* 21: 523-537, 1963.

22. **Julius S and Majahalme S**. The changing face of sympathetic overactivity in hypertension. *Ann Med* 32: 365-370, 2000.

23. **Kazda S, Pohlova I, Bibr B and Kockova J**. Norepinephrine content of tissues in Doca-hypertensive rats. *Am J Physiol* 216: 1472-1475, 1969.

24. **Keller NR, Diedrich A, Appalsamy M, Tuntrakool S, Lonce S, Finney C, Caron MG and Robertson DM**. Norepinephrine transporter-deficient mice exhibit excessive tachycardia and elevated blood pressure with wakefulness and activity. *Circulation* 110: 1191-1196, 2004.

25. **Kopin IJ, Rundqvist B, Friberg P, Lenders J, Goldstein DS and Eisenhofer G**. Different relationships of spillover to release of norepinephrine in human heart, kidneys, and forearm. *Am J Physiol* 275: R165-R173, 1998.

26. **Krakoff LR, Ben Ishay D and Mekler J**. Reduced sympathetic neuronal uptake (uptake1) in a genetic model of desoxycorticosterone-NaCl hypertension. *Proc Soc Exp Biol Med* 178: 240-245, 1985.

27. **LeLorier J, Hedtke JL and Shideman FE**. Uptake of and response to norepinephrine by certain tissues of hypertensive rats. *Am J Physiol* 230: 1545-1549, 1976.

28. **Li H, Ma SK, Hu XP, Zhang GY and Fei J**. Norepinephrine transporter (NET) is expressed in cardiac sympathetic ganglia of adult rat. *Cell Res* 11: 317-320, 2001.

29. **Li W, Knowlton D, Van Winkle DM and Habecker BA**. Infarction alters both the distribution and noradrenergic properties of cardiac sympathetic neurons. *Am J Physiol Heart Circ Physiol* 286: H2229-H2236, 2004.

30. **Lopes HF, Silva HB, Consolim-Colombo FM, Barreto Filho JA, Riccio GM, Giorgi DM and Krieger EM**. Autonomic abnormalities demonstrable in young normotensive subjects who are children of hypertensive parents. *Braz J Med Biol Res* 33: 51-54, 2000.

31. **Luo M, Hess MC, Fink GD, Olson LK, Rogers J, Kreulen DL, Dai X and Galligan JJ**. Differential alterations in sympathetic neurotransmission in mesenteric arteries and veins in DOCA-salt hypertensive rats. *Auton Neurosci* 104: 47-57, 2003.

32. **Nishimura M, Sato K, Shimada S and Tohyama M**. Expression of norepinephrine and serotonin transporter mRNAs in the rat superior cervical ganglion. *Brain Res Mol Brain Res* 67: 82-86, 1999.

33. **Oparil S, Zaman MA and Calhoun DA**. Pathogenesis of hypertension. *Ann Intern Med* 139: 761-776, 2003.

34. **Pardini BJ, Lund DD and Schmid PG**. Organization of the sympathetic postganglionic innervation of the rat heart. *J Auton Nerv Syst* 28: 193-201, 1989.

35. **Rascher W, Schomig A, Dietz R, Weber J and Gross F**. Plasma catecholamines, noradrenaline metabolism and vascular response in desoxycorticosterone acetate hypertension of rats. *Eur J Pharmacol* 75: 255-263, 1981.

36. **Reja V, Goodchild AK and Pilowsky PM**. Catecholamine-related gene expression correlates with blood pressures in SHR. *Hypertension* 40: 342-347, 2002.

37. **Schlaich MP, Lambert E, Kaye DM, Krozowski Z, Campbell DJ, Lambert G, Hastings J, Aggarwal A and Esler MD**. Sympathetic augmentation in hypertension: role of nerve firing, norepinephrine reuptake, and Angiotensin neuromodulation. *Hypertension* 43: 169-175, 2004.

38. **Shannon JR, Flattem NL, Jordan J, Jacob G, Black BK, Biaggioni I, Blakely RD and Robertson DM**. Orthostatic intolerance and tachycardia associated with norepinephrine- transporter deficiency. *N Engl J Med* 342: 541-549, 2000.

39. **Smith PA, Graham LN, Mackintosh AF, Stoker JB and Mary DA**. Sympathetic neural mechanisms in white-coat hypertension. *J Am Coll Cardiol* 40: 126-132, 2002.

40. **Ueno Y, Mohara O, Brosnihan KB and Ferrario CM**. Characteristics of hormonal and neurogenic mechanisms of deoxycorticosterone-induced hypertension. *Hypertension* 11: I172-I177, 1988.

41. **Ungerer M, Chlistalla A and Richardt G**. Upregulation of cardiac uptake 1 carrier in ischemic and nonischemic rat heart. *Circ Res* 78: 1037-1043, 1996.

42. **Wallis D, Watson AH and Mo N**. Cardiac neurones of autonomic ganglia. *Microsc Res Tech* 35: 69-79, 1996.

43. **Zahniser NR and Doolen S**. Chronic and acute regulation of Na+/Cl- -dependent neurotransmitter transporters: drugs, substrates, presynaptic receptors, and signaling systems. *Pharmacol Ther* 92: 21-55, 2001.

44. **Zsoter TT and Wolchinsky C**. Norepinephrine uptake in arteries of spontaneously hypertensive rats. *Clin Invest Med* 6: 191-195, 1983.

CHAPTER 3: NOREPINEPHRINE TRANSPORTER mRNA IS PRESENT IN THE HEART BEFORE AND AFTER SYMPATHETIC DENERVATION

Abstract

Reduced function of cardiac neuronal norepinephrine (NE) transporter (NET) has been proposed to mediate several cardiovascular diseases. Genetic and epigenetic factors that reduce NET mRNA could lead to reduced NET protein in the diseased heart. Although the stellate ganglia are considered to be the source of NET mRNA associated with the heart, we demonstrated for the first time that NET mRNA was present in extracts from all heart chambers. Real time qPCR was used to assess NET mRNA expression in the bilateral stellate ganglia and heart chambers from normal rats. NET mRNA was expressed in greater amounts in the right versus the left stellate ganglia (1.5-fold higher, $p<0.05$). Freshly dissected heart chambers were immediately processed since delayed processing or the use of frozen heart tissue resulted in a reduction or absence of NET mRNA in heart extracts even though a control gene was viable. NET mRNA in the heart is labile and expressed at low levels compared to the stellate ganglia. The stellate ganglia contained up to 17,332-fold higher NET mRNA than the lowest expressing heart chamber ($p<0.0001$). The atria express significantly more NET mRNA than the ventricles ($p<0.05$). Chemical and surgical sympathetic denervation depleted tissue NE but failed to reduce NET mRNA from heart extracts. Therefore, NET mRNA is not present in sympathetic nerve terminals, but instead is localized to other cells in the heart. The finding of NET

mRNA in heart extract is novel and opens up a new area of research into the regulation of NET in cardiovascular disease.

Introduction

The stellate ganglia support a majority of sympathetic innervation to the heart. The heart chambers, in particular the atria, are highly innervated by the sympathetic nervous system , and sympathetic nerve activity to the non-diseased heart is greater than to other organs and tissues (33; 48). Stellate innervation in rat is largely bilateral to all heart chambers and there is substantial crossover to the contralateral heart from each stellate (40; 41). The sympathetic neurotransmitter norepinephrine (NE) is released in the heart upon stellate ganglion stimulation and its actions are attenuated by reuptake into nerve terminals (20). Reuptake occurs via the membrane transporter NE transporter (NET) or "uptake-1". NE clearance from the neuroeffector junction removes excess NE, prevents adrenergic receptor desensitization, and reduces spillover of NE into the circulation. The capacity and efficiency of NE reuptake varies in different organs and tissues (27). A highly efficient NE reuptake system exists in the heart in which a majority (~90 percent) of released NE is quickly cleared by reuptake into the neuron; however, a small amount (~10 percent) of NE is lost into the plasma as spillover (27).

Sympathetic nervous system activation and reduction in NE reuptake have been indicated in cardiovascular disorders, including heart failure, hypertension,

orthostatic intolerance, and postural tachycardia (9; 13; 14; 17; 25; 37; 42; 44-46; 49; 51). Sympathetic nerve activity to the diseased heart is significantly elevated compared to the healthy heart (33; 48) resulting in substantial local junctional NE and NE spillover into the circulation. This is exacerbated when coupled with a reduction in NE reuptake. Changes in NET function associated with diseases suggest that there is regulated modulation of NET, and this is an active research area.

The regulation of NET protein function has been studied extensively in cell culture with limited studies assessing these regulatory processes or the genetic regulation of NET *in vivo*. NET function is regulated acutely by membrane potential, substrate exposure, pre-synaptic receptor manipulation, and second messenger systems that mediate phosphorylation (56). The acute regulation occurs quickly with a subcellular redistribution of transporter from the plasma membrane to intracellular sites, or by changing the transport efficiency while inserted in the membrane (56). Other known modulators of transport function include reactive oxygen species, nitric oxide, angiotensin II, nerve growth factor, and endothelin-1 (1; 4; 29).

Cardiac NET can also be regulated at the genetic and epigenetic level. NET mRNA has never been detected in heart extract (31; 55) thus the stellate ganglia have been the primary site of assessment of genetic regulation of cardiac NET. The stellate ganglia contain the genetic machinery for transcription and

translation of NET, and contain a large amount of NET mRNA (31; 41). The right stellate ganglion expresses higher levels of NET mRNA than the left stellate ganglion (31). NET mRNA in stellate ganglia is unchanged with heart failure even though there is a reduction in NET protein function in the heart suggesting a post-transcriptional mechanism (5). Stellate NET mRNA is also unchanged after myocardial infarction even though there is a reduction in left ventricular [^{3}H]-nisoxetine binding (32). Therefore, decreased NE reuptake in the heart is not associated with downregulation of NET mRNA in the stellate ganglia. Thus, it is not possible to infer NET function in the heart by examining mRNA in the stellate ganglia.

Since NET mRNA in the stellate does not predict NET protein function in cardiac sympathetic terminals, either NET is regulated post-transcriptionally or there are alternative sites of expression of NET mRNA that do predict cardiac NET protein expression. Additional sites of genetic regulation of NET may occur within the heart itself. This is an appealing option since local regulation at the level of the tissue would be beneficial as opposed to regulation only in the distant ganglia. There is good evidence that neurons contain machinery to selectively deliver certain RNAs from the cell body to the axons and dendrites, and that there is local axonal translation of that RNA into protein providing for a tissue level synthesis of vital nerve terminal proteins (8; 30; 35; 57). NET mRNA could be one of the RNAs that is delivered to the nerve terminals and would be present in heart extracts.

This paper provides a method to isolate NET mRNA from the heart and reports for the first time that NET mRNA is present in heart extract. We tested if sympathetic nerve terminals contain NET mRNA by using cardiac sympathetic denervation. This report of NET mRNA in the heart reveals novel sites for regulation of NET that were previously unknown.

Materials and Methods

Animals

Adult male, Sprague-Dawley rats, 8 weeks old (250-275 g, Charles River, Portage, MI) were used. All animal experiments were performed in accordance with the "Guide for the Care and Usage of Laboratory Animals" (National Research Council) and were approved by the Animal Use and Care Committee of Michigan State University. Animals were housed two per cage in temperature and humidity-controlled rooms with a 12 hour/12 hour light-dark cycle. Standard pellet rat chow and water were given *ad libitum*.

Stellate ganglionectomy

Rats were administered atropine sulphate (0.4 mg/kg, i.p.), anesthetized with isoflurane, intubated and ventilated with a Harvard rodent ventilator (model 683, Harvard Apparatus; South Natick, MA). A midline thoracotomy was performed by first making a midline skin incision and then cutting the sternum from the mid-manubrium to the ziphoid process and opening the incision with a retractor. The

stellate ganglia were exposed by moving the upper lobe of the right lung caudally and medially with saline soaked gauze. The entire ganglion was removed bilaterally and the upper lung lobe is returned to its original position. The chest was closed by suturing the bone, muscle, and skin in 3 separate layers. Negative intrathoracic air pressure is reestablished bilaterally by inserting a 23-guage needle into the lower thoracic cavity and suctioning with a 3 ml syringe. Upon arousal from anesthesia, the rat was taken off the ventilator and spontaneous ventilation was reestablished. Animals with successful denervation were noted to have post-surgical ptosis. Hearts were collected two weeks following surgery for confirmation of denervation with cardiac NE assessment or analysis of NET mRNA (detailed procedure below). Control animals underwent anesthesia and thoracotomy, but the stellate ganglia were left intact.

6-hydroxydopamine Denervation Procedure

The neurotoxin 6-hydroxydopamine hydrochloride (6-OHDA, St. Louis, MO) was used to destroy sympathetic nerve terminals and NET containing cells. It was prepared in a mixture of 0.9 % (154 mM) sodium chloride and 0.5 % (28.4 mM) ascorbic acid solution fresh before each administration and kept protected from light. Animals were dosed (250 mg/kg) with subcutaneous injection of 6-OHDA to the loose skin between the shoulder blades (25 gauge needle) with three consecutive injections during one week on day one, three and five. On day seven, two days after the final dose, the animals were sacrificed and hearts were

collected as described below for analysis of RNA and NE content. Age and sex matched control animals were untreated.

Tissue Collection

Rats were anesthetized with sodium pentobarbital (Sigma-Aldrich Corp, St. Louis, MO, 65 mg/kg, i.p.) followed by thoracotomy. Freshly dissected hearts were removed quickly from anesthetized rats and immediately placed into chilled (4 °C) phosphate buffered saline (PBS, 137 mM sodium chloride, 2.7 mM potassium chloride, 4.3 mM sodium phosphate dibasic and 1.4 mM potassium phosphate monobasic) for rinsing and separation of chambers. While in buffer, the chambers were quickly separated in the following order: right atrium, left atrium, right ventricle outer wall, ventricular septal wall, and left ventricle outer wall. For comparisons of RNA isolation from fresh versus frozen hearts, "fresh" hearts were immediately processed as described below while "frozen" hearts were first frozen on dry ice then homogenized for RNA isolation. The freshly dissected heart chambers were immediately placed into Trizol (2ml for atria and 4 ml for ventricles) or frozen and then placed into Trizol. Hearts were then processed using a variable speed Omni TH-115 homogenizer with 7mm saw tooth generator probe (Omni International Inc., Warrenton, VA) for ~30 seconds at high speed and allowed to stand on ice for ~10 minutes. Total RNA was isolated immediately or from Trizol homogenates stored less than 1 week at -80°C. Other tissues were dissected in the following order after the heart was processed: right and left stellate, and adrenal gland. These tissues were placed

into Trizol reagent (300uL for ganglia and 1 ml for adrenal gland) immediately and allowed to stand on ice for ~20 minutes to ensure penetration of Trizol into the tissue, then stored at -80°C for less than one week until RNA isolation. For preparation of tissue for NE analyses see below.

Additional information regarding RNA handling for cardiac tissue

Fresh heart tissue needs to be removed under anesthesia, separated quickly by chamber in cold buffer, and immediately processed in Trizol with a motorized tissue grinder. Due to time sensitivity of processing, the ventricular septal wall was not separated from the outer ventricular wall. This tissue homogenate should be used immediately if possible for RNA isolation but can be frozen briefly at -80°C, assuming that the RNA is to be isolated within 1-week of processing. Slow dissection and separation of chambers and longer storage of tissue at -80°C resulted in loss of NET mRNA. We determined that (i) if there was any delay in removing or homogenizing the heart in Trizol reagent, (ii) if heart homogenate was stored more than 1 week before RNA isolation, (iii) if PCR-amplification was performed with a low starting amount (<2μg) of RNA for reverse transcription, or (iv) if amplified in real time PCR using less than 40 cycles, the NET mRNA signal was often not detectable or was attenuated. Importantly, if heart tissue was frozen prior to processing, NET mRNA was lost even though other high copy number genes, such as GAPDH were amplified and detectable after RT-PCR and real time PCR. Even with care taken with all the above recommendations, it should be noted that the cardiac mRNA samples for NET and GAPDH show

higher variability than that from stellate ganglia. There are instances in which the appropriate cautions are taken and NET mRNA will still not amplify properly. It was common to use additional animals to increase sample size due to NET mRNA instability.

RNA isolation and integrity

Frozen ganglia and adrenal gland in Trizol were thawed on ice then were homogenized in Trizol using an RNase-free Kontes Pellet Pestle® with hand-held motor in a compatible RNase-free Kontes mircocentrifuge tube (Fisher Scientific, Hanover Park, IL). Homogenized heart tissue in Trizol was thawed on ice. Total RNA was isolated from all tissues using the standard TRIzol® procedure (GIBCO Life Technologies, Carlsbad, CA) with the use of glycogen as an RNA carrier for ganglia. The RNA pellet was dried for 5 minutes, resuspended in an appropriate volume of TE Buffer (Ambion, Austin, TX) and stored at -80°C. The concentration and purity/integrity of RNA was ascertained spectrophotometrically (A260/A280 and A260/A230) using a Nanodrop ND-1000 Spectrophotometer (Nanodrop, Wilmington, DE). To eliminate residual genomic DNA in the preparation, total RNA samples were treated with diluted RNase-free DNase I (10U/μl, Roche Diagnostics, Nutley, NJ) for 30 minutes at 37°C; DNase I was inactivated by heating for 10 minutes at 75°C.

Primers

NET primers were derived from the Rattus Norvegicus NET gene (Ascension # Y13223) National Center for Biotechnology Information GenBank). Primers were developed using Primer3 software (http://frodo.wi.mit.edu/), Massachusetts Institute of Technology). A NCBI basic local alignment search tool (BLAST) search ensured the specificity of primer sequences for rat NET and the primers were synthesized at the Macromolecular Structure, Sequencing and Synthesis Facility at Michigan State University. Three primer pairs were designed in this study because of different requirements for sequencing, real-time RT-PCR and regular PCR. Predicted sequences of PCR amplification products were aligned with other rat sequences in GenBank to examine the stringency. Primer sequences are listed in Table 1. Primers were tested to determine efficiency and this value used in calculations of fold-change.

Reverse transcription polymerase chain reaction (RT-PCR) and Real Time PCR

All samples to be compared were run on a single 96 well plate when possible to allow for accurate comparisons. A two-step RT–PCR was performed. The first strand complementary DNA (cDNA) was synthesized from a starting amount of 70 ng total DNase treated RNA for real time PCR and 2 µg total DNase treated RNA for conventional PCR by adding the following components into a nuclease-free microcentrifuge tube (20 µl reaction volume): Oligo(dT) (500 µg/ml) (Invitrogen, Carlsbad, CA), 10mM dNTP mix (Invitrogen, Carlsbad, CA), 5X first

strand buffer, 0.1 M DTT (dithiothreitol), RNase inhibitor (Roche Diagnostics, Indianapolis, IN), and Superscript II RNase H- reverse transcriptase (Invitrogen, Carlsbad, CA). Samples were mixed, incubated at 42°C for 60 minutes, and inactivated by heating at 70°C for 15 minutes. Conventional PCR products were analyzed on 2% (w/v) agarose gel in 1X TAE buffer (2.42g Tris, 0.57ml glacial acetic acid, 0.37g EDTA-sodium in 500ml dH_20, pH 8.5). 100bp DNA ladder was loaded on the gel to measure the length of RT-PCR products. Gels were run at 65V for 45-60 minutes then stained with ethidium bromide for eight minutes followed by destaining in distilled water for 20 minutes. DNA bands were visualized under UV light using a Syngene ChemiGenius® gel documentation system (Syngene, Frederick, MD). RT-PCR for beta-actin was also performed as an internal positive control to assure even loading and no genomic DNA contamination in each sample. In addition, samples were run without reverse transcriptase enzyme (no RT) to rule out contamination and a negative control was run in which no cDNA template was added to the PCR reaction (No Template Control). For real time PCR, a 25 μl PCR reaction volume was prepared with cDNA (70ng/μl) from the first-strand reaction, forward primer (20mM), reverse primer (20 mM), SYBR Green Supermix (Applied Biosystems, Bedford, MA) and DEPC-treated distilled water (Ambion, Austin, TX). Real time PCR thermal profile was set up according to manufacturers instructions for SYBR green and run for 60 cycles to achieve full amplification of NET in the heart. A dissociation protocol (60-95 °C melt) was done at each end of the experiment to verify that only one amplicon was formed during the process of amplification.

Relative quantification of mRNA was measured against the internal control, GAPDH. End point, used in qPCR quantification and Ct value, is defined as the PCR cycle number that crosses an arbitrarily placed signal threshold. Relative expression value calculation and statistical analysis was performed by Pair Wise Fixed Reallocation Randomization Test© (http://www.gene-quantification.info) using Relative Expression Software Tool (REST) (43)

Amplicon Sequencing

PCR amplicons were purified using QIAquick PCR Purification Kit (Qiagen, Valencia, CA). The concentrations of purified DNA amplicons were determined spectrophotometrically. The identities of amplicons were confirmed by sequencing the mixture of 20ng DNA amplicon and 30 picomoles forward primer on an ABIPRISM® 3100 Genetic Analyzer (Applied Biosystems, Foster City, CA) at the Genomic Technology Support Facility at Michigan State University.

Tissue Norepinephrine Measurements

Heart chambers were homogenized in ice-cold 0.1 M perchloric acid. The homogenate was then centrifuged at 10,000 rpm for 15 min at 4°C and the supernatant was further processed by solid phase extraction (SPE) using Oasis MCX cartridges, 30 mg / 1cc (Waters, Milford, MA, USA) as previously described (10). The eluate was analyzed by capillary electrophoresis with electrochemical detection (CE-EC). CE-EC using boron-doped diamond electrode for detection was employed for norepinephrine determination in the heart chambers. The CE-

EC system, electrochemical detection cell, and electrode fabrication was described elsewhere (36; 39). The separation and detection was performed using following conditions: 76 cm long, 362 μm o.d., 29 μm i.d. capillary, 250 mM boric acid - 1 M potassium hydroxide run buffer of pH 8.8, separation voltage 24 kV, detection potential +0.86 V vs Ag/AgCl and electrokinetic injection at 18 kV for 8 sec.

Results

NET mRNA amplification in heart is dependent upon tissue handling

Freshly dissected hearts were either immediately processed for RNA isolation or frozen prior to RNA isolation then real-time qPCR was performed. qPCR amplification plots are shown for all heart chambers. Glyceraldehyde phosphate dehydrogenase (GAPDH), a common control gene, was readily detected in extracts from both fresh and frozen heart chambers. However, NET mRNA was amplified only in extracts isolated from fresh tissues. NET mRNA from frozen right atrium (RA, Figure 1A), right ventricle (RV, Figure 1C), and left ventricle (LV, Figure 1D) was not amplified even after 60 cycles of qPCR as shown by a flat amplification profile at baseline (indicated by black arrowhead). Interestingly, NET mRNA expression from the frozen left atrium (LA) was detectable with only a slight decrease in expression compared to that in fresh LA (Figure 1B). In stellate ganglia there was no difference in NET mRNA expression between fresh and frozen tissues (data not shown). Freezing of heart chambers prior to RNA isolation reduces or eliminates NET mRNA.

NET mRNA is differentially expressed in stellate ganglia and in heart chambers

Using conventional RT-PCR NET mRNA was present in adrenal gland, stellate ganglia and in fresh extracts of all four heart chambers (Figure 2). In all tissues the amplicons were of the predicted size and sequence.

The relative amounts of NET mRNA in the stellate ganglia and in each of the heart chambers were compared using qPCR (Figure 3). All values were normalized to LV. There was dramatically more NET mRNA in the stellate ganglia compared to the heart; up to 17,332-fold higher in the right stellate ganglion than the LV (Figure 3A). Also, the amount of NET mRNA in the right stellate ganglion was 1.5-fold higher than in the left stellate ganglion. Lastly, the amount of NET mRNA in the atria was significantly greater than the amount in the ventricles (Figure 3A). For example, the RA was 8.3-fold higher and LA was 9.7-fold higher than the LV; however, the amounts were not different between the atria (i.e., RA=LA) or the ventricles (i.e., RV=LV). These differences are also apparent from the mean cycle threshold (Ct) values for each tissue (Figure 3B).

Surgical sympathetic denervation: stellate ganglionectomy

To test the hypothesis that the source of NET mRNA in the heart was sympathetic fibers and nerve terminals, we performed bilateral stellate ganglionectomy and assessed heart NET mRNA levels. NE content of all chambers in innervated control hearts was similar to that reported previously (39)

and was significantly reduced in all chambers of ganglionectomized hearts after denervation (Figure 4A). The denervated RA, LA, RV, and LV were depleted of NE by 97.50%, 94.82%, 97.32%, and 96.97%, respectively. Although the hearts were sympathetically denervated, there was no change in the amount of NET mRNA present in three of the four chambers analyzed (Figure 4B). The exception was the LA in which the amount of NET mRNA was 3.1-fold elevated. These differences are also apparent from the mean Ct values for each tissue (Figure 4C).

Chemical Sympathetic Denervation: 6-OHDA

Since stellate ganglionectomy did not reduce NET mRNA in heart extracts, we tested an alternative method of sympathetic denervation by administering the neurotoxin 6-OHDA. Since 6-OHDA is taken up by NET (28; 53), the toxin should have effects on all NET-expressing cells in the heart and thereby cause a reduction in NET mRNA. Following 6-OHDA treatment, the NE content of all heart chambers was significantly reduced compared to control hearts, but the NE content of atria was reduced to a lesser extent than ventricles (Figure 5A). NE values following denervation range from below the limit of detection in the ventricles to 0.75 µg/g tissue in the atria. The RA, LA, RV, and LV were depleted of NE by the following percentages: 68.74%, 60.55%, >97.20%, and >99.97%, respectively. Although these reductions in NE content indicated that the hearts were sympathetically denervated by the 6-OHDA treatment, there was no reduction in NET mRNA in RA, RV or LV (Figure 5B). However, NET mRNA

expression in the LA was reduced by 2.9-fold in the 6-OHDA treated animals. These differences are also apparent from the mean Ct values for each tissue (Figure 5C).

Discussion

NET mRNA exists in stellate ganglia (19; 31). The stellate ganglia were assumed to be the primary source of cardiac-associated NET mRNA and thus the site of genetic regulation of cardiac NET. This paper reports for the first time that NET mRNA exists in extracts from fresh, but not frozen, heart chambers suggesting that cardiac NET mRNA is exceptionally labile. Heart NET mRNA is expressed in low abundance compared to ganglia and is present in greater amounts in the atria than the ventricles. Since the pattern of NET mRNA expression mirrors sympathetic innervation density and chamber NE content, we hypothesized that NET mRNA in heart extracts was derived from sympathetic nerve terminals. However, because surgical and chemical sympathetic denervation of the heart did not reduce the NET mRNA we conclude that NET mRNA is present in non-sympathetic sources in the heart.

NET mRNA presence in heart extract

Sympathetic ganglia contain the cell bodies of neurons whose axons project to end organs such as the heart. Additionally, adrenal medullary cells are "neuron-like" and therefore would also contain the genetic machinery necessary for the production of NET mRNA and protein. We confirmed that sympathetic ganglia

and adrenal gland have expectedly high expression of NET mRNA (18; 19; 31; 32; 38). We also report for the first time that NET mRNA exists in heart extracts, outside the cell bodies of sympathetic neurons. The expression level of NET mRNA in heart extract is substantially lower than that of the ganglia and adrenal gland.

Heart NET mRNA is labile so could only be amplified from hearts that were dissected fresh and immediately homogenized, but not from frozen hearts. GAPDH was not labile and was amplified in extracts of fresh heart, frozen heart, and stellate ganglia to a similar extent. Previous studies on NET mRNA in the heart used frozen tissue for RNA isolation and demonstrated a lack of NET mRNA in the heart even though GAPDH was still abundant (31; 55). We replicated this finding in frozen tissue. The labile nature of this mRNA results in a loss of NET mRNA in three of four frozen heart chambers. The loss of NET mRNA could be due to its low copy number in heart such that even a slight loss of total RNA that likely occurs with RNA isolation may cause this particular mRNA to fall below the limit of detection while other higher copy genes are virtually unchanged; however, this is not valid in the LA since freezing this chamber did not dramatically alter NET mRNA levels suggesting that there are different regulatory processes or cellular locations of NET mRNA in the LA. Alternatively, an inherent instability of NET transcript in the heart, or a specific degradation process that selectively breaks down NET mRNA leaving other genes, such as GAPDH, intact may account for this loss of signal (15).

The comparatively low level of expression in the heart is consistent with the idea that NET mRNA comes from a small portion of the total heart extract, such as nerve terminals or a subset of cardiac cells. Since the atria have greater expression of NET mRNA than do the ventricles and this pattern is consistent with both high sympathetic nerve density (11) (32) and NE content in the atria (39), we suggested that NET mRNA could be found in sympathetic nerve terminals. Neurons contain machinery to selectively deliver certain RNAs from the cell body to the axons and dendrites, and there is local axonal translation of that RNA into protein providing for a tissue level synthesis of vital nerve terminal proteins (8; 30; 35; 57). Therefore, it could be that NET mRNA is axonally transported similar to tyrosine-hydroxylase mRNA (34).

Localization of cardiac NET mRNA: Cardiac Denervation

Stellate ganglionectomy removes the primary cardiac-projecting sympathetic chain ganglion and a majority of sympathetic axonal inputs to the heart (40; 41). The procedure destroys the extrinsic sympathetic innervation to the heart (7) and reduced NE uptake (22). If NET mRNA was present in sympathetic nerve axons and/or terminals, then the destruction of these fibers by ganglionectomy would reduce the amount of NET mRNA amplified in the heart extracts. It is known that acute surgical denervation procedures do not immediately alter NE reuptake and time is needed for the nerves to degenerate (i.e., greater than 5 days) (21). We performed studies two weeks post-denervation to ensure that the nerves were

degenerated. In this study, NE content was depleted in the denervated groups yet surprisingly NET mRNA was not reduced in any chamber, indicating that the mRNA is not located in sympathetic fibers. Interestingly, there was actually an increase in NET mRNA in the LA following denervation suggesting that there are cells in the LA whose expression of NET mRNA is repressed by extrinsic sympathetic innervation.

Since stellate ganglionectomy did not reduce NET mRNA in heart extracts, we used a neurotoxic NET substrate, 6-OHDA, to damage all NET-expressing cells. This neurotoxin is transported into cells by NET (28; 47; 53) where it is converted to a chemically-active oxidative intermediate to destroy sympathetic nerve terminals. NE concentrations in sympathetically-innervated tissues are dramatically reduced after 6-OHDA treatment (26). In this study, the depletion of NE from the hearts of treated animals indicates that 6-OHDA had the expected effect; however, the continued expression of NET mRNA in all heart chambers suggests that some components of neuron structure remained in the heart. The ability of sympathetic nerves to regenerate several weeks after 6-OHDA treatment suggests that the nerve terminals are temporarily depleted of neurotransmitter, but some or all of the sympathetic axons remain in the tissues (12; 16; 54). Thus, it is possible that genetic material in sympathetic axons and other NET-expressing cells remains intact after treatment. Interestingly, however, there was a decrease in NET mRNA expression in the LA after 6-OHDA treatment. It may be that, in contrast to the other heart chambers, there is

a population of NET expressing cells in the LA that are susceptible to 6-OHDA treatment.

Alternative Cellular Sources of NET mRNA

Since neither stellate ganglionectomy not 6-OHDA denervation depleted NET mRNA from the heart, we suggest that the source of NET mRNA is not nerve terminals, but is non-sympathetic cells types.

Intrinsic cardiac adrenergic cells:

In addition to localization in sympathetic fibers in the heart (32; 50), NET protein has been reported in intrinsic cardiac adrenergic (ICA) cells, a type of non-neuronal cardiocyte present throughout the heart (23; 24). These independent cells contain NET protein and transport [^{3}H]NE (23); therefore ICA cells must contain NET mRNA and would be a source of the NET mRNA amplified in heart extracts. There is a higher number of ICA cells in the atria than in the ventricles (23; 24); this could be the reason for the higher expression of NET mRNA in the atria rather that the higher sympathetic innervation to the atria.

ICA cells are expressed throughout the heart even before sympathetic innervation develops (23) and should be intact following stellate ganglionectomy supporting that ICA cells are a likely source of NET mRNA in heart extracts. Following chemical denervation there was a reduction of NET mRNA in the LA only while the other chambers remained unchanged. ICA cells, although

clustered in the atria, are present throughout the heart. If 6-OHDA was capable of destroying those cells and reducing NET mRNA all chambers would show a decrease in NET mRNA not just the LA. The lack of reduction of NET mRNA in other chambers suggests that the decrease in NET mRNA in the LA is not due to loss of ICA cells. Importantly, this does not rule out ICA cells as a source of NET mRNA since ICA cells display different NET kinetics for uptake of NE than nerve terminals (23) and NET function is not inhibited to the same extent by the NET antagonist nisoxetine. Thus ICA cells are likely not affected in the same manner by 6-OHDA as other NET containing cells, and therefore may still be viable post-denervation with a normal expression of NET mRNA.

Intrinsic cardiac neurons:

Intrinsic cardiac neuron cell bodies cluster in cardiac ganglia and are highly concentrated in the atria (2; 3) and could contribute to high NET mRNA levels in the same chambers. Extrinsic sympathetic input from the stellate ganglion directly innervates intrinsic neurons (6) supporting the idea that there are catecholamines released in the cardiac intrinsic ganglia with a need for NE reuptake mechanisms. Some intrinsic neurons, although primarily parasympathetic/cholinergic, have components of the catecholaminergic phenotype (6), and it is possible that NET mRNA and protein are present in a subset of these cells. There is also evidence for NE in cardiac intrinsic neurons from some species (52).

Stellate ganglionectomy resulted in an increase in expression of NET mRNA in the LA. The extrinsic innervation from the stellate ganglia may serve as a negative regulator of NET expression in LA intrinsic neurons as we show that NET mRNA expression is elevated following surgical removal of the extrinsic sympathetic inputs. To the contrary, the decreased NET mRNA expression following 6-OHDA treatment in the LA could be due to susceptibility of intrinsic ganglion neurons in the LA to 6-OHDA. There are also intrinsic neurons in the RA; however, these may be functionally different that those in the LA such that they are not damaged by 6-OHDA.

Unique nature of LA NET mRNA:

NET mRNA in the LA exhibits unique features: 1) NET mRNA can be amplified in the fresh or frozen LA while in other chambers the use of frozen tissue eliminated NET mRNA, 2) chemical denervation reduced NET mRNA in the LA while other chambers were unchanged, and 3) surgical denervation increased NET mRNA from the LA while other chambers were unchanged. Further studies are needed to determine the nature of NET and its functional relevance in the LA. Of particular interest is the role of NET in modulating extrinsic sympathetic input from the stellate to cardiac intrinsic neurons and the physiological effect of catecholaminergic-phenotype neurons, that may contain NET, in the parasympathetic intrinsic ganglia.

Summary and Conclusion

This paper presents a method for isolating labile mRNA from heart and reports for the first time that NET mRNA is present in heart extract. The amount of NET mRNA is significantly lower in heart extract than in stellate ganglia suggesting that the cellular source of NET mRNA in the heart is a small proportion of the total heart extract. NET mRNA expression is higher in the atria than the ventricles and could be due to high numbers of atrial ICA cells and intrinsic cardiac neurons clustered in the atria. NET mRNA was not eliminated by sympathetic denervation thus is not present in cardiac sympathetic nerve terminals in any appreciable amounts. The primary sources of NET mRNA in heart extract are likely ICA cells throughout the myocardium and intrinsic cardiac ganglion neurons clustered in the atria. Further studies are needed to confirm localization to NET mRNA in the heart.

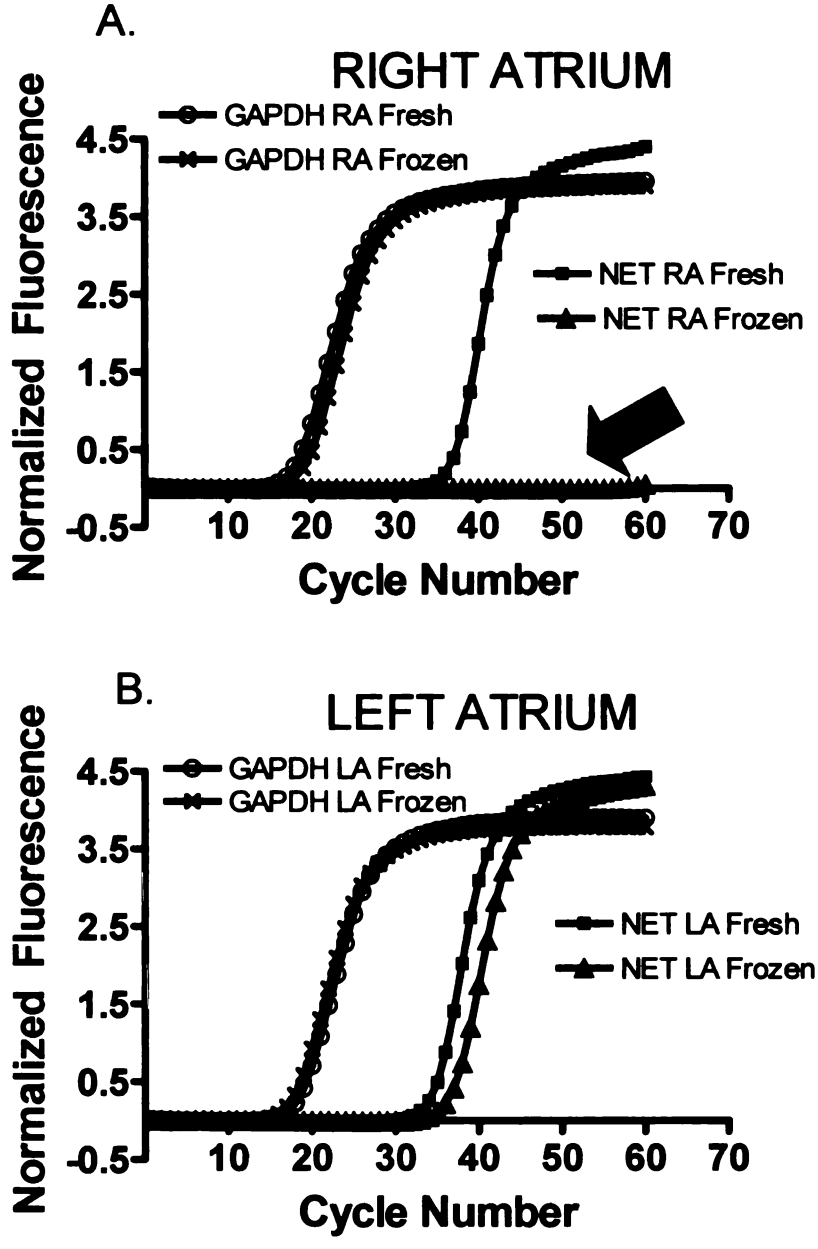

Figure 3.1: NET mRNA is amplified from fresh but not frozen heart extracts. qPCR amplification plots for NET and GAPDH from extracts of fresh and frozen heart chambers (□: GAPDH fresh tissue, Δ: GAPDH frozen tissue, ■: NET fresh tissue, ▲: NET frozen tissue). Representative raw amplification plots were normalized to ROX dye: A) right atrium, B) left atrium, C) right ventricle, and D) left ventricle. GAPDH amplification profiles were similar in fresh and frozen extracts. NET is not amplified from frozen RA, RV and LV as indicated by an arrow and the flat plot (▲) at baseline, but is amplified from fresh samples (■). D) NET from the LA can be amplified from extracts of both fresh and frozen hearts.

Figure 3.1 (continued)

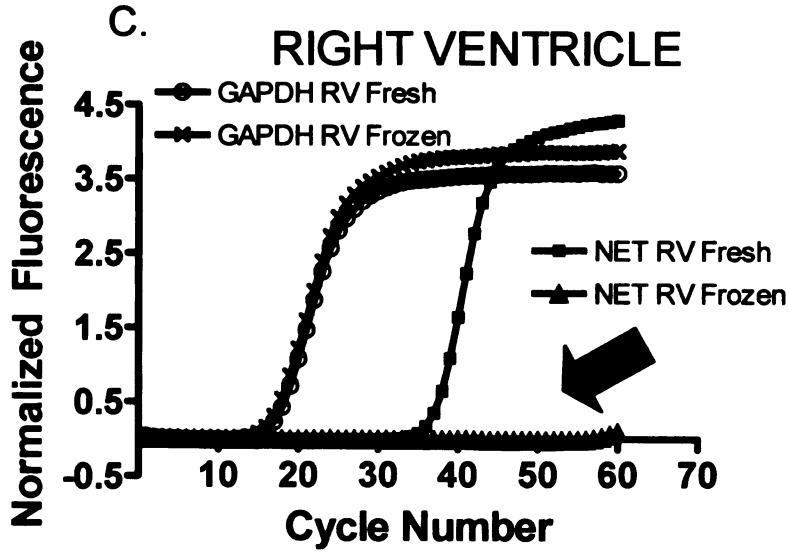

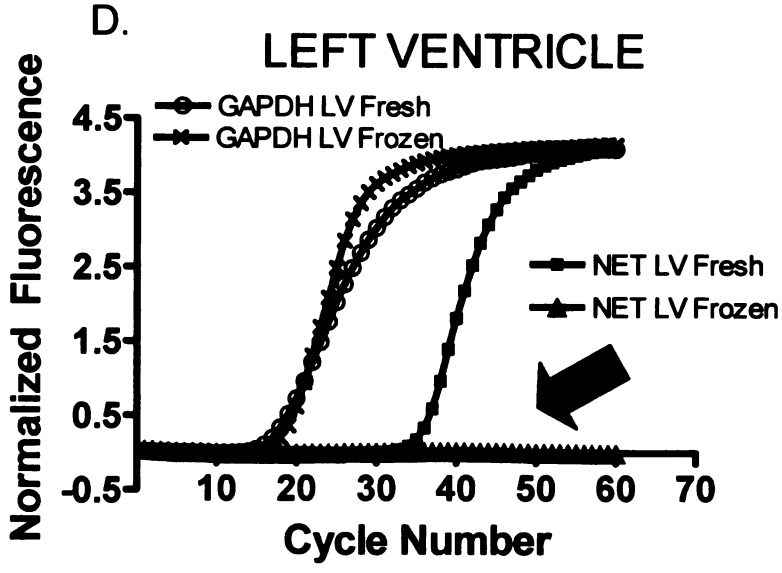

Figure 3.2: NET mRNA is present in all heart chambers, stellate ganglia, and adrenal gland. The RT-PCR amplified NET signal was present in all tissues analyzed and is visualized at 200 base pairs (bp) on a 2% agarose gel using ethidium bromide for band visualization (from left to right, adrenal gland (AG), stellate ganglia (St), right atrium (RA), left atrium (LA), right ventricle (RV), and left ventricle (LV)). Beta-actin was used as a loading control and is shown as a band at 500 bp on the right side of the gel. A no template control (NTC) for each primer and no reverse transcriptase enzyme control (no RT) for each sample was run to confirm purity of reagents and lack of DNA contamination. The NET NTC is shown at the far right. PCR was run for 40 cycles of amplification using 4 μg of starting RNA.

A.

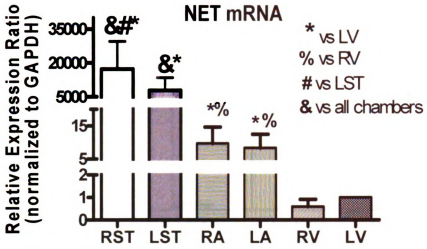

B.

Tissue	Mean NET Ct	NET Ct SE	Mean GAPDH Ct	GAPDH Ct SE	N
Right Stellate	22.46	± 0.38	18.53	± 0.42	6
Left Stellate	21.68	± 0.49	16.58	± 0.34	4
Right Atria	31.53	± 0.59	15.48	± 0.47	4
Left Atria	31.64	± 0.56	15.49	± 0.35	6
Right Ventricle	33.95	± 0.26	15.17	± 0.91	4
Left Ventricle	33.63	± 0.30	14.79	± 0.29	5

Figure 3.3: NET mRNA expression in stellate ganglia and heart chambers using qPCR. A) Graphical representation of the fold differences of NET mRNA relative to left ventricle (LV, equal 1) in right stellate ganglion (RST), left stellate ganglion (LST), right atrium (RA), left atrium (LA), right ventricle (RV). Ct values from qPCR and efficiencies of primers were used together to calculate relative expression ratio between control and sample gene expression. Standard error of fold difference was determined using Taylor's series. REST® 384 software was used with 2000 pair-wise randomizations to determine statistical significance. * $p<0.05$ vs LV; % $p<0.05$ vs RV; # $p<0.05$ vs LST; & $p<0.05$ vs all heart chambers. B) Descriptive statistics from REST® 384 analysis of NET mRNA. Data for NET and GAPDH are shown as average cycle threshold of amplification of each gene along with standard error of cycle threshold and sample size.

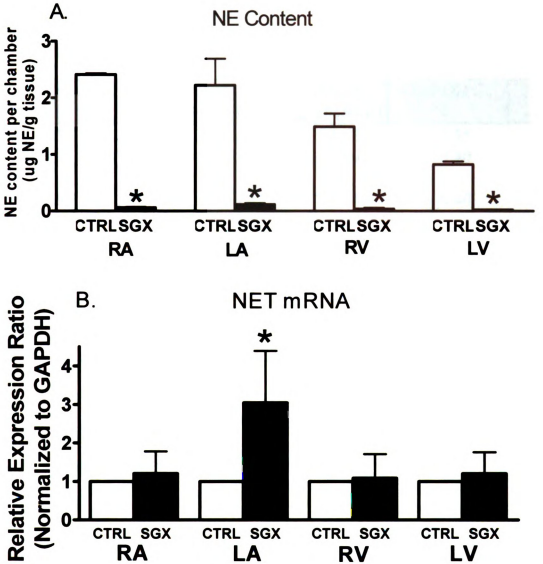

Figure 3.4: Stellate ganglionectomy depletes NE but does not reduce NET mRNA in heart chambers. A) NE was depleted in all heart chambers (RA: right atrium; LA: left atrium; RV: right ventricle; LV: left ventricle) following bilateral stellate ganglionectomy. NE was measured by capillary electrophoresis and is reported as µg/g tissue. Significance was determined between control (CTRL) and ganglionectomized (SGX) using ANOVA. B) NET mRNA is unchanged in three of four heart chambers as determined by qPCR. The LA NET mRNA was significantly increased. Data are shown as relative expression ratio using GAPDH as a control gene. For each chamber, the control average is set to one and the denervated is analyzed compared to control. Calculations of fold change and significance were run separately for each chamber using pair-wise randomization on REST® 384 software. Control and denervated samples from each chamber were run together on the same qPCR plate. C) Descriptive statistics from REST® 384 analysis of NET mRNA.

Figure 3.4 continued

C. Descriptive statistics for qPCR

Tissue	Mean NET Ct	NET Ct SE	Mean GAPDH Ct	GAPDH Ct SE	N
RA CTRL	33.62	± 0.40	14.62	± 0.35	3
RA SGX	33.41	± 0.15	14.69	± 0.40	4
LA CTRL	32.91	± 0.19	15.64	± 0.40	4
LA SGX	31.13	± 0.20	15.47	± 0.42	5
RV CTRL	34.74	± 0.63	14.94	± 0.35	3
RV SGX	35.37	± 0.18	15.69	± 0.40	4
LV CTRL	36.45	± 0.22	16.69	± 0.30	7
LV SGX	35.96	± 0.35	16.48	± 0.46	4

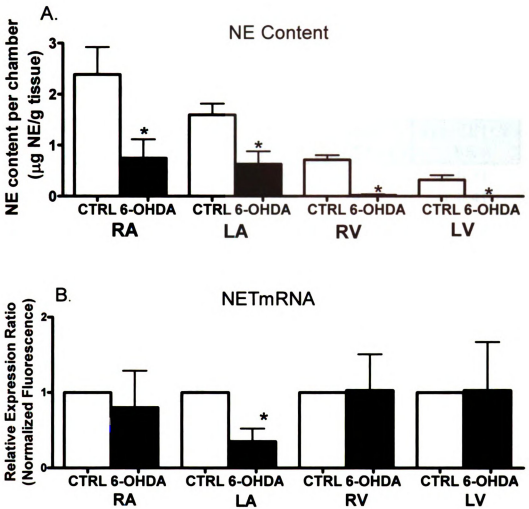

Figure 3.5: Chemical denervation with 6-hydroxydopamine depletes NE, but does not reduce NET mRNA from heart chambers. A) NE was depleted in all heart chambers (RA: right atrium; LA: left atrium; RV: right ventricle; LV: left ventricle) following chemical denervation. NE was measured by capillary electrophoresis and is reported as µg/g tissue. Significance was determined between control (CTRL) and denervated (6-OHDA) for each separate chamber using ANOVA. B) NET mRNA was unchanged in three of four heart chambers as determined by qPCR. The LA NET mRNA is significantly reduced. Data are shown as relative expression ratio using GAPDH as a control gene. For each chamber, the control average is set to one and the denervated is analyzed compared to control. Calculations of fold change and significance were run separately for each chamber using randomization and standard error from the REST® 384 software. Control and denervated samples from each chamber were run together on the same qPCR plate. C) Descriptive statistics from REST® 384 analysis.

Figure 3.5 continued

C. Descriptive statistics for qPCR

Tissue	Mean NET Ct	NET Ct SE	Mean GAPDH Ct	GAPDH Ct SE	N
RA CTRL	33.48	± 0.37	14.49	± 0.51	5
RA 6OHDA	33.55	± 0.48	14.25	± 0.41	4
LA CTRL	32.72	± 0.38	15.17	± 0.39	5
LA 6OHDA	34.42	± 0.35	15.34	± 0.33	5
RV CTRL	35.35	± 0.45	15.23	± 0.35	6
RV 6OHDA	36.08	± 0.23	16.00	± 0.29	3
LV CTRL	33.76	± 0.83	14.56	± 0.41	6
LV 6OHDA	33.86	± 0.54	14.36	± 0.63	3

Primer Name	Primer Sequence
RT-PCR NET Forward	5'-TCC TCA TTG CCC TCT ATG TTG-3'
RT-PCR NET Reverse	5'-CGG TGT GAA CTT GTA TTT GGA-3'
qPCR NET Forward	5'-GCC TGA TGG TCG TTA TCG TT-3'
qPCR NET Reverse	5'-CAT GAA CCA GGA GCA CAA AG-3'
Sequencing NET Forward	5'-TCC TCA TTG CCC TCT ATG TTG-3'
Sequencing NET Reverse	5'-CGG TGT GAA CTT GTA TTT GGA-3'
RT-PCR Actin Forward	5'-TAC TCC TGC TTG CTG ATC CAC -3'
RT-PCR Actin Reverse	5'-GGC TAC AGC TTC ACC ACC AC -3'
qPCR GAPDH Forward	5'-ATC ACT GCC ACT CAG AAG-3'
qPCR GAPDH Reverse	5'-AAG TCA CAG GAG ACA ACC -3'

Table 3.1: Primer sequences RT-PCR, real time PCR (qPCR), and cDNA sequencing for NET, GAPDH, and Actin. Primers were designed using Primer 3® software. All sequences are shown 5' to 3'.

Reference List

1. **Amara SG, Sonders MS, Zahniser NR, Povlock SL and Daniels GM**. Molecular physiology and regulation of catecholamine transporters. *Adv Pharmacol* 42: 164-168, 1998.

2. **Armour JA**. *Neurocardiology Anatomical and Functional Principals*. 2003.

3. **Armour JA**. Cardiac neuronal hierarchy in health and disease. *Am J Physiol Regul Integr Comp Physiol* 287: R262-R271, 2004.

4. **Backs J, Bresch E, Lutz M, Kristen AV and Haass M**. Endothelin-1 inhibits the neuronal norepinephrine transporter in hearts of male rats. *Cardiovasc Res* 67: 283-290, 2005.

5. **Backs J, Haunstetter A, Gerber SH, Metz J, Borst MM, Strasser RH, Kubler W and Haass M**. The neuronal norepinephrine transporter in experimental heart failure: evidence for a posttranscriptional downregulation. *J Mol Cell Cardiol* 33: 461-472, 2001.

6. **Baluk P and Gabella G**. Some parasympathetic neurons in the guinea-pig heart express aspects of the catecholaminergic phenotype in vivo. *Cell Tissue Res* 261: 275-285, 1990.

7. **Bell C and McLachlan EM**. Dependence of deoxycorticosterone/salt hypertension in the rat on the activity of adrenergic cardiac nerves. *Clin Sci (Lond)* 57: 203-210, 1979.

8. **Campenot RB and Eng H**. Protein synthesis in axons and its possible functions. *J Neurocytol* 29: 793-798, 2000.

9. **Carson RP, Diedrich A and Robertson DM**. Autonomic control after blockade of the norepinephrine transporter: a model of orthostatic intolerance. *J Appl Physiol* 93: 2192-2198, 2002.

10. **Cvacka J, Quaiserova V, Park J, Show Y, Muck A, Jr. and Swain GM**. Boron-doped diamond microelectrodes for use in capillary electrophoresis with electrochemical detection. *Anal Chem* 75: 2678-2687, 2003.

11. **Dawson R, Jr. and Meldrum MJ**. Norepinephrine content in cardiovascular tissues from the aged Fischer 344 rat. *Gerontology* 38: 185-191, 1992.

12. **de Champlain J**. Degeneration and regrowth of adrenergic nerve fibers in the rat peripheral tissues after 6-hydroxydopamine. *Can J Physiol Pharmacol* 49: 345-355, 1971.

13. **de Champlain J, Krakoff LR and Axelrod J**. A reduction in the accumulation of H3-norepinephrine in experimental hypertension. *Life Sci* 5: 2283-2291, 1966.

14. **Eisenhofer G, Friberg P, Rundqvist B, Quyyumi AA, Lambert G, Kaye DM, Kopin IJ, Goldstein DS and Esler MD**. Cardiac sympathetic nerve function in congestive heart failure. *Circulation* 93: 1667-1676, 1996.

15. **Garneau NL, Wilusz J and Wilusz CJ**. The highways and byways of mRNA decay. *Nat Rev Mol Cell Biol* 8: 113-126, 2007.

16. **Goldman H and Jacobowitz D**. Correlation of norepinephrine content with observations of adrenergic nerves after a single dose of 6-hydroxydopamine in the rat. *J Pharmacol Exp Ther* 176: 119-133, 1971.

17. **Goldstein DS, Holmes C, Frank SM, Dendi R, Cannon RO, III, Sharabi Y, Esler MD and Eisenhofer G**. Cardiac sympathetic dysautonomia in chronic orthostatic intolerance syndromes. *Circulation* 106: 2358-2365, 2002.

18. **Habecker BA, Grygielko ET, Huhtala TA, Foote B and Brooks VL**. Ganglionic tyrosine hydroxylase and norepinephrine transporter are decreased by increased sodium chloride in vivo and in vitro. *Auton Neurosci* 107: 85-98, 2003.

19. **Habecker BA, Klein MG, Cox BC and Packard BA**. Norepinephrine transporter expression in cholinergic sympathetic neurons: differential regulation of membrane and vesicular transporters. *Dev Biol* 220: 85-96, 2000.

20. **Hertting G and Axelrod J**. Fate of tritiated noradrenaline at the sympathetic nerve-endings. *Nature* 192: 172-173, 1961.

21. **Hertting G, Axelrod J, Kopin IJ and Whitby LG**. Lack of uptake of catecholamines after chronic denervation of sympathetic nerves. *Nature* 189: 66, 1961.

22. **Hertting G and Schiefthaler T**. The effect of stellate ganglion excision on the catecholamine content and the uptake of H3-norepinephrine in the heart of the cat. *Int J Neuropharmacol* 3: 65-69, 1964.

23. **Huang MH, Bahl JJ, Wu Y, Hu F, Larson DF, Roeske WR and Ewy GA**. Neuroendocrine properties of intrinsic cardiac adrenergic cells in fetal rat heart. *Am J Physiol Heart Circ Physiol* 288: H497-H503, 2005.

24. **Huang MH, Friend DS, Sunday ME, Singh K, Haley K, Austen KF, Kelly RA and Smith TW**. An intrinsic adrenergic system in mammalian heart. *J Clin Invest* 98: 1298-1303, 1996.

25. **Julius S and Valentini M**. Consequences of the increased autonomic nervous drive in hypertension, heart failure and diabetes. *Blood Press* Suppl 3: 5-13, 1998.

26. **Kawamura K, Ando K and Takebayashi S**. Perivascular innervation of the mesenteric artery in spontaneously hypertensive rats. *Hypertension* 14: 660-665, 1989.

27. **Kopin IJ, Rundqvist B, Friberg P, Lenders J, Goldstein DS and Eisenhofer G**. Different relationships of spillover to release of norepinephrine in human heart, kidneys, and forearm. *Am J Physiol* 275: R165-R173, 1998.

28. **Kostrzewa RM and Jacobowitz DM**. Pharmacological actions of 6-hydroxydopamine. *Pharmacol Rev* 26: 199-288, 1974.

29. **Kreusser MM, Haass M, Buss SJ, Hardt SE, Gerber SH, Kinscherf R, Katus HA and Backs J**. Injection of nerve growth factor into stellate ganglia improves norepinephrine reuptake into failing hearts. *Hypertension* 47: 209-215, 2006.

30. **Lee SK and Hollenbeck PJ**. Organization and translation of mRNA in sympathetic axons. *J Cell Sci* 116: 4467-4478, 2003.

31. **Li H, Ma SK, Hu XP, Zhang GY and Fei J**. Norepinephrine transporter (NET) is expressed in cardiac sympathetic ganglia of adult rat. *Cell Res* 11: 317-320, 2001.

32. **Li W, Knowlton D, Van Winkle DM and Habecker BA**. Infarction alters both the distribution and noradrenergic properties of cardiac sympathetic neurons. *Am J Physiol Heart Circ Physiol* 286: H2229-H2236, 2004.

33. **Mancia G, Grassi G, Giannattasio C and Seravalle G**. Sympathetic activation in the pathogenesis of hypertension and progression of organ damage. *Hypertension* 34: 724-728, 1999.

34. **Melia KR, Trembleau A, Oddi R, Sanna PP and Bloom FE**. Detection and regulation of tyrosine hydroxylase mRNA in catecholaminergic terminal fields: possible axonal compartmentalization. *Exp Neurol* 130: 394-406, 1994.

35. **Mohr E and Richter D**. Axonal mRNAs: functional significance in vertebrates and invertebrates. *J Neurocytol* 29: 783-791, 2000.

36. **Muna GW, Quaiserova-Mocko V and Swain GM**. Chlorinated phenol analysis using off-line solid-phase extraction and capillary electrophoresis coupled with amperometric detection and a boron-doped diamond microelectrode. *Anal Chem* 77: 6542-6548, 2005.

37. **Munch G, Rosport K, Bultmann A, Baumgartner C, Li Z, Laacke L and Ungerer M**. Cardiac overexpression of the norepinephrine transporter uptake-1 results in marked improvement of heart failure. *Circ Res* 97: 928-936, 2005.

38. **Nishimura M, Sato K, Shimada S and Tohyama M**. Expression of norepinephrine and serotonin transporter mRNAs in the rat superior cervical ganglion. *Brain Res Mol Brain Res* 67: 82-86, 1999.

39. **Novotny M, Quaiserova-Mocko V, Wehrwein EA, Kreulen DL and Swain GM**. Determination of endogenous norepinephrine levels in different chambers of the rat heart by capillary electrophoresis coupled with amperometric detection. *J Neurosci Methods* 163: 52-59, 2007.

40. **Pardini BJ, Lund DD and Schmid PG**. Organization of the sympathetic postganglionic innervation of the rat heart. *J Auton Nerv Syst* 28: 193-201, 1989.

41. **Pardini BJ, Lund DD and Schmid PG**. Innervation patterns of the middle cervical--stellate ganglion complex in the rat. *Neurosci Lett* 117: 300-306, 1990.

42. **Patel KP, Zhang K and Carmines PK**. Norepinephrine turnover in peripheral tissues of rats with heart failure. *Am J Physiol Regul Integr Comp Physiol* 278: R556-R562, 2000.

43. **Pfaffl MW, Horgan GW and Dempfle L**. Relative expression software tool (REST) for group-wise comparison and statistical analysis of relative expression results in real-time PCR. *Nucleic Acids Res* 30: e36, 2002.

44. **Qin F, Vulapalli RS, Stevens SY and Liang CS**. Loss of cardiac sympathetic neurotransmitters in heart failure and NE infusion is associated with reduced NGF. *Am J Physiol Heart Circ Physiol* 282: H363-H371, 2002.

45. **Robertson DM, Shannon JR, Biaggioni I, Ertl AC, Diedrich A, Carson R, Furlan R, Jacob G and Jordan J**. Orthostatic intolerance and the postural tachycardia syndrome: genetic and environment pathophysiologies. Neurolab Autonomic Team. *Pflugers Arch* 441: R48-R51, 2000.

46. **Rumantir MS, Kaye DM, Jennings GL, Vaz M, Hastings JA and Esler MD**. Phenotypic evidence of faulty neuronal norepinephrine reuptake in essential hypertension. *Hypertension* 36: 824-829, 2000.

47. **Sachs C and Jonsson G**. Mechanisms of action of 6-hydroxydopamine. *Biochem Pharmacol* 24: 1-8, 1975.

48. **Schlaich MP, Lambert E, Kaye DM, Krozowski Z, Campbell DJ, Lambert G, Hastings J, Aggarwal A and Esler MD**. Sympathetic augmentation in hypertension: role of nerve firing, norepinephrine reuptake, and Angiotensin neuromodulation. *Hypertension* 43: 169-175, 2004.

49. **Schroeder C, Tank J, Boschmann M, Diedrich A, Sharma AM, Biaggioni I, Luft FC and Jordan J**. Selective norepinephrine reuptake

inhibition as a human model of orthostatic intolerance. *Circulation* 105: 347-353, 2002.

50. **Schroeter S, Apparsundaram S, Wiley RG, Miner LH, Sesack SR and Blakely RD**. Immunolocalization of the cocaine- and antidepressant-sensitive l- norepinephrine transporter. *J Comp Neurol* 420: 211-232, 2000.

51. **Shannon JR, Flattem NL, Jordan J, Jacob G, Black BK, Biaggioni I, Blakely RD and Robertson DM**. Orthostatic intolerance and tachycardia associated with norepinephrine- transporter deficiency. *N Engl J Med* 342: 541-549, 2000.

52. **Singh S, Johnson PI, Javed A, Gray TS, Lonchyna VA and Wurster RD**. Monoamine- and histamine-synthesizing enzymes and neurotransmitters within neurons of adult human cardiac ganglia. *Circulation* 99: 411-419, 1999.

53. **Thoenen H and Tranzer JP**. Chemical sympathectomy by selective destruction of adrenergic nerve endings with 6-Hydroxydopamine. *Naunyn Schmiedebergs Arch Exp Pathol Pharmakol* 261: 271-288, 1968.

54. **Thoenen H and Tranzer JP**. The pharmacology of 6-hydroxydopamine. *Annu Rev Pharmacol* 13: 169-180, 1973.

55. **Ungerer M, Chlistalla A and Richardt G**. Upregulation of cardiac uptake 1 carrier in ischemic and nonischemic rat heart. *Circ Res* 78: 1037-1043, 1996.

56. **Zahniser NR and Doolen S**. Chronic and acute regulation of Na+/Cl- -dependent neurotransmitter transporters: drugs, substrates, presynaptic receptors, and signaling systems. *Pharmacol Ther* 92: 21-55, 2001.

57. **Zheng JQ, Kelly TK, Chang B, Ryazantsev S, Rajasekaran AK, Martin KC and Twiss JL**. A functional role for intra-axonal protein synthesis during axonal regeneration from adult sensory neurons. *J Neurosci* 21: 9291-9303, 2001.

CHAPTER 4: CARDIAC NOREPINEPHRINE TRANSPORTER PROTEIN EXPRESSION IS INVERSELY CORRELATED TO CHAMBER NOREPINEPHRINE CONTENT

Abstract

The cardiac neuronal norepinephrine (NE) transporter (NET) in sympathetic nerve fibers is responsible for uptake of released NE from the neuroeffector junction. Since sympathetic innervation density is highest in the atria, we predicted that NET protein expression would be highest in the atria; however, the ventricles have a greater uptake capacity for NE than the atria indicating that there is a ventricular predominance of NET protein. Therefore, the purpose of this study was to assess chamber distribution of cardiac NET protein and establish if there was a positive correlation of NE content to NET protein amount. NET distribution was also determined in the bilateral stellate ganglia that innervate the heart. Three molecular weight variants of NET protein (80kD, 54kD, and 46kD) exist in the heart and stellate ganglia. Using two methods to measure NET protein, we determined that NET was present in higher amounts in the ventricles than the atria. Even though NET was visualized in sympathetic nerve fibers along with tyrosine hydroxylase, a significant negative correlation of NET to NE content per chamber was observed. NE content is lowest in the ventricles where NET protein is high, while the atria contain high NE and low NET. The neurotoxin 6-hydroxydopamine, a NET substrate, reduced NE content more in the ventricles than the atria demonstrating functional significance of high ventricular NET protein. In summary, there is a ventricular predominance of NET

protein that corresponds to a high NE reuptake capacity in the ventricles, yet does negatively correlates to tissue NE content.

Introduction

Norepinephrine (NE) released from cardiac sympathetic nerve terminals is removed from the neuroeffector junction by the neuronal NE transporter (NET). NET is in sympathetic nerve fibers of the heart (2; 15; 35) and is enriched in nerve varicosities (55; 56). NET in sympathetic fibers is critical for removal of extracellular NE in the heart and reuptake function is reduced in sympathetically denervated animals (2; 19; 24). There are numerous studies that indicate the presence of NET in the heart and altered reuptake in the diseased heart (12; 13; 15; 18; 35). From whole organ NE reuptake studies, it is known that neuronal reuptake in the heart is highly efficient, it is estimated that ~90% of released NE is cleared from the neuroeffector junction by NET (14; 15). There is approximately a 20:1 ratio of released NE to NE "spillover", in which only ~one out of twenty molecules of released NE is lost to the plasma (30). However, these studies do not address any chamber specific differences in NE uptake capacity. It has been shown that the ventricles have a greater NE uptake capacity then the atria (20) and there are also regional differences in reuptake within a single heart chamber (3; 9).

NET (also known as solute carrier family (SLC) 6A2) is a plasma membrane protein that contains twelve membrane spanning domains and belongs to the large gene family of Na^+/Cl^- dependent neurotransmitter

transporters (7; 8; 49). NET has a large extracellular loop between transmembrane domains three and four, which contains a variable number of glycosylation sites (67). Based on the level of glycosylation there are three molecular weight variants of NET in transfected cells: a fully glycosylated 80kD, a partially glycosylated 54kD, and a 46kD core protein (5; 42; 43; 46). Inhibition of N-glycosylation of NET reduces substrate transport and radioligand binding (43). The 80 kD NET protein is the mature functional protein enriched in the plasma membrane (42; 43). The 54kD and 46kD NET variants reach the cell membrane to a lesser extent than the 80kD form. The 46kD NET has reduced transport capacity and is relatively unstable (43). Recently, Parrish *et al* reported for the first report that this same complement of three NET variants exists in rat heart (51).

The cardiac sympathetic axons and nerve terminals containing NET originate in the cell bodies of the bilateral stellate ganglia. The cardiac targets of stellate axons are the sinoatrial node, the conducting system, cardiomyocytes, and coronary vessels (61). In the rat, all heart chambers receive bilateral innervation from the right and left stellate ganglia; however, the majority of the rat right ventricular innervation arises in the left stellate ganglion and there is substantial ipsilateral innervation to the atrial appendages (50). Bilateral stellate ganglionectomy in the rat reduces cardiac NE content by 89-100% (50). It is unknown if NET protein expression is different in the right versus left stellate ganglia, but NET mRNA is expressed at higher levels in the right stellate ganglion (34).

Although NET is found in sympathetic fibers, it is not known if the amount of NET protein is proportional to the sympathetic innervation density of the heart chambers. The atria are highly innervated by the sympathetic nervous system (28) and contain high levels of NE (47); therefore it is likely that the atria contain more NET than the less densely innervated ventricles. This idea is supported by the work of Lee *et al* which showed that NET binding sites are reduced when NE is depleted with reserpine, while NET binding is increased when NE levels are raised by treatment with monoamine oxidase inhibitors (32). This is true for other transmitter systems as well. Acetylcholine release influences the uptake of choline by neurons such that an increase in cholinergic activity and acetylcholine release is coupled to an increase in choline uptake and vice versa (25). Taken together, we hypothesized that a positive correlation would exist between NET and NE with high levels of NET corresponding to the high innervation density in the atria. The purpose of this study was to assess regional expression of NET protein in stellate ganglia and heart chambers, and determine if NET protein expression correlated to cardiac sympathetic innervation density.

Materials and Methods

Animals

Adult male, Sprague-Dawley rats, 8 weeks old (250-275 g, Charles River, Portage, MI) were used. All animal experiments were performed in accordance with the "Guide for the Care and Usage of Laboratory Animals" (National

Research Council) and were approved by the Animal Use and Care Committee of Michigan State University. Animals were housed two per cage in temperature and humidity-controlled rooms with a 12 hour/12 hour light-dark cycle. Standard pellet rat chow and water were given *ad libitum*. For the denervation study, the animals were randomly divided into control (untreated) and denervated group (see details below).

6-hydroxydopamine denervation procedure

The neurotoxin 6-hydroxydopamine hydrochloride (6-OHDA, St. Louis, MO) was used as a NET substrate (31; 54; 60) to selectively impair sympathetic nerve terminals and functionally denervate the treated group by depleting NE. 6-OHDA was prepared in a mixture of 0.9 % (154 mM) sodium chloride and 0.5 % (28.4 mM) ascorbic acid solution fresh before each administration and kept protected from light. A subcutaneous injection of 6-OHDA (250 mg/kg) was administered to the loose skin between the shoulder blades with three consecutive injections during one week on day one, three and five. On day seven, two days after the final dose, the animals were sacrificed. Age- and sex-matched control animals were untreated.

Tissue collection

Rats were anesthetized with a lethal dose of sodium pentobarbital (Sigma-Aldrich Corp, St. Louis, MO, 65 mg/kg, intra-peritoneal) followed by thoracotomy. Hearts were removed quickly and immediately placed into chilled (4 °C) phosphate

buffered saline (PBS, 137 mM sodium chloride, 2.7 mM potassium chloride, 4.3 mM sodium phosphate dibasic and 1.4 mM potassium phosphate monobasic) for separation of chambers. While in buffer, the chambers were quickly separated in the following order: right atrium, left atrium, right ventricle outer wall, ventricular septal wall, and left ventricle outer wall. The dissected heart chambers were frozen immediately by contact with dry ice and stored at -80 °C until further processing.

Tissue processing for western blotting

Frozen heart chambers were pulverized on dry ice and then transferred to a mortar and pestle that had been pre-chilled with liquid nitrogen. Tissue was further processed by grinding, then suspended in the appropriate amount of homogenization buffer (10mM HEPES (Sigma, St. Louis, MO), 0.15M NaCl (VWR, West Chester, PA), 1mM EDTA (Sigma, St. Louis, MO), 1mM phenol methane sulfanyl fluoride (PMSF, Roche, Indianapolis, IN), 1μg/ml leupeptin (Roche, Indianapolis, IN), and 1μg/ml aprotinin (Roche, Indianapolis, IN), amount per tissue). The suspended tissue was then homogenized using a variable speed Omni TH-115 homogenizer with 5mm saw tooth generator probe (Omni International Inc., Warrenton, VA) for ~30 seconds at high speed. Finally, the processed tissue in solution was transferred to a 10 ml glass hand-held homogenizer for 10 strokes of further processing. The homogenate was centrifuged (Sorvall RC 5B Plus) at 700xg for 5 min at 4°C to remove nuclei and cellular debris, assessed in triplicate for protein concentration using a modified

Bradford protein assay (Bio-Rad, Hercules, CA), and the supernatant containing total protein was frozen until use at -80ºC.

Western blotting

Standard western blotting was performed. Samples containing 50μg protein were prepared, loaded into 4% stacking gel/10% resolving gels and run at 100 V for ~90 minutes until the leading edge of samples traveled to the bottom of gel. All heart chambers from an animal were run on the same gel to ensure accurate comparison across chambers. Transfer to polyvinylidene fluoride (PVDF) membranes (Bio-Rad, Hercules, CA) was performed at a constant voltage of 100 V at 4°C for 60 minutes. The membranes were blocked with 5% non-fat dry milk in PBS containing 0.1% Tween-20 for one hour with shaking at room temperature. Membranes were then incubated overnight at 4°C with rabbit anti-rat NET 11-A primary antibody (Alpha Diagnostics Intl Inc, San Antonio, TX) diluted 1:250 in 5% milk solution. The primary antibody was prepared fresh and was not reused. The membranes were rinsed with PBS containing 0.1% Tween-20 and incubated for one hour at room temperature with anti-rabbit IgG horseradish peroxidase (HRP) secondary antibody (Santa Cruz Biotech, Santa Cruz, CA) diluted 1:2000 in 5% milk solution. Immunoreactivity was detected using Femto® chemiluminescence kit (Pierce Chemical, Rockford, IL) to visualize bands. The membrane was imaged using Syngene ChemiGenius Gel Documentation System with GeneSnap software and was quantified using GeneTools software (Syngene, Frederick, MD). All membranes were counter-

stained with Coomassie Blue (Invitrogen, Carlsbad, CA) to verify equal protein loading. Data were normalized for protein loading using Coomassie Blue staining. Data are expressed as arbitrary density units normalized for protein loading. Total NET was calculated as the sum of the normalized densities of all three molecular weight variants per chamber.

Immunohistochemistry

Whole mount atria immunolocalization: After the hearts were removed the left and right atria were dissected and rinsed to remove blood. Each atrium was fixed as a whole mount using Zamboni's fixative (59) for 20 minutes at room temperature. Fixed atria were washed in PBS and incubated for 24 hours (4°C) with antibody in PBS containing 1% bovine serum albumin (BSA) and 0.3% Triton X-100. Antibodies used were rabbit anti-NET 411(55) (courtesy of RD Blakely, Vanderbilt University) and mouse anti-tyrosine hydroxylase (TH) (1:250) (Chemicon, Temecula, CA) and rabbit anti-TH (1:500) (Chemicon, Temecula, CA) After 24 hours, atria were washed in PBS (3 x 5 minutes) followed by incubation for 2 hours (25°C) in secondary antibody (goat anti-mouse IgG conjugated to AlexaFluor 488 (Molecular Probes, Carlsbad, California) 1:1000 dilution in PBS containing BSA (1%) and Triton (0.3%) and goat anti-rabbit IgG conjugated to AlexaFluor 594 (Molecular Probes, Carlsbad, California) 1:1000 dilution in PBS containing BSA (1%) and Triton (0.3%). Atria were washed 3 x 5 minutes in PBS and were mounted on slides and viewed using a confocal microscope (Zeiss LSM 510). Filter settings for Alexa Fluor 488 were bandpass

505-530 and Alexa Fluor 594 were bandpass 585-615. Samples were optically sectioned in 2 μm slices and then digitally reconstructed to attain a projection encompassing multiple layers of the tissue.

Ganglia immunohistochemistry: Stellate ganglia were fixed in 10% neutral buffered formalin for 2 hours then transferred to 70% ethanol, routinely processed, embedded in paraffin and sectioned on a rotary microtome at 5μM. Sections were placed on slides coated with 2% 3-Aminopropyltriethoxysilane, dried at 56°C overnight then deparaffinized in Xylene and hydrated through descending grades of ethyl alcohol to distilled water. After incubation in Tris buffered saline (TBS, pH 7.4) for 5 minutes, slides were antigen retrieved utilizing citrate buffer pH 6.0 (Biogenex, San Ramon CA) in a vegetable steamer (Oster, Boca Raton FL) for 30 minutes at 100°C, allowed to cool on the counter at room temperature for 10 minutes and rinsed in several changes of distilled water. Endogenous peroxidase was blocked utilizing 3% hydrogen peroxide for 30 minutes followed by running tap and distilled water rinses. Standard avidin-biotin complex staining steps were performed at room temperature on the DAKO Autostainer. After blocking with normal goat serum for 30 minutes, slides were incubated 15 minutes each in avidin D (Vector, Burlingame CA) and d-biotin (Sigma, St. Louis MO) to block endogenous avidin and biotin. Slides were then rinsed in several changes of TBS + Tween 20 (TBS-T), incubated for 60 minutes at room temperature with the polyclonal primary antibody NET 48411 (1:250 in Scytek normal antibody diluent (Scytek, Logan, UT)). Slides were then rinsed in

several changes of TBS-T then incubated in biotinylated goat anti-rabbit IgG H+L (Vector, Burlingame CA) in normal antibody diluent 1:200 for 30 minutes. Slides were rinsed in TBS-T followed by the application of Vectastain® Elite ABC Reagent (Vector, Burlingame CA) for 30 minutes. The slides were rinsed with TBS-T and developed using Nova Red Peroxidase substrate kit (Vector, Burlingame CA) for 15 minutes. Slides were rinsed in distilled water, counterstained using Lerner 2 hematoxylin for 1 minute, differentiated in 1% aqueous glacial acetic acid, and rinsed in running tap water then dehydrated through ascending grades of ethyl alcohol, cleared through several changes of xylene and cover slipped using Flotex (Lerner, Pittsburgh PA) permanent mounting media.

Sections of right and left stellate ganglia from an animal were mounted on the same slide for a direct comparison under the same experimental conditions. Images were viewed using standard brightfield microscopy (Olympus BX60, Center Valley, PA). NET staining in ganglia was quantified by assessing all individual neuron cell bodies in a single section of stellate ganglia using NIH Image J Version 1.37 software. The nucleus did not stain positive for NET and was not included in the determination of staining intensity. The arbitrary intensity of NET staining was determined on color inverted images by using the straight line measurement tool and drawing a line in a region defined by the user to contain cytoplasmic NET staining in every cell in a section from each ganglion. The mean intensity values in arbitrary units for individual neurons were then

averaged to determine total NET staining intensity per ganglia. Staining intensity of right stellate ganglia was compared to left stellate ganglia using a paired t-test.

Tissue norepinephrine content

Capillary electrophoresis with electrochemical detection (CE-EC) using boron-doped diamond electrode was employed for norepinephrine determination in the heart chambers. The CE-EC system, electrochemical detection cell and electrode fabrication was described elsewhere (10; 45). The protocol is similar to that described previously (47). The separation and detection was performed using following conditions: 76 cm long, 362 μm o.d., 29 μm i.d. capillary, 250 mM boric acid - 1 M potassium hydroxide run buffer of pH 8.8, separation voltage 24 kV, detection potential +0.86 V vs Ag/AgCl and electrokinetic injection at 18 kV for 8 s. Heart chamber was homogenized using a variable speed Omni TH-115 homogenizer with 5mm diameter EZ-Gen generator probe (Omni International Inc., Warrenton, VA) in ice-cold 0.1 M perchloric acid for 3 min at 35,000 rpm (2 mL/0.5 g tissue - left and right ventricles and the ventricular septum and 5 mL/0.5 g tissue - right and left atria). The homogenate was then centrifuged at 10,000 rpm for 15 min at 4°C and the supernatant was further processed by solid phase extraction (SPE) using Oasis MCX cartridges, 30 mg / 1cc (Waters, Milford, MA, USA). SPE sorbent was conditioned by 1mL of methanol and 2 mL of ultrapure water. Then, 0.7 – 1 mL of the sample supernatant was loaded onto a SPE cartridge at a flow rate < 0.5 mL/min. The sorbent was washed by 2 mL of 0.1 M hydrochloric acid and then 1 mL of methanol. The elution was accomplished from

the vacuum dried sorbent by 0.7 – 1 mL (same volume as loaded) CE run buffer at a flow rate < 0.5 mL/min. The eluate was analyzed by CE-EC.

Immunoprecipitation

Rabbit anti-rat NET primary antibody (NET 11A, Alpha Diagnostics; San Antonio, TX) or rabbit anti-actin primary antibody (Sigma; St. Louis, MO) was immobilized on to coupling gel using the Seize™ Primary Immunoprecipitation Kit (Pierce Biotechnologies; Rockford, IL). Rat heart or stellate ganglion were homogenized in HEPES buffer then denatured by adding 0.05% sodium dodecyl sulfate (SDS) solution (1:1 tissue homogenate to SDS) and heating for 5 minutes at 65°C. Denatured protein was incubated overnight at 4°C with the immobilized antibody. The coupling gel/antibody/protein complex was washed with BupH™ Tris immunoprecipitation buffer (Pierce Biotechnologies; Rockford, IL) to remove non-specific proteins. The antibody and protein were separated from the gel/antibody/protein complex by boiling (3 min, 100°C) and centrifugation. The supernatant containing protein and antibody was mixed with non-reducing SDS buffer and loaded into 4% stacking gel/10% resolving polyacrylamide gels then run at 110 V for ~90 minutes until the leading edge of samples traveled to the bottom of gel. Gels were then stained using SilverSNAP® Stain (Pierce Biotechnologies; Rockford, IL) and appropriate bands were visualized and cut from the gel for sequence analysis using mass spectrometry.

Experimental Liquid Chromatography-Tandem Mass Spectrometry (LC-MS/MS)

Gel bands were subjected to in-gel tryptic digestion (26; 58) or when applicable the coupling gel/antibody/protein complex was digested without running a gel. The extracted peptides were then automatically injected by a Waters nanoAcquity sample manager (Waters Corporation, Milford, MA, USA) and loaded for 5 minutes onto a Waters Symmetry C18 peptide trap (5µm, 180µm x 20mm) at 4µl/min in 2% Acetonitrile/0.1%Formic Acid. The bound peptides were then eluted onto a Waters BEH C18 nanoAcquity column (1.7um, 100um x 100mm) and eluted over 35 minutes with a gradient of 5% B to 90% B, 25 minutes using a Waters nanoAcquity UPLC (Buffer A = 99.9% Water/0.1% Formic Acid, Buffer B = 99.9% /0.1% Formic Acid) into a ThermoFisher LTQ mass spectrometer (Thermo Scientific, Waltham. MA, USA) equipped with a Michrom Axial Desolvation Vacuum Assisted Nano Capillary Electrospray (ADVANCE) beta nanospray source (Michrom Bioresources, Auburn, CA, USA) at a flow rate of 1µl/min. The top five ions in each survey scan were then subjected to data-dependant zoom scans followed by low energy collision-induced dissociation and the resulting MS/MS spectra are converted to peak lists using BioWorks Browser v 3.2 (Thermo Scientific, Waltham. MA, USA). The peak list data were searched against all rat protein sequence entries available from NCBI, downloaded 12-13-2007, using the Mascot® searching algorithm v2.2 (Matrix Science, Boston, MA, USA). Spectral assignments were then validated using Scaffold® (Proteome Software Inc., Portland OR, USA). Matches were

considered correct if the confidence level of the Scaffold® identification was greater than 95%. Sequencing was performed by the Michigan State University Research Technology Support Proteomics Core Facility.

[^{3}H]-Nisoxetine binding

Preparation of cardiac membranes: Frozen heart chambers were pulverized on dry ice and then transferred to a mortar and pestle that had been pre-chilled with liquid nitrogen. Tissue was further processed by grinding and then suspended in the appropriate amount of homogenization buffer without detergent to keep membranes intact (50 mM Tris pH 7.4, 120 mM NaCl, 5 mM KCl). The suspended tissue in solution was transferred to an ice cold 10 ml glass hand-held homogenizer for 10 strokes of further gentle processing in ice. For ventricular tissue, the homogenate was centrifuged (Sorvall RC 5B Plus) at 700 xg for 10 min at 4°C to remove nuclei and cellular debris, and atrial membranes were used without centrifugation. Samples were spun at 40,000 xg for 30 minutes after which the supernatant was discarded and the pellet resuspended in an additional 4 ml of buffer. A second identical spin was performed, the supernatant discarded, and the pellet stored at -80°C until use.

Binding assay: NET protein expression in cardiac membranes from individual heart chambers was estimated from B_{max} values of full saturating binding curves using [^{3}H]-Nisoxetine (Perkin-Elmer, Waltham, MA).in a manner similar to that described previously (35; 68). Frozen membrane pellets were resuspended in

ice cold incubation buffer (50mM Tris pH 7.4, 300mM NaCl, 5 mM KCl) on ice just prior to use. The resuspended membranes were loaded in quadruplicate into 96-well reaction plates and aliquots were used in parallel for a Bradford protein assay to determine protein concentration. Samples were assessed for total and background binding. Full saturating binding curves were run in duplicate using 0.37-50 nM [^{3}H]-Nisoxetine; additional duplicate wells with 1.5 mM desipramine were used to determine non-specific binding. Samples were incubated on a shaker for a minimum of 4 hours at 0° C then filtered through glass fiber filters presoaked in 0.5% polyethylenimine using a 96-well Filtermate cell harvester (Packard Biosciences, Shelton, CT, USA). Standard scintillation counting was performed using Ecolite scintillation fluid (ICN Biomedicals, Irvine CA, USA).

Data analysis

Data are presented as mean ± SEM for the number of animals. Statistical significance was assessed by a Student's t-test or One-way ANOVA were appropriate using Prism 4.0 software (GraphPad Software, San Diego, CA). Data were statistically significant if $p<0.05$.

Results

NET in sympathetic fibers

Immunohistochemical localization using confocal microscopy was performed to assess the cellular site of NET protein in the heart. NET staining in nerve fibers

in the atria is shown in red (Figure 1A). Tyrosine hydroxylase (TH) was used as a marker of sympathetic neurons and is shown in green (Figure 1B). NET/TH co-localization is shown in an overlay image (Figure 1C) in which yellow indicates regions where NET and TH are colocalized in sympathetic fibers. We determined that NET protein is found in sympathetic nerve fibers in the rat atria and sought to determine if NET protein is found in proportion to sympathetic innervation density.

Sympathetic innervation density: chamber NE content

NE tissue content is a reflection of sympathetic innervation density. Based on our findings the atria were more densely innervated than the ventricles and had a greater amount if NE per gram of tissue. NE values from heart chambers are similar to previously reported values (47): RA 2.387 μg/g tissue, LA 1.597 μg/g tissue, RV 0.713 μg/g tissue, LV 0.3567 μg/g tissue. NE content of the RA was significantly higher than all other chambers (*, $p<0.05$), while the LA was significantly higher than RV, VS, and LV (&, $p<0.05$). NE tissue content per chamber was RA>LA>RV=LV (Figure 2). We then examined NET protein level in all heart chambers to determine if there was a positive correlation of NE to NET.

NET western blotting of the heart

There are three reported molecular weight variants of NET protein in human NET transfected cell lines, yet there are differing reports of the NET variants found in

other cells types and native tissue. We assessed the NET protein profile in heart chambers to determine which variants are present. NET amount by chamber was assessed using western blotting. NET has three molecular weight variants (~80, 54, 46 kD) in all heart chambers (Figure 3). The amount of 80 kD NET was the same in all heart chambers (Figure 3A). The 54 kD form was significantly higher in ventricular septal wall (VS) and LV than in RA and LA (Figure 3B, * $p<0.05$ vs RA, # $p<0.05$ vs LA, n=5) showing a ventricular predominance of this form of NET. The 46 kD form in LV was significantly higher than RA (Figure 3C, * $p<0.05$, n=5) while there was no difference between any other chamber for this NET variant. Therefore, there are chamber differences in expression of the 54 kD and 46 kD forms of NET, while the 80 kD NET is uniformly distributed.

The relative proportion of the three molecular weight NET variants (i.e., the ratio of 80 vs 54 vs 46 kD NET) within a chamber is not uniform across the heart. In the RA and VS, the 54kD NET was significantly higher than other forms. In the RV and LV, there was an equal distribution of the three forms. The LA contained equal amounts of 80kD and 54kD, both of which were significantly greater than the 46kD NET.

Relationship of total NET protein determined by western blotting to tissue NE content

Since NET is found in sympathetic fibers (Figure 1) and the density of innervation is highest in the atria (Figure 2), we hypothesized that NET protein would be

found in proportion to chamber NE with the atria containing high levels of NE and NET. Total NET within each chamber is calculated by summing the normalized densities of western blot bands of each of the three variants (80kD+54kD+46kD=total NET). This calculation was done for each chamber separately to determine the total amount of NET protein contained within each chamber. The total amount of NET protein in chambers is variable with the ventricles containing the most and the atria containing the least (Figure 4A). The total NET content in the RV, VS, and LV is significantly greater than the RA (* $p<0.05$, n=5), and the LV total NET content is also significantly greater than the LA (# $p<0.05$, n=5).

We compared total NET protein measured by western blotting to tissue NE content in order to determine if NET was present in proportion to sympathetic innervation. If NET protein is found only in sympathetic nerves where it functions to clear released NE then NET protein expression should mirror innervation density and NE content in the heart. However, we observed a significant negative correlation between NE content and NET protein (Figure 4B, $p<0.02$, $r^2=0.95$). Therefore, the NE content is greatest in the atria, where the NET is the lowest; likewise, sympathetic innervation density and NE content is the least in the ventricles where NET is the highest.

NE depletion by 6-hydroxydopamine (6-OHDA)

To assess functional relevance of high NET expression in the ventricles, we used the neurotoxic NET substrate, 6-OHDA, to deplete NE. The atria are less affected by treatment than the ventricles. The RA and LA show a 68.5% ($n=5$, $p<0.05$) and 61.3% ($n=5$, $p<0.05$) reduction in NE content per chamber, respectively. The RV ($n=5$, $p<0.0001$), and LV ($n=5$, $p<0.0001$) were highly affected by treatment as indicated by a reduction in NE content per chamber to below the limit of detection.

Stellate ganglion western blotting

We aimed to determine if ventricular predominance of NET expression in the heart was associated with differential NET expression in stellate ganglion neurons that innervate the heart. Western blotting was used to determine that there are three molecular weight variants of NET (80, 54, and 46 kD) present in equal amounts in both the right and left stellate ganglia (Figure 5A). There was no difference in the amount of any individual molecular weight variant (Figure 5A) or total NET protein (Figure 5B) between right and left stellate ganglia. Total NET protein was determined by summing the normalized densities of all three NET variant bands observed in western blotting.

Stellate ganglia immunohistochemistry

Stellate NET protein expression level by western blotting was confirmed using immunohistochemical techniques. NET immunoreactivity (red) is present in all visible neuron cell bodies in a single section of left and right stellate ganglia

(Figure 6A and 6B). At high magnification, NET protein is visible throughout the cytoplasm of neurons of the bilateral stellate ganglion with limited membrane localization discernable (Figure 6C). NET immunoreactivity cannot distinguish between the molecular weight variants of NET thus represents total NET protein expression. Similar to western blotting, there is no difference in total NET protein between right and left stellate using quantified NET immunoreactivity (Figure 6E). Although there was unequal distribution of NET in different parts of the heart, there was no corresponding difference in NET protein in the bilateral stellate ganglia.

NET antibody validation for western blotting: NET knockout mouse heart and immunoprecipitation of NET protein for sequence analysis

Verification of the NET 11-A primary antibody used in western blotting was performed to ensure that our finding of an inverse relationship of NE to NET in heart chambers was valid. Western blotting was performed on wild type and NET knockout mouse heart on the same membrane as rat LV (Figure 7A). The three NET variants are present in all lanes, including in the NET KO heart, along with an additional band at ~30kD that has not been previously reported and is likely a breakdown product of NET containing the antigenic sequence (Figure 7A). A control peptide from the manufacturer was used to determine which bands represent specific binding of the primary antibody to its designated antigenic sequence (Figure 7B). The bands at 54kD and 30kD (shown in boxes in panels A and B) are absent in the presence of control peptide suggesting that

these bands only are specifically recognized by this NET primary antibody even though there are reports of all three variant forms (51). Therefore, although there are known NET variants that have been reported in many tissues and we can visualize all three known forms in western blotting, we were unable to validate this antibody in a manner suitable to confirm that all bands are specific to NET. This antibody recognizes the same molecular weight NET bands in the NET KO mouse heart as in wild type mouse and rat tissue and therefore raised doubt as to its specificity. We sequenced the protein bands obtained with the antibody to validate the presence of NET protein.

Further analysis of antibody specificity was performed using immunoprecipitation of heart and sympathetic ganglion protein followed by mass spectrometry sequencing. To confirm our immunoprecipitation procedure we performed a control study using heart protein with beads coupled to an antibody for actin. We were able to successfully pull-down actin protein then run a gel using immunoprecipitated protein and visualize a band at the appropriate molecular weight (Figure 8B). Mass spectrometry revealed the presence of actin sequence in the sample. Using the NET 11-A antibody for immunoprecipitation followed by gel running of bound protein, five bands (80, 65, 54, 46, and 30kD) of the approximate sizes of NET protein were visualized on silver stained gels of immunoprecipitated protein from heart (Figure 8A). These bands are the same molecular weight as those seen in western blotting for NET using the same antibody and are aligned in Figure 8B. This is strong evidence that the

immunoprecipitation protocol for the antibody was successful. Bands were individually digested and analyzed by mass spectrometry. There was no evidence of NET protein sequence in any of the bands from heart. Similarly, for immunoprecipitates of stellate ganglion protein there was no signal for peptide sequences occurring in NET.

Relationship of total NET protein determined by antagonist binding to tissue NE content

Given the aforementioned issues with validating the NET primary antibody, we wanted to use a completely independent method to quantify NET protein heart chambers. Cardiac membranes from all heart chambers were used in saturation binding assays with [^{3}H]-nisoxetine to estimate the B_{max} of NET binding sites per chamber. A representative binding curve is shown (Figure 10A). The plot shows specific binding (total binding minus non-specific binding determined by addition of despiramine). Individual B_{max} values from each sample were averaged by chamber to get mean B_{max}. There were significantly more NET binding sites in the LV than in any other heart chamber (Figure 10B; RA 221.8 ± 46.4, LA 315 ± 91.25, RV 418.2 ± 68.76, and LV 768.2 ± 128.1 fmol binding/mg tissue). Similar to western blotting, NET protein measured by antagonist binding was inversely correlated to tissue NE content and showed a pattern of ventricular predominance of NET protein. There is a significant negative correlation between NE content and NET binding (Figure 10C, $p=.04$, $r^2=0.922$). Therefore, the NE content is greatest in the atria, where the NET binding is the lowest;

likewise, sympathetic innervation density is the least in the ventricles where NET binding is the highest.

Discussion

We found that NET protein expression in the stellate ganglia did not predict a heterogeneous distribution of NET in the heart as both ganglia express the same amount of NET protein. Strikingly, even though NET protein was present in sympathetic nerve fibers co-localized to TH, the abundance of NET protein in the heart chambers was negatively correlated to NE content of each chamber (i.e., the ventricles contained the most NET and the least NE). The ventricular predominance of NET protein had functional consequence as treatment with the neurotoxin 6-OHDA, a NET substrate, (54; 60) (31) had greater effect on depletion of NE in the ventricles than the atria.

NET protein

There are three molecular weight forms of NET reported from studies of human NET transfected cell lines (42; 43). The 80 kD form is the mature fully glycosylated form enriched in surface membranes, the 54 kD is partially glycosylated intermediate, and the 46 kD is the immature core protein which is the least abundant and considered to be unstable (42; 43). In western blotting studies of PC12 cells and native tissue, reports vary on the form of NET investigated. The 80 kD form was reported in PC12 cells (38), 80 and 54 kD in human neuroblastoma cells (16), 54kD in cultured superior cervical ganglia (16),

80 and 54 kD in human NET transfected cells (56), 90, 60, and 50 kD in human NET transfected cells (46), and 80, 54, and 46 kD in heart (51). We found three forms of NET in all heart chambers and in stellate ganglia and consistent with studies in human NET transfected cells. To our knowledge, this is the first report of all three forms on NET observed in stellate ganglia; however, a recent report by Parrish et al (51) demonstrated these three forms exist in heart. Since three forms have been reported previously to exist, we show data from all forms even though there are studies that report only single NET variants. It is important to note that there are several antibodies for NET reported in the literature and therefore some differences in results of NET western blotting may exist based on the antibody used.

Protein maturation by glycosylation as described in transfected cells also takes place within native neuronal cell bodies as evident by our finding of all three forms of NET in the stellate ganglia. This indicates that the synthetic and processing machinery for NET is present in native tissue. However, it is of interest then that all three forms are also found in heart homogenate. Either all three forms are synthesized in stellate ganglion neurons and shipped via axonal transport from the cell bodies in sympathetic ganglia to nerve terminals, or that the full complement of NET synthetic machinery exists in the heart itself such that all three forms can be locally synthesized and processed in the heart in sympathetic nerve terminals or in other cell types in the heart.

The finding of all three forms of NET in the heart could be due to NET synthesis outside sympathetic axons. NET protein is present outside sympathetic axons in the heart in intrinsic cardiac adrenergic (ICA) cells, a non-neuronal cardiocyte that expresses NET protein and has NE uptake capacity (21). In the case of ICA cells, the process of glycosylation and the existence of all three NET variants is feasible since a full complement of protein processing machinery should exist in the cell. Alternatively, selected mRNAs are shipped in a regulated manner to nerve terminals where local translation occurs (33; 48). NET mRNA is present in the heart (63) thus local protein synthesis of NET within sympathetic axons and/or nerve terminals is possible. However, for axonal translation via rudimentary translational machinery it is difficult to understand how advanced protein processing such as glycosylation could occur in axons.

NET in stellate ganglia

Using multiple techniques, there was no difference in NET protein expression between the right and left stellate even though there is higher NET mRNA in the right stellate ganglia (34). Neurons in stellate ganglia stain positive for NET protein similar to expression in cultured superior cervical ganglia, brain, and adrenal gland (29; 56). The expression in stellate ganglia is largely cytoplasmic with limited membrane localization. However, in transfected HEK cells NET protein was localized in cell surface membrane (55). Cultured superior cervical ganglion cells from newborn rats have NE uptake capacity, indicating that NET can be inserted into the plasma membrane and function in native sympathetic

neuron cell bodies (18; 39; 57) (36) and presumably NET trafficking and function in stellate ganglia occurs in a similar manner .

The vast majority of stellate ganglion neurons are noradrenergic, but there is a small subset of cholinergic neurons present (1). These cholinergic neurons are found in loose clusters at the core of the ganglion and project to the sweat glands and rib periosteum (1). During development, noradrenergic neurons that innervate the sweat glands undergo a phenotypic switch to cholinergic neurons and stop expressing NET mRNA in the cell bodies and NET protein in their axons (17). Cultured superior cervical ganglion cells that are noradrenergic cease to express NET mRNA and protein when administered neurokines that induce a switch to the cholinergic phenotype (41). Together, these studies suggest that sympathetic cholinergic neurons do not express NET. We observed single sections of ganglia rather than observing all cell bodies in the entire ganglion using serial sections and observed that all cell bodies were positive for NET Presumably these single sections did not contain examples of cholinergic cell bodies that are NET-negative.

There are cell bodies in the stellate complex that are non-cardiac, which innervate the lung, or cause vasoconstriction and piloerection (44; 61). We examined the entire ganglion for mRNA and protein studies, rather than putative cardiac neurons alone. It is important to determine if the regional distribution of NET in cardiac nerve terminals is ultimately based in heterogeneity of stellate

neuron cell bodies, such that particular neurons destined for the ventricle would contain a higher amount of NET protein as compared to those neurons with an atrial target.

Relationship of NET to innervation density

As demonstrated by immunohistochemistry in this study and by others (35; 56), NET protein is found in sympathetic nerve terminals in the heart. NE content is a marker of sympathetic innervation density. The atria are highly innervated by the sympathetic nervous system (28) and contain high amounts of NE (47); therefore it is likely that the atria contain more NET than the lesser innervated ventricles. The number of NE uptake sites in brain is regulated by transmitter content (32). NET binding with [^{3}H]-desipramine is reduced when NE is depleted with reserpine, while NET sites are increased when NE levels are raised by treatment with monoamine oxidase inhibitors (32). NE and NET would be expected to change in parallel such that when there are high synaptic levels of NE, NET protein would also be high.

We hypothesized that NET protein in the heart would correlate with chamber NE content such that the atria would contain both high NE and NET. We report for the first time that there are differences in protein distribution of NET among heart chambers. Our measurements of NE content in the myocardium fit with previous findings that the sympathetic innervation density and NE content is greatest in the atria and least in the ventricles (47; 65); however, the total NET protein

measured with western blotting and binding unexpectedly has a negative correlation with this index of innervation density. NET is found in the highest amount in the LV which has the lowest NE content per gram of tissue, while the RA has the lowest NET and the highest NE content per gram of tissue. This is contrary to out expectations that NE levels dictate NET expression. Recently, it was determined that cells did not directly sense NE level to regulate NET (64). Using mice deficient in tyrosine hyrdoxylase (lack NE and dopamine) or dopamine beta hyrdoxylase (lack NE), it was shown that NET levels are regulated by total catecholamines and substrate transport rather by NE levels alone (64).

The ventricular predominace of NET has functional relevance suggesting that there is a physiological role for high NET in the ventricles. The ventricles take up more NE per gram of tissue than the atria (20) and this is consistent with our findings of high levels of ventricular NET. Furthermore, the neurotoxin 6-OHDA, a NET substrate (54; 60), had a greater toxic effect in the guinea pig ventricles when compared to the atria (4) indicative of high levels of NET protein in the ventricles. The greater toxic effect of 6-OHDA in ventricles is supportive of high amount of NET protein available to transport this neurotoxin resulting is a greater effect on NE depletion. We treated animals with 6-OHDA in rat heart and as expected from our finding of low NET protein in the atria, these chambers are less affected by 6-OHDA than the ventricles (i.e., there is less uptake capacity for

NE and 6-OHDA in the atria thus the neurotoxic effects are lower than in the ventricles where the uptake capacity for NE and 6-OHDA is higher).

Aside from our report of ventricular predominance of NET, other examples of regional and transmural differences in NE and NE uptake exist. The ventricles take up more NE per gram of tissue than in the atria (20). In right ventricular heart failure there is a reduction in right ventricular NET while left ventricular NET is unchanged (37). In pressure overload hypertrophy, there is a reduction in NET in the left ventricle while the right ventricle was unchanged (6). Regional patterns of NE uptake exist not only among different chambers, but also within a chamber (9). There is conflicting evidence about the distribution of NE and NE uptake across the heart wall. Sympathetic fibers and NE are more abundant in the subepicardium than the subendocardium (23) supporting a positive correlation of NE content to NET protein; however, others report that NE distribution and uptake follows a consistent pattern across the ventricular wall with no epicardial-to-endocardial gradient (52). There is a relatively uniform distribution of transmural NE uptake in the non-diseased heart while there is a dramatic reduction in subendocardial regions compared to subepicardial regions in the failing heart (3).

Tools for studying NET: antibody verification

We utilized two different NET antibodies for our studies: NET 48411 for immunohistochemistry and ADI NET 11-A for western blotting. The

immunohistochemical antibody recognizes an internal sequence on the C-terminal cytoplasmic tail of NET and has been shown to be selective to NET by the absence of immunoreactivity in brain from NET knockout mice (56). This antibody has been used in cultured primary superior cervical ganglion neurons, brain, and atria (56). The western blotting antibody has been used in heart, PC12 cells, and brain to measure NET protein (27; 40; 51). It recognizes a 22-amino acid peptide of rat NET located in the N-terminal extracellular domain. This antigenic sequence is available as a control peptide to determine which western blot bands are specifically recognized by this antibody. We show the three reported NET variants, 80, 54 and 46 kD, are present in western blotting on rat heart but also exist in NET knockout mouse hearts using this antibody. The mouse NET sequence is 100% homologous to the rat antigenic sequence of NET recognized by this antibody and therefore NET is similarly recognized in the wild type rat and mouse. The NET KO mouse has been reported to be devoid of functional NET and NET binding (62; 66) thus would be expected to serve as a negative control in these studies since the specific antigenic sequence for which the antibody was raised should not be present in these animals.

The NET variant forms of reported size are present in our studies; however, our control peptide studies using NET 11-A indicate that only the 54 kD band and an unreported 30 kD band are specifically recognized by the antibody. Thus, even though three molecular weight variants of NET have been previously reported and we show this data, the control peptide studies indicate that only the 54kD

form is valid using this primary antibody. Protein sequencing of five bands (80, 65, 54, 46, and 30 kD) visible after heart immunoprecipitation with NET 11-A did not reveal the presence of NET protein in any band. This result is however not conclusive as to the absence of NET protein due to the sensitivity of mass spectrometry sequencing.

Given the inconclusive results obtain while verifying the antibody, we also used [^{3}H]-nisoxetine binding as an alternative technique of measuring NET protein in cardiac membranes. Interestingly, the results of antagonist binding and western blotting matched suggesting that total NET protein can be measured successfully by either technique. We cautiously report all data from forms of NET in this study, but urge a critical assessment of all studies using NET antibodies without verification using other methods.

Summary

NET protein distribution is inversely correlated to the NE content of the heart chambers such that the ventricles have the lowest NE content, but the highest NET protein expression. A neurotoxic NET substrate affects the ventricles more than the atria, supporting the idea that there is more functional NET protein in the ventricles than the atria. The ventricles have higher NET uptake capacities for NE and 6-OHDA at least partly due to higher NET protein expression, but not related to a sidedness to stellate ganglion NET expression patterns. Since altered NET function plays a role in the diseased heart it is important to

recognize that the heart is not homogeneous in NE uptake function and that there may be some key regional changes in NET that have not been recognized in whole organ uptake studies.

Perspectives

Although NET protein is highly expressed in the ventricles, ventricular sympathetic innervation density and NE content per gram of tissue are low. 1) It is possible that there may be substantially more NET per nerve fiber in the ventricles compared to the atria. This could be assessed by measuring the amounts of NET mRNA and protein in individual stellate ganglion neuron cell bodies that have a ventricular target (53; 61) versus those neurons with an atrial target. However, it has not been clearly established if rat ventricular nerve fibers originate in a ganglionic cell body dedicated to ventricular control or if these fibers extend from discrete sub-branches of a particular axon that innervates other parts of the heart. 2) It is possible that some of the NET examined in the study was from sources aside from sympathetic fibers. This is supported by findings in stellate ganglionectomized cats showing that there is uptake of NE in the sympathetically denervated heart suggesting other sites of NET aside from sympathetic axons (20). Other cellular sources of NET protein need to be examined, including ICA cells (21; 22) and intrinsic cardiac neurons.

High levels of ventricular NET could related to reuptake function: 1) It may also be that the NET protein in ventricles is present in greater amounts because it is

less efficient at recapturing NE such that more total NET protein is required to clear NE. This could be due to reduced transporter efficiency or membrane insertion of NET. 2) The alternative NE clearance pathway, extraneuronal uptake (uptake-2) via organic cation transporter-3 (11), could play a smaller role in the clearance of NE in the ventricles such that NE reuptake in these chambers is more reliant on NET that in the atria.

Importantly, we must keep in mind that sympathetic fibers, and thus NET protein, in the heart comes from multiple sites of innervation including myocardium, coronary vessels, and nodal tissue. By using heart homogenate we are unable to assess discrete differences in expression or function of NET protein in these different regions of the heart. This study only reports on the predominance of NET in various chambers so the physiologically relevance of regional differences remains to be determined.

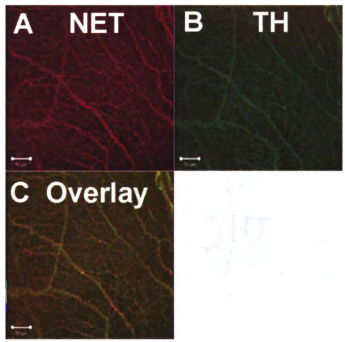

Figure 4.1: NET immunoreactivity localized to sympathetic nerve fibers in atria. Fixed atria from normal rats were stained using NET 411 or tyrosine hyrdoxylase (TH) primary antibodies with fluorescent secondary antibodies as described in Methods section. Samples were viewed as a whole-mount using confocal microscopy. A) NET staining (red) is shown in nerve fibers throughout the atria. B) TH staining (green) in sympathetic nerve fibers in the atria. C) NET and TH are co-localized (yellow) confirming the presence of NET in sympathetic fibers in the atrium. Scale bar: 50 μm. Images in this dissertation are presented in color.

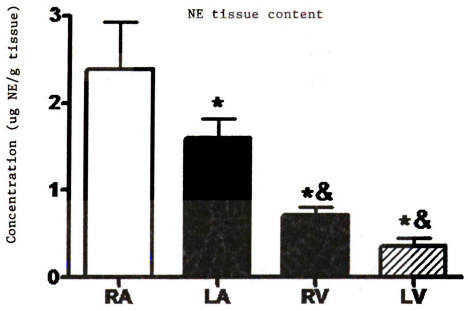

Figure 4.2: NE content, a marker of sympathetic innervation density, is greater in the atria than the ventricles. Capillary electrophoresis with electrochemical detection using a boron-doped diamond electrode was employed for NE determination in homogenized heart chambers. The amount of NE is highest in the RA and lowest in the LV and the atria have more NE per gram of tissue than do the ventricles. NE content is expressed in μg NE/g tissue ± 95% confidence interval (n=5 for each chamber). RA=right atrium, LA=left atrium, RV=right ventricle, LV=left ventricle. (* $p<0.05$ vs RA, & $p<0.05$ vs LA).

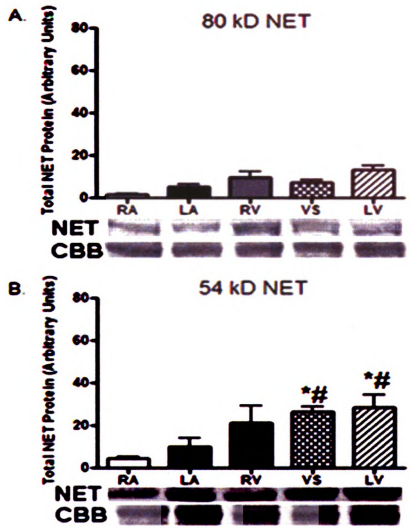

Figure 4.3: NET protein exists in three molecular weight variants in heart chambers. Homogenized heart chambers were used in western blotting for NET. All chambers from a single heart were run on the same gel and membranes were counterstained with Coomassie Brilliant Blue (CBB) to verify equal protein loading in all lanes. CBB was used to normalize samples. Representative membrane images of NET western blotting are shown below each graphed data set. For each panel, the top row of images represents NET western blotting and the lower row of images shows CBB stained bands. A) 80 kD NET, B) 54 kD NET, and C) 46 kD NET. RA=right atrium, LA=left atrium, RV=right ventricle, VS=ventricular septal wall, and LV=left ventricle. Data were analyzed using ANOVA with Tukey's post-hoc test (* $p<0.05$ vs RA, # $p<0.05$ vs LA, n=6).

Figure 4.3 continued

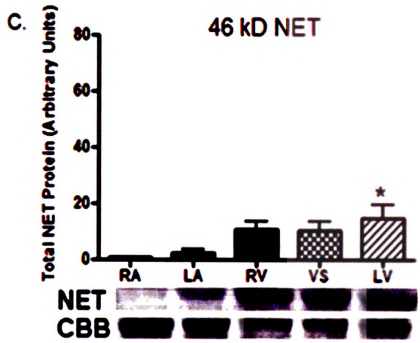

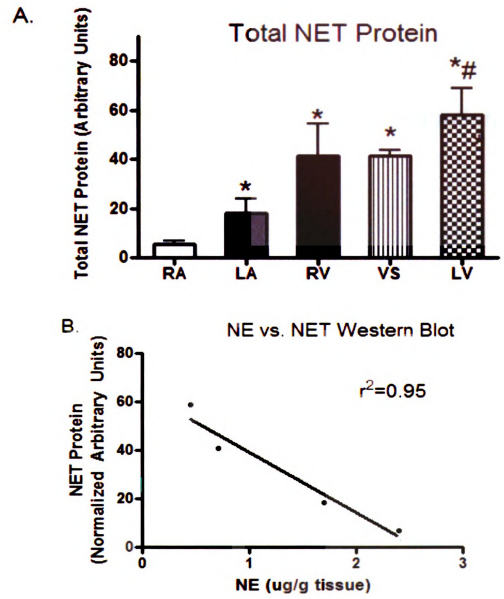

Figure 4.4: Total NET protein is expressed at higher levels in the ventricles than the atria and is inversely correlated to chamber NE content. Western blotting for NET was performed on heart homogenate and the normalized densities of the three molecular weight variants of NET were summed to obtain total NET for each chamber. A) Total NET protein by chamber obtained from western blotting indicates that NET protein is highly expressed in the ventricles compared to the atria (* $p<0.05$ vs RA, # $p<0.05$ vs LA). Data were analyzed using ANOVA with Tukey's post-hoc test. B) A negative correlation exists between total NET protein and NE content per chamber. A linear regression was performed to obtain a best fit line and a correlation analysis was performed using GraphPad Prism software.

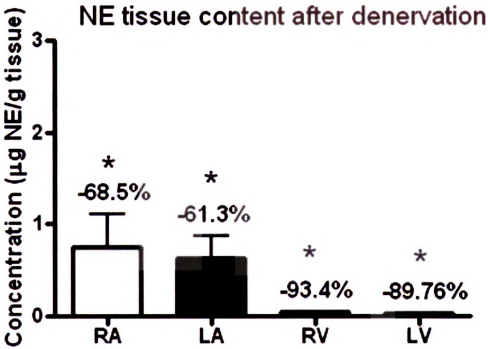

Figure 4.5: 6-OHDA treatment reduces ventricular NE more than atrial NE. Capillary electrophoresis with electrochemical detection using a boron-doped diamond electrode was employed for NE determination in the heart chambers. There was a significant reduction in NE content in all chambers with systemic 6-OHDA treatment, although the atria are more resistant than the ventricles and show less NE depletion in response to treatment. NE content is expressed in µg NE/g tissue $\pm$ 95% confidence interval (n=5). The percent decrease in NE content in treated animals compared to control is shown (* $p<0.05$ vs untreated control heart chamber). Limit of detection for NE by chamber: LV 0.034µg/g tissue, RV and VS 0.043 µg/g tissue, LA and RA 0.23 µg/g tissue.

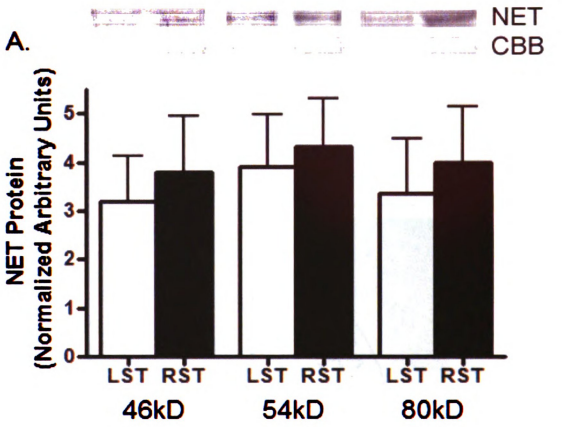

Figure 4.6: NET protein expression is not significantly different between the right and left stellate ganglia. Homogenized stellate ganglia were used in western blotting for NET. Right and left ganglia were run on the same gel in alternating lanes and membranes were counterstained with Coomassie Brilliant Blue (CBB) to verify equal protein loading in all lanes. A) Three molecular weight variants of NET were observed (46, 54, and 80kD) and there is no difference between RST and LST. Representative membrane images are shown above each graphed data set. The top row of images represents NET western blotting and the lower row of images represents CBB stained membrane used to normalize data. Comparisons between RST and LST for each NET variant were made using a paired t-test. RST=right stellate ganglion (n=6), LST=left stellate ganglia (n=5). B) The normalized densities of the three molecular weight variants of NET obtained from western blotting were summed to obtain total NET. There is no difference in total NET protein between RST and LST.

Figure 4.6 continued

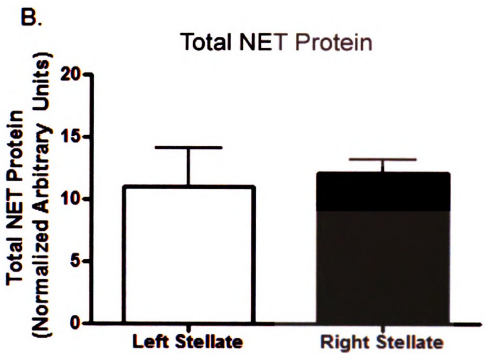

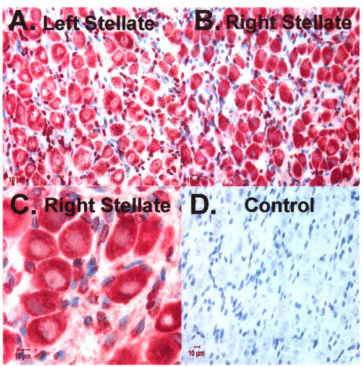

Figure 4.7: NET immunoreativity in cell bodies of sympathetic neurons in the stellate ganglion. Stellate ganglia from normal adult animals were fixed, embedded in paraffin, and sectioned at 5μM. NET 411 primary antibody was used with NOVA RED chromagen such that NET immunoreactivity is shown in red. Images were captured using standard brightfield microscopy. NET immunoreactivity is observed in all neurons of: A) Left stellate (40X magnification) and B) Right stellate ganglia (40X magnification). C) Right stellate ganglion neurons at high magnification with cytoplasmic staining of NET observed surrounding large nuclei (100X oil objective) (n=4). D) No primary antibody control image counterstained with hematoxylin to show cellular structure and antibody specificity. E) Quantification of NET immunoreactivity indicates that there is no difference between left and right ganglia (p=0.38; left stellate n=518 neurons; right stellate n=596 neurons). Scale bar=10 μM. Images in this dissertation are presented in color.

Figure 4.7 continued

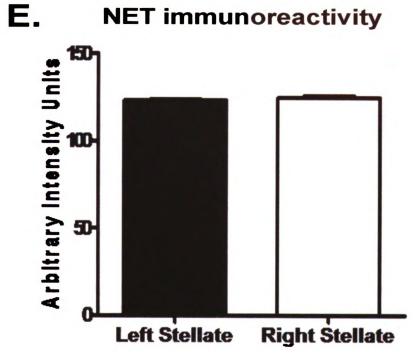

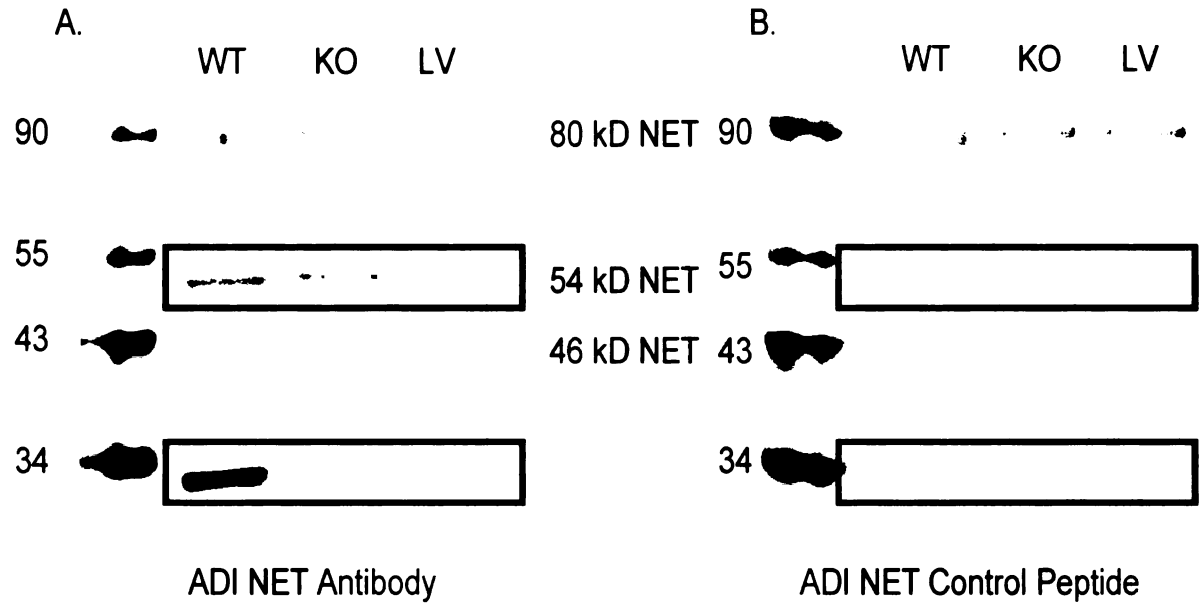

Figure 4.8: Validation of NET primary antibody in western blotting using NET KO hearts and control peptide. Heart homogenates from mouse wild type (WT) and NET knockout (KO) hearts were run on the same gel as rat left ventricle (LV) and the molecular weights markers are shown in the far left lane. Western blot membranes are shown with NET 11-A primary antibody chemiluminescence. In the center of the two membrane images, the three NET variant molecular weights are listed next the corresponding band on the membrane. A) Western blot membrane from NET primary antibody showing all bands visible following incubation with NET primary antibody and chemiluminescent detection of bands. The three known NET variants, 80, 54, and 46 kD are shown as well as bands observed at ~65 and ~30 kD. B) Western blot membrane image showing all bands visible following chemiluminescent detection. NET primary antibody was pre-incubated its control peptide antigenic sequence. Pre-incubation of primary antibody with excess control peptide will specifically remove primary antibody from solution and allow determination of band specificity on western blotting. The 54 kD and 30kD bands are absent in the presence of control peptide and are thus considered to contain the NET 11-A antigen sequence. These bands are indicated by boxes in panel A and B.

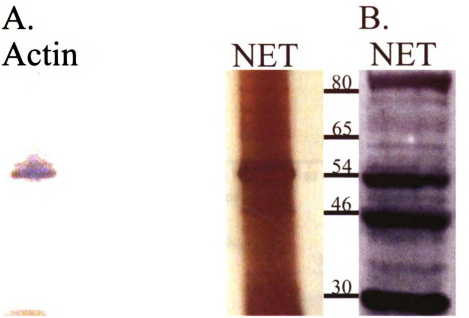

Figure 4.9: Immunoprecipitation (IP) using NET primary antibody. NET primary antibody was immobilized on a coupling gel, incubated with heart homogenate, and protein bound to the antibody was examined. Bound protein was run on a gel then stained using SilverSNAP® Stain and appropriate bands were cut from the gel for sequence analysis using mass spectrometry. A) Image of a representative gel showing IP of bound protein from actin (left) and NET 11-A (right) primary antibodies. Approximate molecular weights (kD) of bands are indicated to the right of figure. B) Western blot membrane using the same NET primary antibody. Approximate molecular weights (kD) of bands are indicated to the left of figure indicating alignment of the bands obtained used NET IP and NET western blotting. Images in this dissertation are presented in color.

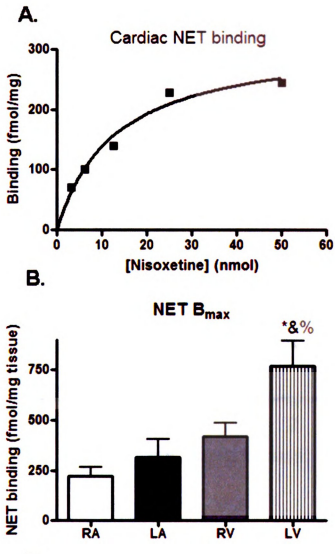

Figure 4.10: NET protein assessed by binding in cardiac membranes is negatively correlated to chamber NE content. Cardiac membranes were used in binding studies with [^{3}H]-nisoxetine to determine amount of NET protein in each chamber of the heart. A) Representative saturable binding curve for [^{3}H]-nisoxetine in cardiac membranes. Binding is desipramine-sensitive and plot represents specific binding after non-specific binding is subtracted. Total Binding minus non-specific binding= specific binding. B) B_{max} values were obtained from binding curves using curve fitting in GraphPad Prism. Mean B_{max} was obtained by averaging all B_{max} values from individual chambers. The LV has the greatest amount of binding and highest estimated amount of NET protein. C) NET B_{max} by chamber was compared to chamber NE content. A negative correlation exists between NET protein amount and NE content per chamber.

Figure 4.10 continued

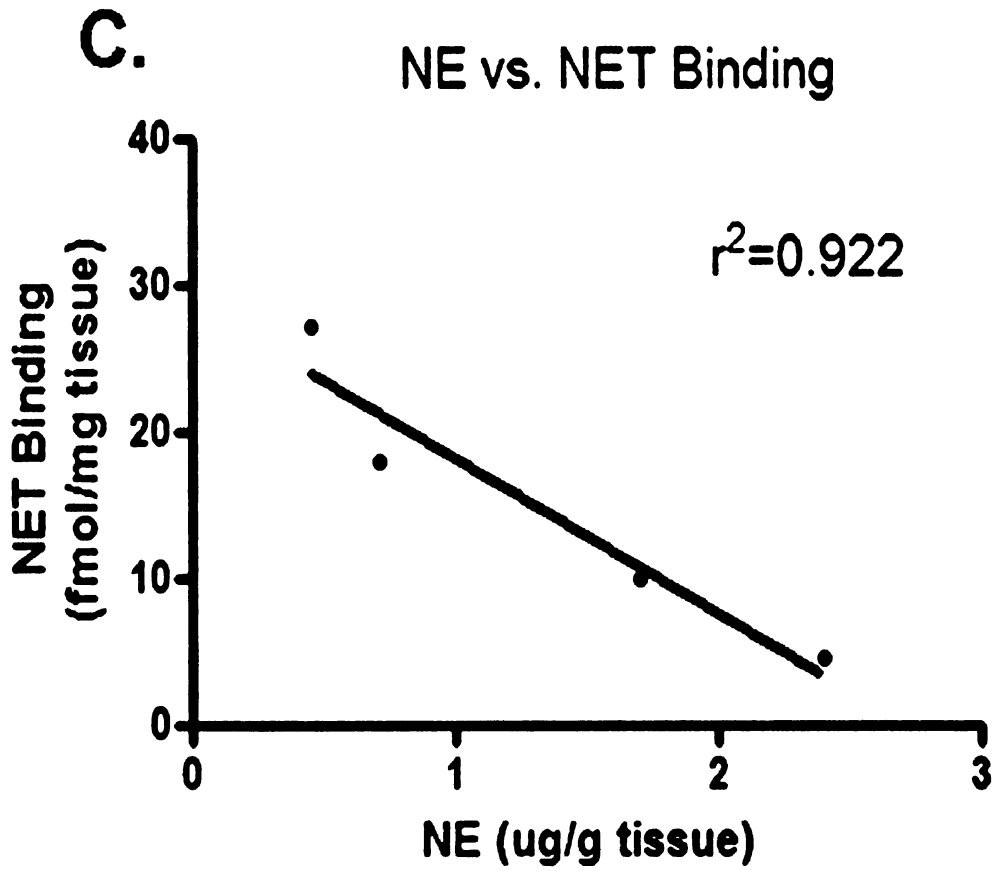

Reference List

1. **Anderson CR, Bergner A and Murphy SM**. How many types of cholinergic sympathetic neuron are there in the rat stellate ganglion? *Neuroscience* 2006.

2. **Axelrod J and Kopin IJ**. The uptake, storage, release, and metabolism of noradrenaline in sympathetic nerves. *Prog Brain Res* 31: 21-32, 1969.

3. **Beau SL and Saffitz JE**. Transmural heterogeneity of norepinephrine uptake in failing human hearts. *J Am Coll Cardiol* 23: 579-585, 1994.

4. **Bentley JA, Shibata S and Cheng JB**. Differences in effect of 6-hydroxydopamine on the right and left atria from guinea-pig. *Med Biol* 54: 129-136, 1976.

5. **Blakely RD, De Felice LJ and Hartzell HC**. Molecular physiology of norepinephrine and serotonin transporters. *J Exp Biol* 196: 263-281, 1994.

6. **Bohm M, Castellano M, Flesch M, Maack C, Moll M, Paul M, Schiffer F and Zolk O**. Chamber-specific alterations of norepinephrine uptake sites in cardiac hypertrophy. *Hypertension* 32: 831-837, 1998.

7. **Bonisch H and Bruss M**. The noradrenaline transporter of the neuronal plasma membrane. *Ann N Y Acad Sci* 733: 193-202, 1994.

8. **Bruss M, Porzgen P, Bryan-Lluka LJ and Bonisch H**. The rat norepinephrine transporter: molecular cloning from PC12 cells and functional expression. *Brain Res Mol Brain Res* 52: 257-262, 1997.

9. **Chilian WM, Boatwright RB, Shoji T and Griggs DM, Jr.** Regional uptake of [3H]norepinephrine by the canine left ventricle (41491). *Proc Soc Exp Biol Med* 171: 158-163, 1982.

10. **Cvacka J, Quaiserova V, Park J, Show Y, Muck A, Jr. and Swain GM**. Boron-doped diamond microelectrodes for use in capillary electrophoresis with electrochemical detection. *Anal Chem* 75: 2678-2687, 2003.

11. **Eisenhofer G**. The role of neuronal and extraneuronal plasma membrane transporters in the inactivation of peripheral catecholamines. *Pharmacol Ther* 91: 35-62, 2001.

12. **Eisenhofer G**. Sympathetic nerve function--assessment by radioisotope dilution analysis. *Clin Auton Res* 15: 264-283, 2005.

13. **Eisenhofer G, Esler MD, Meredith IT, Dart A, Cannon RO, III, Quyyumi AA, Lambert G, Chin J, Jennings GL and Goldstein DS**. Sympathetic nervous function in human heart as assessed by cardiac spillovers of dihydroxyphenylglycol and norepinephrine. *Circulation* 85: 1775-1785, 1992.

14. **Esler M, Jennings G, Lambert G, Meredith I, Horne M and Eisenhofer G**. Overflow of catecholamine neurotransmitters to the circulation: source, fate, and functions. *Physiol Rev* 70: 963-985, 1990.

15. **Goldstein DS, Brush JE, Jr., Eisenhofer G, Stull R and Esler M**. In vivo measurement of neuronal uptake of norepinephrine in the human heart. *Circulation* 78: 41-48, 1988.

16. **Habecker BA, Grygielko ET, Huhtala TA, Foote B and Brooks VL**. Ganglionic tyrosine hydroxylase and norepinephrine transporter are decreased by increased sodium chloride in vivo and in vitro. *Auton Neurosci* 107: 85-98, 2003.

17. **Habecker BA, Klein MG, Cox BC and Packard BA**. Norepinephrine transporter expression in cholinergic sympathetic neurons: differential regulation of membrane and vesicular transporters. *Dev Biol* 220: 85-96, 2000.

18. **Habecker BA, Willison BD, Shi X and Woodward WR**. Chronic depolarization stimulates norepinephrine transporter expression via catecholamines. *J Neurochem* 2006.

19. **Hertting G and Axelrod J**. Fate of tritiated noradrenaline at the sympathetic nerve-endings. *Nature* 192: 172-173, 1961.

20. **Hertting G and Schiefthaler T**. The effect of stellate ganglion excision on the catecholamine content and the uptake of H3-norepinephrine in the heart of the cat. *Int J Neuropharmacol* 3: 65-69, 1964.

21. **Huang MH, Bahl JJ, Wu Y, Hu F, Larson DF, Roeske WR and Ewy GA**. Neuroendocrine properties of intrinsic cardiac adrenergic cells in fetal rat heart. *Am J Physiol Heart Circ Physiol* 288: H497-H503, 2005.

22. **Huang MH, Friend DS, Sunday ME, Singh K, Haley K, Austen KF, Kelly RA and Smith TW**. An intrinsic adrenergic system in mammalian heart. *J Clin Invest* 98: 1298-1303, 1996.

23. **Ieda M, Kanazawa H, Kimura K, Hattori F, Ieda Y, Taniguchi M, Lee JK, Matsumura K, Tomita Y, Miyoshi S, Shimoda K, Makino S, Sano M, Kodama I, Ogawa S and Fukuda K**. Sema3a maintains normal heart rhythm through sympathetic innervation patterning. *Nat Med* 13: 604-612, 2007.

24. **Iversen LL, Glowinski J and Axelrod J**. Reduced uptake of tritiated noradrenaline in tissues of immunosympathectomized animals. *Nature* 206: 1222-1223, 1965.

25. **Jenden DJ, Jope RS and Weiler MH**. Regulation of acetylcholine synthesis: does cytoplasmic acetylcholine control high affinity choline uptake? *Science* 194: 635-637, 1976.

26. **Jensen ON, Wilm M, Shevchenko A and Mann M**. Sample preparation methods for mass spectrometric peptide mapping directly from 2-DE gels. *Methods Mol Biol* 112: 513-530, 1999.

27. **Kantor L, Park YH, Wang KK and Gnegy M**. Enhanced amphetamine-mediated dopamine release develops in PC12 cells after repeated amphetamine treatment. *Eur J Pharmacol* 451: 27-35, 2002.

28. **Kawano H, Okada R and Yano K**. Histological study on the distribution of autonomic nerves in the human heart. *Heart Vessels* 18: 32-39, 2003.

29. **Kippenberger AG, Palmer DJ, Comer AM, Lipski J, Burton LD and Christie DL**. Localization of the noradrenaline transporter in rat adrenal

medulla and PC12 cells: evidence for its association with secretory granules in PC12 cells. *J Neurochem* 73: 1024-1032, 1999.

30. **Kopin IJ, Rundqvist B, Friberg P, Lenders J, Goldstein DS and Eisenhofer G**. Different relationships of spillover to release of norepinephrine in human heart, kidneys, and forearm. *Am J Physiol* 275: R165-R173, 1998.

31. **Kostrzewa RM and Jacobowitz DM**. Pharmacological actions of 6-hydroxydopamine. *Pharmacol Rev* 26: 199-288, 1974.

32. **Lee CM, Javitch JA and Snyder SH**. Recognition sites for norepinephrine uptake: regulation by neurotransmitter. *Science* 220: 626-629, 1983.

33. **Lee SK and Hollenbeck PJ**. Organization and translation of mRNA in sympathetic axons. *J Cell Sci* 116: 4467-4478, 2003.

34. **Li H, Ma SK, Hu XP, Zhang GY and Fei J**. Norepinephrine transporter (NET) is expressed in cardiac sympathetic ganglia of adult rat. *Cell Res* 11: 317-320, 2001.

35. **Li W, Knowlton D, Van Winkle DM and Habecker BA**. Infarction alters both the distribution and noradrenergic properties of cardiac sympathetic neurons. *Am J Physiol Heart Circ Physiol* 286: H2229-H2236, 2004.

36. **Li W, Knowlton D, Woodward WR and Habecker BA**. Regulation of noradrenergic function by inflammatory cytokines and depolarization. *J Neurochem* 86: 774-783, 2003.

37. **Liang CS, Fan TH, Sullebarger JT and Sakamoto S**. Decreased adrenergic neuronal uptake activity in experimental right heart failure. A chamber-specific contributor to beta-adrenoceptor downregulation. *J Clin Invest* 84: 1267-1275, 1989.

38. **Mao W, Iwai C, Qin F and Liang CS**. Norepinephrine induces endoplasmic reticulum stress and downregulation of norepinephrine transporter density in PC12 cells via oxidative stress. *Am J Physiol Heart Circ Physiol* 288: H2381-H2389, 2005.

39. **Mason JN, Farmer H, Tomlinson ID, Schwartz JW, Savchenko V, DeFelice LJ, Rosenthal SJ and Blakely RD**. Novel fluorescence-based approaches for the study of biogenic amine transporter localization, activity, and regulation. *J Neurosci Methods* 143: 3-25, 2005.

40. **Matsunaga W, Isobe K and Shirokawa T**. Involvement of neurotrophic factors in aging of noradrenergic innervations in hippocampus and frontal cortex. *Neurosci Res* 54: 313-318, 2006.

41. **Matsuoka I, Kumagai M and Kurihara K**. Differential and coordinated regulation of expression of norepinephrine transporter in catecholaminergic cells in culture. *Brain Res* 776: 181-188, 1997.

42. **Melikian HE, McDonald JK, Gu H, Rudnick G, Moore KR and Blakely RD**. Human norepinephrine transporter. Biosynthetic studies using a site-directed polyclonal antibody. *J Biol Chem* 269: 12290-12297, 1994.

43. **Melikian HE, Ramamoorthy S, Tate CG and Blakely RD**. Inability to N-glycosylate the human norepinephrine transporter reduces protein stability, surface trafficking, and transport activity but not ligand recognition. *Mol Pharmacol* 50: 266-276, 1996.

44. **Mo N, Wallis DI and Watson A**. Properties of putative cardiac and non-cardiac neurones in the rat stellate ganglion. *J Auton Nerv Sys* 47: 7-22, 1994.

45. **Muna GW, Quaiserova-Mocko V and Swain GM**. Chlorinated phenol analysis using off-line solid-phase extraction and capillary electrophoresis coupled with amperometric detection and a boron-doped diamond microelectrode. *Anal Chem* 77: 6542-6548, 2005.

46. **Nguyen TT and Amara SG**. N-linked oligosaccharides are required for cell surface expression of the norepinephrine transporter but do not influence substrate or inhibitor recognition. *J Neurochem* 67: 645-655, 1996.

47. **Novotny M, Quaiserova-Mocko V, Wehrwein EA, Kreulen DL and Swain GM**. Determination of endogenous norepinephrine levels in different chambers of the rat heart by capillary electrophoresis coupled with amperometric detection. *J Neurosci Methods* 163: 52-59, 2007.

48. **Olink-Coux M and Hollenbeck PJ**. Localization and active transport of mRNA in axons of sympathetic neurons in culture. *J Neurosci* 16: 1346-1358, 1996.

49. **Pacholczyk T, Blakely RD and Amara SG**. Expression cloning of a cocaine- and antidepressant-sensitive human noradrenaline transporter. *Nature* 350: 350-354, 1991.

50. **Pardini BJ, Lund DD and Schmid PG**. Organization of the sympathetic postganglionic innervation of the rat heart. *J Auton Nerv Syst* 28: 193-201, 1989.

51. **Parrish DC, Gritman K, Van Winkle DM, Woodward WR, Bader M and Habecker BA**. Post-infarct sympathetic hyperactivity differentially stimulates expression of tyrosine hydroxylase and norepinephrine transporter. *Am J Physiol Heart Circ Physiol* 2007.

52. **Pierpont GL, DeMaster EG and Cohn JN**. Regional differences in adrenergic function within the left ventricle. *Am J Physiol* 246: H824-H829, 1984.

53. **Richardson RJ, Grkovic I, Allen AM and Anderson CR**. Separate neurochemical classes of sympathetic postganglionic neurons project to the left ventricle of the rat heart. *Cell Tissue Res* 324: 9-16, 2006.

54. **Sachs C and Jonsson G**. Mechanisms of action of 6-hydroxydopamine. *Biochem Pharmacol* 24: 1-8, 1975.

55. **Savchenko V, Sung U and Blakely RD**. Cell surface trafficking of the antidepressant-sensitive norepinephrine transporter revealed with an ectodomain antibody. *Mol Cell Neurosci* 24: 1131-1150, 2003.

56. **Schroeter S, Apparsundaram S, Wiley RG, Miner LH, Sesack SR and Blakely RD**. Immunolocalization of the cocaine- and antidepressant-sensitive l- norepinephrine transporter. *J Comp Neurol* 420: 211-232, 2000.

57. **Schwartz JW, Blakely RD and DeFelice LJ**. Binding and transport in norepinephrine transporters: Real-time, spatially resolved analysis in single cells using a fluorescent substrate. *J Biol Chem* 2002.

58. **Shevchenko A, Wilm M, Vorm O and Mann M**. Mass spectrometric sequencing of proteins silver-stained polyacrylamide gels. *Anal Chem* 68: 850-858, 1996.

59. **Stefanini M, De MC and Zamboni L**. Fixation of ejaculated spermatozoa for electron microscopy. *Nature* 216: 173-174, 1967.

60. **Thoenen H and Tranzer JP**. Chemical sympathectomy by selective destruction of adrenergic nerve endings with 6-Hydroxydopamine. *Naunyn Schmiedebergs Arch Exp Pathol Pharmakol* 261: 271-288, 1968.

61. **Wallis D, Watson AH and Mo N**. Cardiac neurones of autonomic ganglia. *Microsc Res Tech* 35: 69-79, 1996.

62. **Wang YM, Xu F, Gainetdinov RR and Caron MG**. Genetic approaches to studying norepinephrine function: knockout of the mouse norepinephrine transporter gene. *Biol Psychiatry* 46: 1124-1130, 1999.

63. Wehrwein, E. A., Fink, G. D., and Kreulen, D. L. Norepinephrine transporter mRNA is present in the heart and stellate ganglion, and is differentially regulated in hypertension. American Heart Association, Council for High Blood Pressure Research Abstract . 2006.
Ref Type: Abstract

64. **Weinshenker D, White SS, Javors MA, Palmiter RD and Szot P**. Regulation of norepinephrine transporter abundance by catecholamines and desipramine in vivo. *Brain Res* 946: 239-246, 2002.

65. **Willenbrock R, Stauss H, Scheuermann M, Osterziel KJ, Unger T and Dietz R**. Effect of chronic volume overload on baroreflex control of heart rate and sympathetic nerve activity. *Am J Physiol* 273: H2580-H2585, 1997.

66. **Xu F, Gainetdinov RR, Wetsel WC, Jones SR, Bohn LM, Miller GW, Wang YM and Caron MG**. Mice lacking the norepinephrine transporter are supersensitive to psychostimulants. *Nat Neurosci* 3: 465-471, 2000.

67. **Zahniser NR and Doolen S**. Chronic and acute regulation of Na+/Cl- -dependent neurotransmitter transporters: drugs, substrates, presynaptic receptors, and signaling systems. *Pharmacol Ther* 92: 21-55, 2001.

68. **Zhu MY and Ordway GA**. Down-regulation of norepinephrine transporters on PC12 cells by transporter inhibitors. *J Neurochem* 68: 134-141, 1997.

CHAPTER 5: ALTERNATIVE CELLULAR SOURCES OF NOREPINEPHRINE TRANSPORTER IN THE HEART AND VASCULATURE

Abstract

The actions of norepinephrine (NE) in the heart are attenuated by reuptake into sympathetic nerve terminal by the action of the neuronal NE transporter (NET). NET is localized to sympathetic nerves in the heart and plays an important role in heart function in health and disease. Nonetheless, when we denervated the heart using stellate ganglionectomy or 6-hydroxydopamine, there was no reduction in NET protein although the procedure was successful (i.e., NE was depleted in all chambers). Furthermore, we determined that there are examples NET-positive nerve fibers in the atria that do not colocalize with tyrosine hydroxylase (TH), a marker of sympathetic neurons. These findings led us to investigate alternative cellular sources of NET in the normal heart. First, we confirmed that NET was present and equally expressed in all neurons in the paravertebral sympathetic stellate ganglia that provide the majority of sympathetic input to the heart. NET immunoreactivity (IR) was observed in sympathetic nerve fibers in both atria by use of colabeling with TH as a marker of sympathetic neurons. NET-IR was also observed in all neurons of the prevertebral celiac ganglia and in mesenteric blood vessels colocalized with TH. NET-IR was colocalized with choline acetyltransferase (ChAT) in a subset of intrinsic cardiac ganglion neurons in the left atria and cholinergic nerve fibers in the atria. NET-IR in the sensory nervous system was present in varying amounts in all neuron cell bodies in cervical and upper thoracic dorsal root ganglia that

innervate the heart, yet was not contained in calcitonin gene related peptide (CGRP)-positive sensory neurites in the atria. Similarly, NET-IR was present in all neurons in lumbar dorsal root ganglia and was not colocalized with CGRP-fibers in mesenteric blood vessels. In summary, we found NET in: 1) sympathetic ganglion cell bodies in stellate ganglion and celiac ganglion, 2) postganglionic sympathetic fibers in the atria, 3) intrinsic cardiac neuron cell bodies (parasympathetic postganglionic neurons), 4) cardiac cholinergic neurites, and 5) sensory cervical and thoracic dorsal root ganglia, but not in sensory neurites in the heart.

Introduction

Interest in autonomic innervation of the heart has been the subject of numerous studies for over 70 years. The autonomic innervation of the heart plays a vital functional role in regulation of the rhythmicity and contractility of the heart and has documented functional changes in cardiovascular disease. The heart is richly innervated by the sympathetic nervous system and in particular the atria and nodal tissue have a high density of nerve fibers. Norepinephrine (NE) is the primary neurotransmitter and results in enhanced heart rate, cardiac output, and contractility. There is evidence of enhanced sympathetic drive to the heart in many diseases and thus a better understanding of NE handling in the heart is important.

Early studies of NE in the heart determined that there are two different clearance mechanisms in the heart that attenuate the actions of NE in the neuromuscular junction: uptake-1 which occurs at low amine concentrations and is inhibited by desipramine and uptake-2 which works at high concentrations (22). It was later determined that uptake-1 occurred primarily in sympathetic nerves (12; 18; 23). There is a reduction in NE uptake in sympathetically denervated structures supporting that the site of binding and inactivation of NE was on sympathetic nerves (17). Subsequently, it was determined that uptake-1 into nerve terminals occurred through a membrane transporter known as NE transporter (NET). NET immunoreactivity has now been demonstrated in sympathetic nerves of the heart verifying the early function studies that NET and NE uptake occur in sympathetic fibers (28; 38).

The heart has a very efficient NE uptake system. There is a roughly 20:1 ratio of *released* NE to NE spillover in the heart. The ratio is much lower in other organs, such as the liver and kidney, which have ratios of 4:1 or 8:1, respectively (25). That is to say that the reuptake system in the heart can clear up to 5 times more *released* NE then it does in other organs. Also, the heart is exceptionally dependent on NET for clearance of *circulating* NE, such that while the heart clears nearly 70% of infused NE via NET, other organs clear only 4-14% of circulating NE by neuronal reuptake via NET (13).

Given the compelling evidence of NE uptake in sympathetic nerves, the focus of research on NET has justifiably been in the sympathetic nervous system. However, if the sympathetic nerves were the sole source of NET in the heart, then cardiac denervation should eliminate NET protein and virtually eliminate NE uptake. It is surprising then that there is NE uptake function, albeit reduced, in sympathetically denervated animals that underwent stellate ganglionectomy to remove postganglionic sympathetic inputs to the heart (18). This suggests that NET protein may be found in other cells in the heart. We determined that substantial NET protein is present in the heart following sympathetic denervation thus investigated alternative cellular sources of NET in the normal heart. Parasympathetic intrinsic cardiac neurons and sensory neurons were examined.

Methods

Animals

Adult male, Sprague-Dawley rats, 8 weeks old (250-275 g, Charles River, Portage, MI) were used. All animal experiments were performed in accordance with the "Guide for the Care and Usage of Laboratory Animals" (National Research Council) and were approved by the Animal Use and Care Committee of Michigan State University. Animals were housed two per cage in temperature and humidity-controlled rooms with a 12 hour/12 hour light-dark cycle. Standard pellet rat chow and water were given *ad libitum*.

For the surgical denervation study, the animals were randomly divided into control (sham operated) and stellate ganglionectomized group (denervated). Rats were administered atropine sulphate (0.4 mg/kg, i.p.), anesthetized with isoflurane, intubated and ventilated with a Harvard rodent ventilator (model 683, Harvard Apparatus; South Natick, MA). A midline thoracotomy was performed by first making a midline skin incision and then cutting the sternum from the mid-manubrium to the ziphoid process and opening the incision with a retractor. The stellate ganglia were exposed by moving the upper lobe of the right lung caudally and medially with saline soaked gauze. The entire ganglion was removed bilaterally and the upper lung lobe is returned to its original position. The chest was closed by suturing the bone, muscle, and skin in 3 separate layers. Negative intrathoracic air pressure is reestablished bilaterally by inserting a 23-guage needle into the lower thoracic cavity and suctioning with a 3 ml syringe. Upon arousal from anesthesia, the rat was taken off the ventilator and spontaneous ventilation was reestablished. Animals with successful denervation were noted to have post-surgical ptosis. Hearts were collected two weeks following surgery. Control animals underwent anesthesia and thoracotomy, but the stellate ganglia were left intact.

For the chemical denervation study, the neurotoxin 6-hydroxydopamine hydrochloride (6-OHDA, St. Louis, MO) was used to destroy sympathetic nerve terminals and NET containing cells. It was prepared in a mixture of 0.9 % (154 mM) sodium chloride and 0.5 % (28.4 mM) ascorbic acid solution fresh before

each administration and kept protected from light. Animals were dosed (250 mg/kg) with subcutaneous injection of 6-OHDA to the loose skin between the shoulder blades (25 gauge needle) with three consecutive injections during one week on day one, three and five. On day seven, two days after the final dose, the animals were sacrificed and hearts were collected as described below for analysis of RNA and NE content. Age and sex matched control animals were untreated.

Tissue Collection

Rats were anesthetized with a lethal dose of sodium pentobarbital (Sigma-Aldrich Corp, St. Louis, MO, 65 mg/kg, intra-peritoneal) followed by thoracotomy. Hearts were removed quickly and immediately placed into chilled (4 °C) phosphate buffered saline (PBS, 137 mM sodium chloride, 2.7 mM potassium chloride, 4.3 mM sodium phosphate dibasic and 1.4 mM potassium phosphate monobasic) for separation of chambers. The dissected heart chambers were frozen immediately by contact with dry ice and stored at -80 °C until further processing for binding or western blotting. Alternatively, atria were rinsed and fixed as described below. Stellate and celiac ganglia were dissected and fixed as described below.

[^{3}H]-Nisoxetine Binding

Preparation of Cardiac Membranes: Frozen heart chambers were pulverized on dry ice and then transferred to a mortar and pestle that had been pre-chilled with liquid nitrogen. Tissue was further processed by grinding and then suspended in

the appropriate amount of homogenization buffer without detergent to keep membranes intact (50 mM Tris pH 7.4, 120mM NaCl, 5 mM KCl). The suspended tissue in solution was transferred to an ice cold 10 ml glass hand-held homogenizer for 10 strokes of further gentle processing in ice. For ventricular tissue, the homogenate was centrifuged (Sorvall RC 5B Plus) at 700 xg for 10 min at 4°C to remove nuclei and cellular debris, and atrial membranes were used without centrifugation. Samples were spun at 40,000 xg for 30 minutes after which the supernatant was discarded and the pellet resuspended in an additional 4 ml of buffer. A second identical spin was performed, the supernatant discarded, and the pellet stored at -80°C until use.

Binding Assay: NET protein expression in cardiac membranes from individual heart chambers was estimated from B_{max} values of full saturating binding curves using [^{3}H]-Nisoxetine (Perkin-Elmer, Waltham, MA).in a manner similar to that described previously (15; 28; 45). Frozen membrane pellets were resuspended in ice cold incubation buffer (50mM Tris (pH 7.4), 200mM NaCl, 5 mM KCl) on ice just prior to use. The resuspended membranes were loaded in quadruplicate into 96-well reaction plates and aliquots were used in parallel for a Bradford protein assay to determine protein concentration. Samples were assessed for total and background binding. Full saturating binding curves were run in duplicate using 0.37-50 nM [^{3}H]-Nisoxetine; additional duplicate wells with 15 nM desipramine were used to determine non-specific binding. Samples were incubated on a shaker for a minimum of 4 hours at 0° C then filtered through glass fiber filters

presoaked in 0.5% polyethylenimine using a 96-well Filtermate cell harvester (Packard Biosciences, Shelton, CT, USA). Standard scintillation counting was performed using Ecolite scintillation fluid (ICN Biomedicals, Irvine CA, USA).

Western Blotting

Tissue processing: Frozen heart chambers were pulverized on dry ice and then transferred to a mortar and pestle that had been pre-chilled with liquid nitrogen. Tissue was further processed by grinding, then suspended in the appropriate amount of homogenization buffer (10mM Hepes (Sigma), 0.15M NaCl (VWR), 1mM EDTA (Sigma), 1mM phenol methane sulfanyl fluoride (PMSF, Roche), 1μg/ml leupeptin (Roche), and 1μg/ml aprotinin (Roche), amount per tissue). The suspended tissue was then homogenized using a variable speed Omni TH-115 homogenizer with 5mm saw tooth generator probe (Omni International Inc., Warrenton, VA) for ~30 seconds at high speed. Finally, the processed tissue in solution was transferred to a 10 ml glass hand-held homogenizer for 10 strokes of further processing. The homogenate was centrifuged (Sorvall RC 5B Plus) at 700xg for 10 min at 4°C to remove nuclei and cellular debris, assessed in triplicate for protein concentration using a modified Bradford protein assay (Bio-Rad, Hercules, CA), and the supernatant containing total protein was frozen until use at -80°C.

Western Blotting: Standard Western blotting was performed. Samples containing 50μg protein were prepared, loaded into 4% stacking gel/10% resolving gels and

run at 100 V for ~90 minutes until the leading edge of samples traveled to the bottom of gel. All heart chambers from an animal were run on the same gel to ensure accurate comparison across chambers. Transfer to polyvinylidene fluoride (PVDF) membranes (Bio-Rad, Hercules, CA) was performed at a constant voltage of 100 V at 4°C for 60 minutes. The membranes were blocked with 4% non-fat dry milk in PBS containing 0.1% Tween-20 for one hour with shaking at room temperature. Membranes were then incubated overnight at 4°C with anti-rat NET 11-A primary antibody (Alpha Diagnostics Intl Inc, San Antonio, TX) diluted 1:250 in 4% milk solution. The primary antibody was prepared fresh and was not reused. The membranes were rinsed with PBS containing 0.1% Tween-20 and incubated for one hour at 4°C with anti-rabbit IgG horseradish peroxidase (HRP) secondary antibody (Santa Cruz Biotech, Santa Cruz, CA) diluted 1:2000 in 4% milk solution. Immunoreactivity was detected using Femto® chemiluminescence kit (Pierce Chemical, Rockford, IL) to visualize bands. The membrane was imaged using Syngene ChemiGenius Gel Documentation System with GeneSnap software and was quantified using GeneTools software (Syngene, Frederick, MD). All membranes were counter-stained with Coomassie Blue (Invitrogen, Carlsbad, CA) to verify equal protein loading. Data were normalized for protein loading using Coomassie Blue staining. Data are expressed as arbitrary density units normalized for protein loading. Total NET was calculated as the sum of the normalized densities of all three molecular weight variants per chamber.

Immunohistochemistry

Ganglia Immunohistochemistry: Stellate ganglia and celiac ganglia were fixed in 10% neutral buffered formalin for 2 hours then transferred to 70% ethanol, routinely processed, embedded in paraffin and sectioned on a rotary microtome at 5μM. Sections were placed on slides coated with 2% 3-Aminopropyltriethoxysilane, dried at 56°C overnight then deparaffinized in Xylene and hydrated through descending grades of ethyl alcohol to distilled water. After incubation in Tris buffered saline (TBS, pH 7.4) for 5 minutes, slides were antigen retrieved utilizing citrate buffer pH 6.0 (Biogenex, San Ramon CA) in a vegetable steamer (Oster, Boca Raton FL) for 30 minutes at 100°C, allowed to cool on the counter at room temperature for 10 minutes and rinsed in several changes of distilled water. Endogenous peroxidase was blocked utilizing 3% hydrogen peroxide for 30 minutes followed by running tap and distilled water rinses. Standard avidin-biotin complex staining steps were performed at room temperature on the DAKO Autostainer. After blocking with normal goat serum for 30 minutes, slides were incubated 15 minutes each in avidin D (Vector, Burlingame CA) and d-biotin (Sigma, St. Louis MO) to block endogenous avidin and biotin. Slides were then rinsed in several changes of TBS + Tween 20 (TBS-T), incubated for 60 minutes at room temperature with the polyclonal primary antibody NET 48411 (1:250 in normal antibody diluent (Scytek, Logan, UT)). Slides were then rinsed in several changes of TBS-T then incubated in biotinylated goat anti-rabbit IgG H+L (Vector, Burlingame CA) in normal antibody diluent 1:200 for 30 minutes. Slides were rinsed in TBS-T followed by the

application of Vectastain® Elite ABC Reagent (Vector, Burlingame CA) for 30 minutes. The slides were rinsed with TBS-T and developed using Nova Red Peroxidase substrate kit (Vector, Burlingame CA) for 15 minutes. Slides were rinsed in distilled water, counterstained using Lerner 2 hematoxylin for 1 minute, differentiated in 1% aqueous glacial acetic acid, and rinsed in running tap water then dehydrated through ascending grades of ethyl alcohol, cleared through several changes of xylene and cover slipped using Flotex (Lerner, Pittsburgh PA) permanent mounting media. Images were captured using standard brightfield microscopy (Olympus BX60, Center Valley, PA).

Immunolocalization in Whole Mount Atria and Mesenteric Blood Vessels: After the hearts were removed the left and right atria were dissected and rinsed to remove blood. Mesenteric vessels were rinsed and cleaned of fat while in ice cold PBS. Atria and vessels were fixed using Zamboni's fixative(42) for 20 minutes at room temperature. Fixed tissues were washed in PBS and incubated for 24 hours (4°C) with antibody in PBS containing 1% bovine serum albumin (BSA) and 0.3% Triton X-100. Antibodies used were rabbit anti-NET 411(37) (courtesy of RD Blakely, Vanderbilt University), goat anti-NET (1:100, Santa Cruz, Santa Cruz, CA), mouse anti-tyrosine hydrozylase (TH) (1:250, Chemicon, Temecula, CA), rabbit anti-TH (1:500, Chemicon, Temecula, CA), rabbit anti-calcitonin gene related peptide (CGRP, 1:8000, Sigma, St. Louis, MO), mouse anti-CGRP (1:200, Sigma, St. Louis, MO), goat anti-CGRP (1:250, Santa Cruz, Santa Cruz, CA), goat anti-choline acetyltransferase (ChAT, 1:500, Chemicon,

Temecula, CA), and mouse anti-ChAT (Chemicon, Temecula, CA). After 24 hours, tissues were washed in PBS (3 x 5 minutes) followed by incubation for 2 hours (25°C) in secondary antibody (goat anti-mouse IgG conjugated to AlexaFluor 488 (Molecular Probes, Carlsbad, California) 1:1000 dilution in PBS containing BSA (1%) and Triton (0.3%)) and goat anti-rabbit IgG conjugated to AlexaFluor 594 (Molecular Probes, Carlsbad, California) 1:1000 dilution in PBS containing BSA (1%) and Triton (0.3%)). Tissues were washed 3 x 5 minutes in PBS, mounted on slides, and viewed as a whole mount using a confocal microscope (Zeiss LSM 510). Filter settings for AlexaFluor 488 were bandpass 505-530 and AlexaFluor 594 were bandpass 585-615. Samples were optically sectioned in 2 μm slices and then digitally reconstructed to attain a projection encompassing multiple layers of the tissue.

Results

NET in sympathetic ganglia and sympathetic nerve fibers

Stellate ganglion neurons provide the majority of sympathetic input to the heart. Studies of NET immunoreactivity (IR) were performed in the stellate (paravertebral) sympathetic ganglia and sympathetic fibers of the heart. NET-IR (red) was present throughout the cytoplasm, but never in the nucleus, in all neurons in sectioned left and right stellate ganglia (Figure 1A). NET (green) was colocalized with tyrosine hydroxylase (TH, red) in atrial whole-mount tissue preparations indicating in regions of yellow (lower panel) that NET was present in sympathetic fibers in the heart (Figure 1B).

This pattern of NET localization to sympathetic cell bodies and fibers was also observed in the celiac (prevertebral) sympathetic ganglion innervating the mesenteric blood vessels. Cytoplasmic NET-IR (red) was observed in all visible neurons of the celiac ganglia (Figure 2A). Sympathetic fibers originating in the celiac ganglia innervate the mesenteric vasculature. NET (green) was colocalized with TH (red) in sympathetic nerve fibers (Figure 2B) similar to heart (Figure 1B).

NET protein is present after cardiac sympathetic denervation

NET protein is present in sympathetic fibers thus sympathetic denervation was expected to dramatically reduce NET protein in the heart as it does NE content. Western blotting of heart homogenate was performed on control rats or denervated rats following stellate ganglionectomy (SGX) or 6-OHDA denervation (Figure 3A). Three molecular weight bands of NET were visualized in all lanes at 80, 54, and 46 kD and there was still substantial NET protein present in hearts. [^{3}H]-nisoxetine binding in cardiac membranes following stellate ganglionectomy (Figure 3B) was used to confirm the results from western blotting and also indicated the presence of substantial NET protein in the denervated heart. [^{3}H]-nisoxetine binding curves were saturable and sensitive to the NET antagonist desipramine. The estimated B_{max} for control and denervated hearts were similar 206.4 fmol/mg tissue and 181.0 fmol/mg tissue, respectively (Figure 3B).

NET protein localized outside of sympathetic fibers: non-sympathetic neuritis and intrinsic neurons

Since there was substantial NET present after sympathetic denervation, alternative sources of NET protein besides sympathetic ganglia and nerve fibers were investigated. First, we observed that there were NET-positive fibers in the atria that did not contain TH and vice versa (shown with arrowheads, Figure 4A). NET-IR (red) and TH-IR (green) are visible in nerve fibers in the atria (Figure 4A, upper panels). The overlay image of TH and NET-IR (lower panel) indicates that there are fibers that do not contain both proteins. Although there is evidence for NET and TH colocalization in other areas of the heart (Figure 1), there are sites where that is not the case.

Cardiac intrinsic neurons are largely parasympathetic/cholinergic but there is evidence of catecholaminergic phenotype in some cells. TH (green) is a marker of catecholaminergic cells and is present in intrinsic cardiac neurons along with NET (red) (Figure 5).

NET in cholinergic intrinsic cardiac neurons in the left atria

As described in Figure 5, an alternative source of NET protein in the heart is intrinsic cardiac ganglia which are largely cholinergic. To investigate this possibility, atria were colabeled with NET and choline acetyl transferase (ChAT) (Figure 5A). ChAT (red) was observed in neuron cell bodies of the intrinsic cardiac ganglia these cells also contain NET staining (red) (Figure 6A and B,

upper panels). The overlay image (yellow) shows locations where NET and ChAT are colocalized (Figure 6A and B. lower panel). Thus, NET is present in cardiac intrinsic ganglia in neurons that have cholinergic properties. A low and high magnification image is shown supporting that NET is present in these neuron cell bodies.

In addition to NET localization in cell bodies of cardiac cholinergic neurons, NET is also found in cholinergic nerve fibers in the atria. ChAT (green) marks cholinergic fibers and NET (red) is present in some of these fibers (Figure 7).

NET presence in the sensory nervous system

The presence of NET was examined in dorsal root ganglia (DRG) sections and also using NET double-labeling with the sensory marker calcitonin gene related peptide (CGRP) in the heart. NET protein (red) is highly expressed in all neurons observed in cervical sensory ganglia that provide some of the sensory innervation to the heart (Figure 8A). The intensity of cytoplasmic NET staining is variable among the neurons in the cervical DRG with some neurons highly expressing NET and others with low expression. Generally, NET staining was observed to be throughout the cytoplasm; however, in some neurons NET staining is observed localized to the membrane (Figure 8A, upper right, arrowheads). CGRP-IR (green) and NET-IR (red) were observed in atria (Figure 8B, upper panels). The overlay indicates that NET and CGRP exist in separate fibers (Figure 8B, lower panel).

NET immunoreactivity (red) was also observed in all visible neurons in a section of the lumbar DRG (Figure 9A). Similar to the cervical DRG, there is a variety of staining intensities among neurons in the lumber DRG. The lumbar DRG contain cell bodies that innervate the mesenteric blood vessels. At high power, the separation of NET (green) and CGRP (red) staining in separate fibers is evident indicating that there is no NET protein sensory fibers in the mesentery even though there is NET in the lumbar DRG (Figure 8B).

Discussion

NET in cardiac sympathetic nerves functions to clear NE from the peripheral sympathetic neuroeffector junction and from the circulation. It is surprising then that there is NE uptake function, albeit reduced, in sympathetically denervated animals (18). This suggests that NET protein may be found in other cells in the heart. We determined that substantial NET protein is present in the sympathetically denervated heart then investigated alternative cellular sources of NET in the normal heart. Furthermore, we observed substantial colocalization of NET with TH indicating NET presence in sympathetic fibers, we also observed examples of NET-positive nerve fibers in the heart that were not associated with TH. In summary, we found NET in: 1) sympathetic ganglion cell bodies in stellate, 2) postganglionic sympathetic fibers in the heart, 3) parasympathetic postganglionic neuron cell bodies in cardiac intrinsic ganglia, 4) cardiac cholinergic neurites, and 5) sensory cervical and thoracic dorsal root ganglia.

However, NET is not found in sensory neurites in the heart. These findings were confirmed in the celiac ganglion and mesenteric innervation when possible.

NET in the sympathetically denervated heart

NET is known to be present and functional in sympathetic nerve fibers and sympathetic ganglia. There is a reduction in NE uptake in sympathetically denervated structures suggesting that the site of binding and inactivation of NE was on sympathetic nerves (17). Thus, the focus of research on NET has been in the sympathetic nervous system. However, if the sympathetic nerves were the sole source of NET in the heart, then cardiac denervation should eliminate NET protein, as it does NE content, and virtually eliminate NE uptake via uptake-1.

When the heart is sympathetically denervated using stellate ganglionectomy, there is depletion in endogenous NE content of all heart chambers and to a lesser extent a reduction in NE uptake (18). Approximately 30% of NE uptake capacity of the heart remains intact after stellate ganglionectomy (18). We confirmed that this procedure drastically reduces NE content in all heart chambers, yet it did not affect NET protein content.

NET protein present following denervation and residual NE uptake capacity in the denervated heart suggests a role for non-sympathetic NET in normal heart reuptake function. One example of an alternative site of NET expression is intrinsic cardiac adrenergic (ICA) cells which are non-neuronal cardiocytes found

throughout the myocardium that contain NET protein and display NE uptake capacity (20; 21). NE uptake via extraneuronal monoamine transporter (also known as organic cation transporter-3) in cardiac muscle that could explain the residual NE uptake capacity after sympathetic denervation, this does not explain the presence of NET protein.

It is known that acute denervation procedures do not significantly after NE reuptake and time is needed for the nerves to degenerate (i.e., greater than 5 days) (17). We performed studies two weeks post-denervation to ensure that the nerves were degenerated. Using two independent methods of assessing protein level, we determined that there is substantial NET protein present in the denervated heart. Since stellate ganglionectomy leaves other nervous structures in the heart intact, we investigated cardiac sensory nerves with associated ganglia and intrinsic cardiac neurons for NET protein.

NET in intrinsic neurons

Cardiac intrinsic ganglia contain parasympathetic efferent postganglionic neurons that generally are considered to be of cholinergic phenotype. However, some of these neurons also display noradrenergic/catecholaminergic properties such as expression of catecholamine-synthesizing enzymes (41). This subset of intrinsic neurons is considered to be of mixed phenotype thus do not express the catecholaminergic phenotype in an all-or-nothing manner (8). The neuronal expression profile of various sympathetic and parasympathetic markers vary by

species and tissue innervated (43). The adrenergic neuronal phenotype in parasympathetic intrinsic ganglia is functionally relevant since injection of nicotine to activate these cardiac ganglionic neurons can elicit the classic parasympathetic cardiodepression or an adrenergically mediated cardioaugmentation depending on the subset of ganglion neurons activated (32).

Coexpression of adrenergic (e.g., tyrosine hydroxylase or vesicular monoamine transporter 2 (VMAT2)) and cholinergic (e.g., vesicular acetylcholine transporter (VAChT)) markers with occurs in 40-50% of cardiac intrinsic neurons in the rheses monkey and human heart (43). In these species, the full complement of proteins exists to allow exist to allow sympathetic function. In the mouse, all intrinsic ganglion neurons display cholinergic phenotype while a sub-population have TH and VAChT colocalization (19; 43); however, there is no VMAT2 (43) expression noted. In this case, the lack of VMAT2 indicates that these neurons have a partial adrenergic phenotype.

As to the role of NET in intrinsic ganglia, NE present in the ganglia and would suggest that NET would be required as well. The large amount of NE present in the intrinsic ganglion of the mudpuppy comes from both intrinsic and extrinsic sources (33). NE is released by axons of extrinsic sympathetic innervation and presumably synthesized in the ganglia by catecholamine synthetic enzymes (40). There is direct innervation to intrinsic ganglia by neurons from the stellate ganglia (34; 41). Furthermore, NE is contained in intrinsic neurons in human hearts (40).

Taken together, it is not unreasonable to postulate that these cells would also express NET. We demonstrate that intrinsic neurons in the heart contain NET in the same cells that express ChAT showing that NET is present in parasympathetic neurons. In studies of other mammals, the duality of neurotransmitter expression not only occurs in the cell bodies of extrinsic neurons but also in the nerve endings (43). We visualized NET immunoreactivity in ChAT-positive nerve fibers indicating that NET is present in both cell bodies and nerve terminals of cardiac intrinsic neurons where its role in cardiac function remains to be determined.

NET in sensory nerves

Cardiac sensory neurons are vitally important to heart function as they not only monitor mechanical and chemical changes in the myocardium and associated vasculature but also ultimately determine efferent input to the heart (6). Cardiac sensory neurites in the heart are associated with the nodose ganglia and C7-T4 dorsal root ganglia as well as intrathoracic extracardiac and intrinsic cardiac ganglia (5). Dorsal root ganglion neurons are multi-modal and can transducer mechanical and chemical signals from the specific regions of the myocardium and coronary vascular walls to second order neurons in the central nervous system (4) which relay signals to cardiac efferents destined for the heart.

Sympathetic and sensory neurites are often closely associated anatomically and functionally in the heart. Sympathectomy results in an increase in CGRP

immunoreactivity, particularly in the atria (1; 2), and sympathetic neurotransmitters can modulate sensory neurotransmission in the atria (3; 24). Since sensory nerve fibers respond to adrenergic neurotransmitters, it is feasible that the reuptake system for NE could exist in those same fibers. We investigated if NET was found in sensory neurites.

We did not find evidence of NET in sensory fibers in the heart or mesenteric blood vessels. This is consistent with the finding that sensory denervation in the atria does not alter tissue NE content supporting that there is no uptake or storage of NE in sensory fibers in the heart (29). There is no effect of capsaicin-induced sensory-motor denervation on sympathetic neurotransmission suggesting that there are no functional changes to the sympathetic innervation or function following sensory denervation (36).

Even though NET protein is absent in sensory neurites, NET is found in sensory ganglia at all spinal levels (cervical, thoracic, and lumbar dorsal root ganglia). Dissociated dorsal root ganglion neurons have uptake capacity for NE (26; 44). Further studies are needed to determine the presence of NET in cardiac-associated nodose ganglia. NET in sensory dorsal root ganglia may be associated with uptake of NE from *en passant* sympathetic fibers or perivascular sympathetic fibers in sensory ganglia (30).

Implications

While NET function is known to be important in terminating the adrenergic signal to the heart musculature, vessels, and nodal tissue, the current studies indicate a role of NET in the function of parasympathetic and sensory neurons as well. There is substantial cross-talk between sympathetic, parasympathetic, and sensory nerves in mediating heart function. Dual adrenergic/cholinergic phenotype and expression of NET in postganglionic parasympathetic neurons has functional implication in the heart. If parasympathetic neurons in the heart can synthesize and/or clear NE then there is a possibility of co-release of NE and acetylcholine in the heart. Also, the ability of parasympathetic neurons to respond to and take up NE indicates that NE modulates function of these neurons. These findings may have physiological relevance in the regulation of normal heart function including coronary blood flow, myocardial contractile force, and rate of contraction. Furthermore, the presence of NET in parasympathetic and sensory neurons must be considered in disease states that have known NE reuptake dysfunction as a hallmark such as heart failure (7; 27; 31), orthostatic intolerance (9; 14; 16), hypertension (10; 11; 39), and postural orthostatic tachycardia syndrome (35).

Summary

NET is found in postganglionic sympathetic ganglion neurons, postganglionic sympathetic fibers in the heart and mesentery, parasympathetic postganglionic neuron cell bodies in cardiac intrinsic ganglia, cardiac cholinergic neurites, and sensory cervical, thoracic, and lumbar dorsal root ganglia; however, is not found

in sensory neurites in the heart or mesenteric vasculature. This study has revealed novel sites of NET expression in the rat heart and the functional implications on parasympathetic and sensory neurotransmission and on heart function remain to be determined.

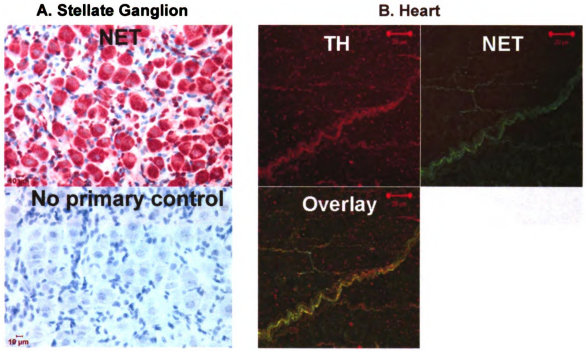

Figure 5.1: NET protein is found in stellate ganglia and is colocalized with tyrosine hydroxylase (TH) in sympathetic fibers in atria. A) Stellate ganglia were fixed, sectioned, and stained with NET primary antibody as described in the methods section. NET immunoreactivity (upper panel, red) is visible under standard brightfield microscopy within the cytoplasm of all neurons in the section. A no primary antibody control section counterstained with hemotoxylin (lower panel) was used to assess specific staining. Scale bar =10 μM. B) Atria were fixed and stained with TH (red, upper left) and NET (green, upper right) to determine colocalization of NET in sympathetic fibers. Images were captured using confocal microscopy of atria whole mount samples. Yellow regions on the overlay image indicate locations were NET and TH staining is present in the same nerve fiber. Scale bar = 20 μM. Images in this dissertation are presented in color.

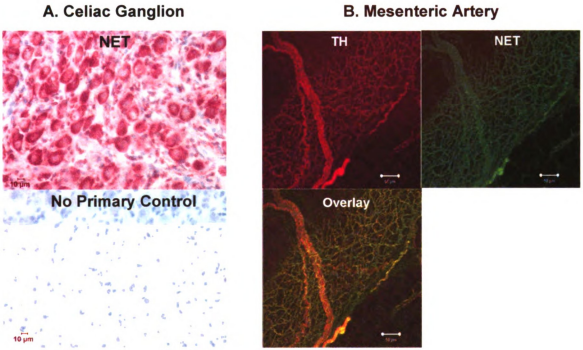

Figure 5.2: NET protein is found in celiac ganglia and is colocalized with tyrosine hydroxylase (TH) in sympathetic fibers in mesenteric vessels. A) Celiac ganglia were fixed, sectioned, and stained with NET primary antibody as described in the methods section. NET immunoreactivity (upper panel, red) is visible under standard brightfield microscopy within the cytoplasm of all neurons in the section. A no primary antibody control section counterstained with hemotoxylin (lower panel) was used to assess specific staining. Scale bar =10 µM. B) Mesenteric vessels were cleaned of fat, fixed, and stained with TH (red, upper left) and NET (green, upper right) to determine colocalization of NET in sympathetic fibers. Images were captured using confocal microscopy of vessel whole mount samples. Yellow regions on the overlay image indicate locations were NET and TH staining is present in the same nerve fiber. Scale bar = 50 µM. Images in this dissertation are presented in color.

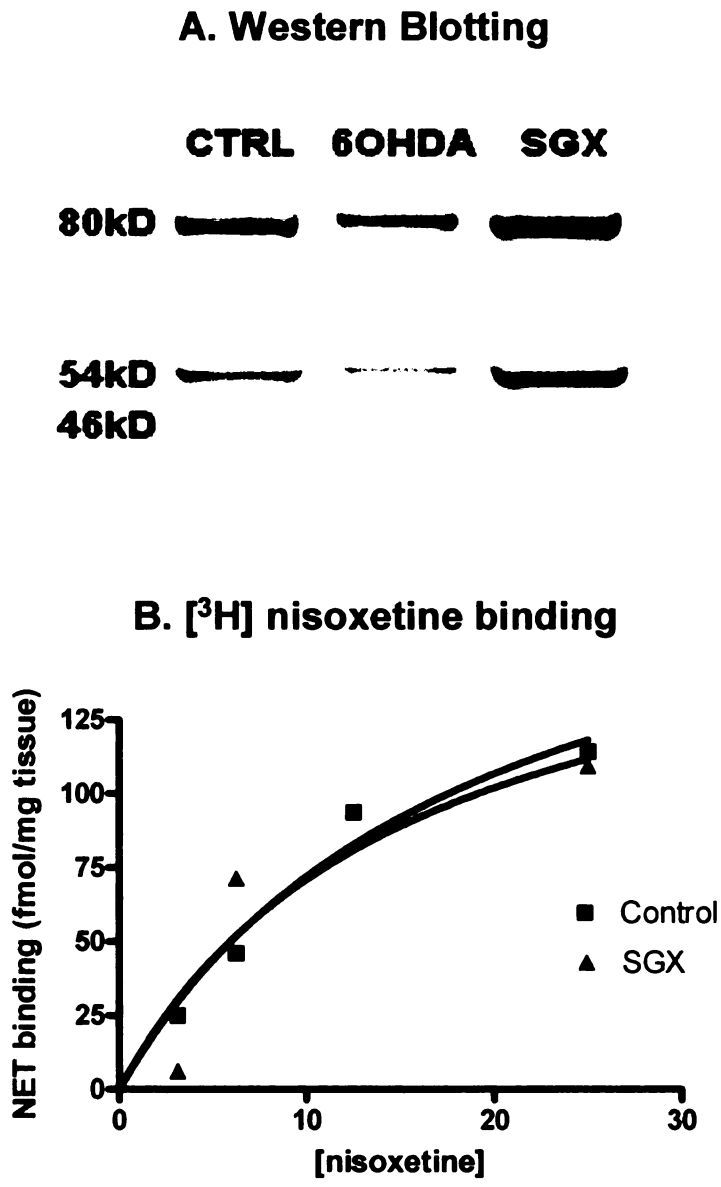

Figure 5.3: NET protein in heart is not depleted by sympathetic denervation. A) Heart homogenate from normal control (CRTL), 6-OHDA denervated (6-OHDA), and stellate ganglionectomized (SGX) rats was used in western blotting for NET. Three molecular weight bands of NET were visualized in all lanes at 80, 54, and 46 kD. There is substantial NET present following sympathetic denervation procedures (n=3). B) Western blot results were confirmed using [^{3}H]-nisoxetine binding in cardiac membranes from normal control and stellate ganglionectomized (SGX) rats. There was no substantial reduction in NET binding in denervated rats (n=1).

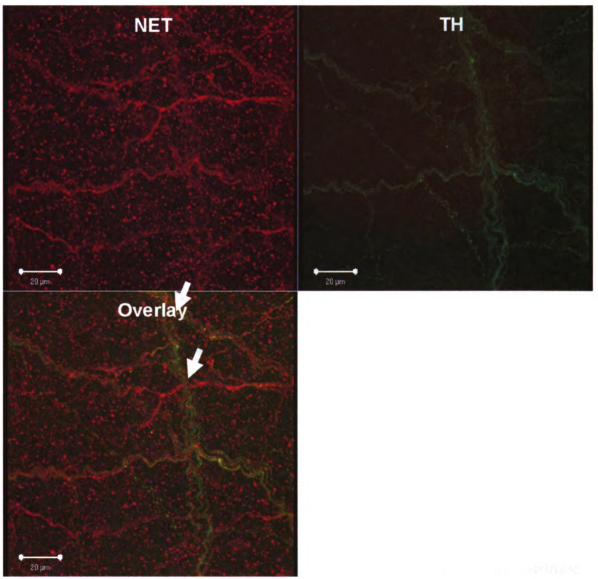

Figure 5.4: NET is found in non-sympathetic fibers in the atria. Atria were fixed and stained with NET (red, upper left) and TH (green, upper right) to determine colocalization of NET in sympathetic fibers. Images were captured using confocal microscopy of atria whole mount samples. Although NET exists in sympathetic fibers in the heart (Fig 1), there are fibers in the heart that are NET-positive/TH-negative (arrowhead on red fiber, lower panel) and vice versa (arrowhead on green fiber, lower panel). Scale bar = 20 µM. Images in this dissertation are presented in color.

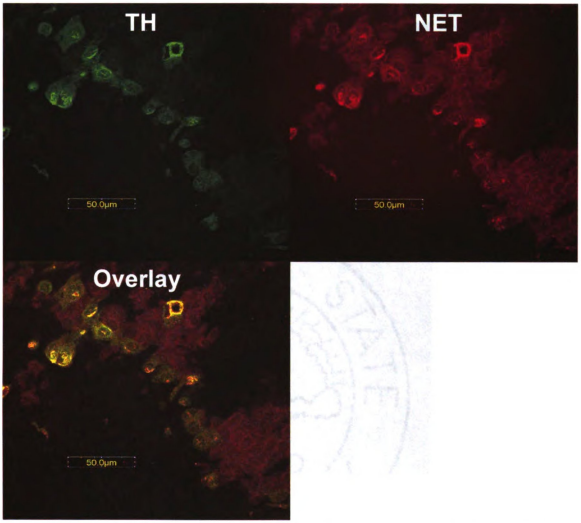

Figure 5.5: NET and tyrosine hydroxylase are colocalized in intrinsic cardiac neurons in the atria. Atria were fixed and stained with TH (green, upper left) and NET (red, upper right) to establish the presence of catecholaminergic proteins in cardiac intrinsic neurons. Images were captured using confocal microscopy of atria whole mount samples. Yellow regions on the overlay image indicate locations were NET and TH staining is present in the same nerve fiber. Scale bar = 50 µM. Images in this dissertation are presented in color.

A.

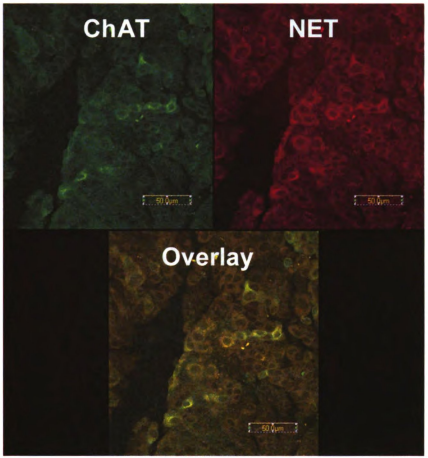

Figure 5.6: NET and choline acetyl transferase (ChAT) are colocalized in intrinsic cardiac neurons in the atria. Atria were fixed and stained with ChAT and NET to establish the presence of catecholaminergic proteins in cardiac intrinsic neurons. A) ChAT (green, upper left) and NET (red, upper right)) are found in the same cells (yellow overlay, lower center). Scale bar = 20 μM. B) At high magnification ChAT (red, upper right) and NET (green, upper right) are found in the same cells (yellow overlay, lower left). Scale bar = 5 μM. Images were captured using confocal microscopy of atria whole mount samples. Yellow regions on the overlay image indicate locations were NET and ChAT staining is present in the same nerve cell body. Images in this dissertation are presented in color.

Figure 5.6 continued

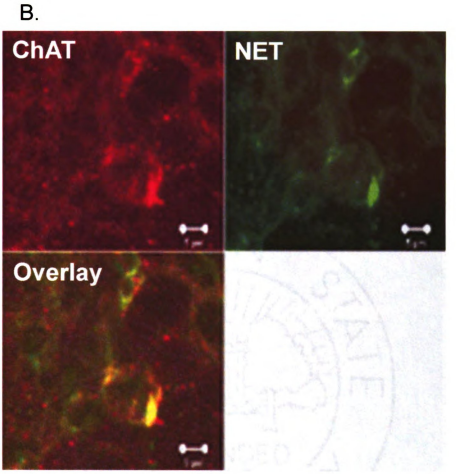

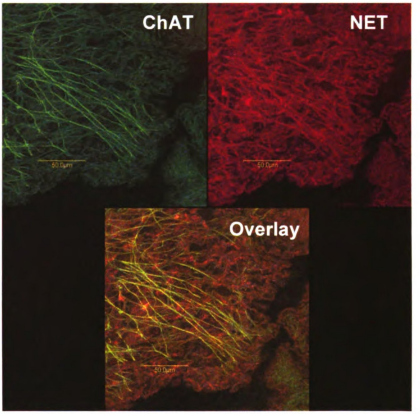

Figure 5.7: NET and choline acetyl transferase (ChAT) are colocalized in cholinergic nerve fibers in the atria. Atria were fixed and stained with ChAT (green, upper left) and NET (red, upper right) to establish the presence of catecholaminergic proteins in cardiac intrinsic neurons. Images were captured using confocal microscopy of atria whole mount samples. Yellow regions on the overlay image indicate locations were NET and ChAT staining is present in the same nerve cell body (lower panel). Scale bar = 50 μM. Images in this dissertation are presented in color.

A. Cervical dorsal root ganglia

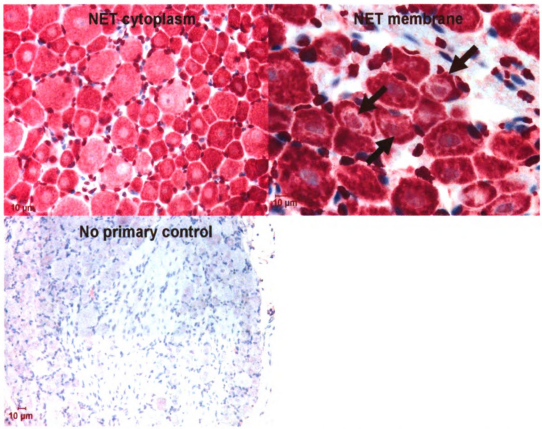

Figure 5.8: NET protein is found in cervical dorsal root ganglia but is not colocalized with calcitonin gene related peptide (CGRP) in sensory fibers in atria. A) Dorsal root ganglia were fixed, sectioned, and stained with NET primary antibody as described in the methods section. NET immunoreactivity (left upper panel, red) is visible under standard brightfield microscopy within the cytoplasm of all neurons in the section. There was membrane localization visualized in some DRG neurons (right upper panel, 100X magnification). A no primary antibody control section counterstained with hemotoxylin (lower panel) was used to assess specific staining. Scale bar =10 µM. B) Vessels were cleaned of fat, fixed, and stained with CGRP (green) and NET (red) to determine colocalization of NET in sensory fibers. Images were captured using confocal microscopy of atria whole mount samples. There was no indication of CGRP and NET colocalization in the same nerve fiber as observed by distinct green and red fibers in the overlay image. Scale bar = 50 µM. Images in this dissertation are presented in color.

Figure 5.8 continued

B. Heart

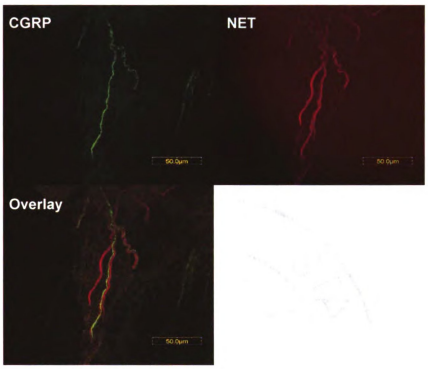

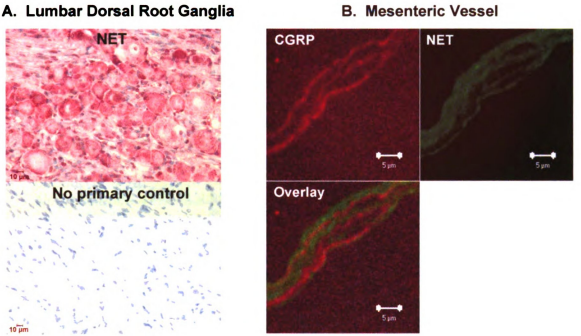

Figure 5.9: NET protein is found in lumbar dorsal root ganglia but is not colocalized with calcitonin gene related peptide (CGRP) in sensory fibers in mesenteric vessels. A) Dorsal root ganglia were fixed, sectioned, and stained with NET primary antibody as described in the methods section. NET immunoreactivity (left upper panel, red) is visible under standard brightfield microscopy within the cytoplasm of all neurons in the section. There was membrane localization visualized in some DRG neurons (right upper panel, 100X magnification). A no primary antibody control section counterstained with hemotoxylin (lower panel) was used to assess specific staining. Scale bar =10 µM. B) Vessels were cleaned of fat, fixed, and stained with CGRP (red) and NET (green) to determine colocalization of NET in sensory fibers. Images were captured using confocal microscopy of atria whole mount samples. There was no indication of CGRP and NET colocalization in the same nerve fiber as observed by distinct green and red fibers in the overlay image. Scale bar = 50 µM. Images in this dissertation are presented in color.

Reference List

1. **Aberdeen J, Corr L, Milner P, Lincoln J and Burnstock G**. Marked increases in calcitonin gene-related peptide-containing nerves in the developing rat following long-term sympathectomy with guanethidine. *Neuroscience* 35: 175-184, 1990.

2. **Aberdeen J, Milner P, Lincoln J and Burnstock G**. Guanethidine sympathectomy of mature rats leads to increases in calcitonin gene-related peptide and vasoactive intestinal polypeptide-containing nerves. *Neuroscience* 47: 453-461, 1992.

3. **Amerini S, Rubino A, Filippi S, Ledda F and Mantelli L**. Modulation by adrenergic transmitters of the efferent function of capsaicin-sensitive nerves in cardiac tissue. *Neuropeptides* 20: 225-232, 1991.

4. **Armour JA**. The little brain on the heart. *Cleve Clin J Med* 74 Suppl 1: S48-S51, 2007.

5. **Armour JA**. Potential clinical relevance of the 'little brain' on the mammalian heart. *Exp Physiol* 93: 165-176, 2008.

6. **Armour JA and Ardell JL**. *Basic and clinical neurocardiology*. Oxford University Press, 2004.

7. **Backs J, Haunstetter A, Gerber SH, Metz J, Borst MM, Strasser RH, Kubler W and Haass M**. The neuronal norepinephrine transporter in experimental heart failure: evidence for a posttranscriptional downregulation. *J Mol Cell Cardiol* 33: 461-472, 2001.

8. **Baluk P and Gabella G**. Some parasympathetic neurons in the guinea-pig heart express aspects of the catecholaminergic phenotype in vivo. *Cell Tissue Res* 261: 275-285, 1990.

9. **Carson RP, Diedrich A and Robertson DM**. Autonomic control after blockade of the norepinephrine transporter: a model of orthostatic intolerance. *J Appl Physiol* 93: 2192-2198, 2002.

10. **Esler M, Alvarenga M, Pier C, Richards J, El-Osta A, Barton D, Haikerwal D, Kaye D, Schlaich M, Guo L, Jennings G, Socratous F and Lambert G**. The neuronal noradrenaline transporter, anxiety and cardiovascular disease. *J Psychopharmacol* 20: 60-66, 2006.

11. **Esler MD, Rumantir M, Kaye DM, Jennings G, Hastings J, Socratous F and Lambert G**. Sympathetic nerve biology in essential hypertension. *Clin Exp Pharmacol Physiol* 28: 986-989, 2001.

12. **Farnebo LO**. Histochemical studies on the uptake of noradrenaline in the perfused rat heart. *Br J Pharmacol* 34: 227P-228P, 1968.

13. **Goldstein DS, Brush JE, Jr., Eisenhofer G, Stull R and Esler M**. In vivo measurement of neuronal uptake of norepinephrine in the human heart. *Circulation* 78: 41-48, 1988.

14. **Goldstein DS, Holmes C, Frank SM, Dendi R, Cannon RO, III, Sharabi Y, Esler MD and Eisenhofer G**. Cardiac sympathetic dysautonomia in chronic orthostatic intolerance syndromes. *Circulation* 106: 2358-2365, 2002.

15. **Habecker BA, Klein MG, Cox BC and Packard BA**. Norepinephrine transporter expression in cholinergic sympathetic neurons: differential regulation of membrane and vesicular transporters. *Dev Biol* 220: 85-96, 2000.

16. **Hahn MK, Robertson DM and Blakely RD**. A Mutation in the Human Norepinephrine Transporter Gene (SLC6A2) Associated with Orthostatic Intolerance Disrupts Surface Expression of Mutant and Wild-Type Transporters. *J Neurosci* 23: 4470-4478, 2003.

17. **Hertting G, Axelrod J, Kopin IJ and Whitby LG**. Lack of uptake of catecholamines after chronic denervation of sympathetic nerves. *Nature* 189: 66, 1961.

18. **Hertting G and Schiefthaler T**. The effect of stellate ganglion excision on the catecholamine content and the uptake of H3-norepinephrine in the heart of the cat. *Int J Neuropharmacol* 3: 65-69, 1964.

19. **Hoard JL, Hoover DB and Wondergem R**. Phenotypic properties of adult mouse intrinsic cardiac neurons maintained in culture. *Am J Physiol Cell Physiol* 293: C1875-C1883, 2007.

20. **Huang MH, Bahl JJ, Wu Y, Hu F, Larson DF, Roeske WR and Ewy GA**. Neuroendocrine properties of intrinsic cardiac adrenergic cells in fetal rat heart. *Am J Physiol Heart Circ Physiol* 288: H497-H503, 2005.

21. **Huang MH, Friend DS, Sunday ME, Singh K, Haley K, Austen KF, Kelly RA and Smith TW**. An intrinsic adrenergic system in mammalian heart. *J Clin Invest* 98: 1298-1303, 1996.

22. **Iversen LL**. The uptake of catechol amines at high perfusion concentrations in the rat isolated heart: a novel catechol amine uptake process. 1964. *Br J Pharmacol* 25: 18-33, 1965.

23. **Iversen LL, Glowinski J and Axelrod J**. Reduced uptake of tritiated noradrenaline in tissues of immunosympathectomized animals. *Nature* 206: 1222-1223, 1965.

24. **Kawasaki H, Nuki C, Saito A and Takasaki K**. Role of calcitonin gene-related peptide-containing nerves in the vascular adrenergic neurotransmission. *J Pharmacol Exp Ther* 252: 403-409, 1990.

25. **Kopin IJ, Rundqvist B, Friberg P, Lenders J, Goldstein DS and Eisenhofer G**. Different relationships of spillover to release of norepinephrine in human heart, kidneys, and forearm. *Am J Physiol* 275: R165-R173, 1998.

26. Kreulen, D. L., Manteuffel, J. L. Rogers J. L., Larson, R. E., Zheng, Z. L., and Olsen, L. K. Norepinephrine transporter in sympathetic and primary sensory neurons. Neuroscience Abstracts . 2001.
Ref Type: Abstract

27. **Kreusser MM, Haass M, Buss SJ, Hardt SE, Gerber SH, Kinscherf R, Katus HA and Backs J**. Injection of nerve growth factor into stellate ganglia improves norepinephrine reuptake into failing hearts. *Hypertension* 47: 209-215, 2006.

28. **Li W, Knowlton D, Van Winkle DM and Habecker BA**. Infarction alters both the distribution and noradrenergic properties of cardiac sympathetic neurons. *Am J Physiol Heart Circ Physiol* 286: H2229-H2236, 2004.

29. **Luthman J, Stromberg I, Brodin E and Jonsson G**. Capsaicin treatment to developing rats induces increase of noradrenaline levels in the iris without affecting the adrenergic terminal density. *Int J Dev Neurosci* 7: 613-622, 1989.

30. **McLachlan EM, Jänig W, Devor M and Michaelis M**. Peripheral nerve injury triggers noradrenergic sprouting within dorsal root ganglia. *Nature* 363: 543-545, 1993.

31. **Munch G, Rosport K, Bultmann A, Baumgartner C, Li Z, Laacke L and Ungerer M**. Cardiac overexpression of the norepinephrine transporter uptake-1 results in marked improvement of heart failure. *Circ Res* 97: 928-936, 2005.

32. **Murphy DA, O'Blenes S, Hanna BD and Armour JA**. Capacity of intrinsic cardiac neurons to modify the acutely autotransplanted mammalian heart. *J Heart Lung Transplant* 13: 847-856, 1994.

33. **Parsons RL, Neel DS, McKeon TW and Carraway RE**. Organization of a vertebrate cardiac ganglion: A correlated biochemical and histochemical study. *The Journal of Neuroscience* 7: 1987.

34. **Richardson RJ, Grkovic I and Anderson CR**. Immunohistochemical analysis of intracardiac ganglia of the rat heart. *Cell Tissue Res* 314: 337-350, 2003.

35. **Robertson DM, Shannon JR, Biaggioni I, Ertl AC, Diedrich A, Carson R, Furlan R, Jacob G and Jordan J**. Orthostatic intolerance and the postural tachycardia syndrome: genetic and environment pathophysiologies. Neurolab Autonomic Team. *Pflugers Arch* 441: R48-R51, 2000.

36. **Rubino A, Ralevic V and Burnstock G**. Sympathetic neurotransmission in isolated rat atria after sensory-motor denervation by neonatal treatment with capsaicin. *J Pharmacol Exp Ther* 282: 671-675, 1997.

37. **Savchenko V, Sung U and Blakely RD**. Cell surface trafficking of the antidepressant-sensitive norepinephrine transporter revealed with an ectodomain antibody. *Mol Cell Neurosci* 24: 1131-1150, 2003.

38. **Schroeter S, Apparsundaram S, Wiley RG, Miner LH, Sesack SR and Blakely RD**. Immunolocalization of the cocaine- and antidepressant-sensitive l- norepinephrine transporter. *J Comp Neurol* 420: 211-232, 2000.

39. **Shibao C, Raj SR, Gamboa A, Diedrich A, Choi L, Black BK, Robertson D and Biaggioni I**. Norepinephrine transporter blockade with atomoxetine induces hypertension in patients with impaired autonomic function. *Hypertension* 50: 47-53, 2007.

40. **Singh S, Johnson PI, Javed A, Gray TS, Lonchyna VA and Wurster RD**. Monoamine- and histamine-synthesizing enzymes and neurotransmitters within neurons of adult human cardiac ganglia. *Circulation* 99: 411-419, 1999.

41. **Slavikova J, Kuncova J, Reischig J and Dvorakova M**. Catecholaminergic neurons in the rat intrinsic cardiac nervous system. *Neurochem Res* 28: 593-598, 2003.

42. **Stefanini M, De MC and Zamboni L**. Fixation of ejaculated spermatozoa for electron microscopy. *Nature* 216: 173-174, 1967.

43. **Weihe E, Schutz B, Hartschuh W, Anlauf M, Schafer MK and Eiden LE**. Coexpression of cholinergic and noradrenergic phenotypes in human and nonhuman autonomic nervous system. *J Comp Neurol* 492: 370-379, 2005.

44. **Zheng ZLXDJJMKLOaDLK**. Characterization of norepinephrine transporter in rat dorsal root ganglia *in vitro*. *J Neuroscience* 0: 0, 2004.

45. **Zhu MY and Ordway GA**. Down-regulation of norepinephrine transporters on PC12 cells by transporter inhibitors. *J Neurochem* 68: 134-141, 1997.

CHAPTER 6: NET mRNA AND PROTEIN ARE NOT REDUCED IN STELLATE GANGLIA AND ARE REGIONALLY DECREASED IN THE HEART CHAMBERS FROM DOCA-SALT HYPERTENSIVE RATS

Abstract

There is substantial evidence of a reduction in cardiac uptake of norepinephrine (NE) via the neuronal NE transporter (NET) in hypertension. The mechanism for this reduction is poorly understood, but it is known that nerve growth factor (NGF) is positively related to NET function. The purpose of this study was to: 1) determine if reduced cardiac NET mRNA and protein in the stellate ganglia and heart chambers is the cause of reduced NE reuptake that occurs in the hypertensive heart, 2) identify if a reduction in NGF occurs in hypertension to cause NET downregulation, and 3) determine if NET mRNA and protein are regionally altered in hypertension. Using the deoxycorticosterone (DOCA)-salt rat model of hypertension, we assessed NET mRNA and protein expression in the stellate ganglion and heart chambers. After 4-weeks of treatment, there was no change in NET mRNA in the either the right or the left stellate ganglia from hypertensive rats ($n=5$-7, $p>0.05$). NET immunoreactivity in the left stellate ganglion was significantly increased ($n=4$, $p<0.05$) while the right stellate ganglion was unchanged ($n=4$, $p>0.05$). In the heart chambers, NE content and NGF were analyzed. NE was significantly reduced in the right atrium ($n=6$, $p<0.05$) of DOCA-salt rats but no other changes were noted with hypertension. NGF was unchanged in all heart chambers in hypertensive rats ($n=4$, $p>0.05$). There was a significant reduction of NET mRNA in the LA of DOCA-salt hearts (relative expression ratio 0.5, $n=5$-6, $p<0.05$). NET protein in the LA was also

significantly reduced. All other heart chambers had unchanged or increased NET expression. Therefore, 1) the functional reduction in whole heart NE reuptake in hypertension is not due to reduced NGF, 2) reduced reuptake in the hypertensive heart is not due to a global reduction in NET mRNA or protein in the stellate ganglion and heart, 3) NET regulation occurs regionally in the heart and stellate ganglion.

Introduction

The sympathetic innervation from the heart arises primarily from the bilateral stellate ganglia. The actions of circulating and released NE in the heart are attenuated primarily by neuronal reuptake of NE into adrenergic nerve terminals (26). This uptake process into nerve terminals occurs through a membrane transporter known as NE transporter (NET) or "uptake-1". Reduced function or pharmacological blockade of NET results in elevated junctional NE and spillover of NE into the circulation; therefore NET has functional relevance in mediating adrenergic responses. For example, NET deficient mice demonstrate elevation of heart rate and mean arterial pressure as well as significantly elevated plasma NE (34).

There is a reduction of cardiac NE reuptake and NE content in hypertension both *in vivo* and in isolated heart preparations (24; 28; 33; 36; 40; 50). For example, there is reduced accumulation of [^{3}H] NE in the heart following tail vein infusion and in an *in vitro* heart perfusion study (13; 14), and this is associated with

reduced endogenous NE content per gram of heart. A highly significant inverse correlation exists between blood pressure and [^{3}H] NE accumulation in the heart *in vivo* (14; 33). This is observed in multiple models of hypertension in both the developmental and sustained phase of blood pressure elevation (33) and occurs in parallel with increased inotropic response to NE and with elevation in blood pressure (40).

Human studies also indicate a reduction in cardiac NE reuptake in hypertension (17; 21; 22; 55). Lean hypertensive patients have increased spillover of NE from the heart, reduced fractional extraction of infused [^{3}H] NE, increased NE extraneuronal metabolites (due to elevated junctional NE), and reduced release of the intraneuronal metabolite [^{3}H] DHPG (due to less reuptake into nerve terminals) (53). In another study, hypertensive patients had elevated muscle sympathetic nerve activity, elevated total and cardiac-specific NE spillover, reduction of DHPG in plasma, and displayed a lesser effect of NET blockade with despiramine (54).

Taken together, the human and animal work provides evidence suggesting that the NET dysfunction in the heart could play a prominent role in hypertension; however, the mechanism by which this happens is unclear. Most studies have examined whole heart NE accumulation or uptake without molecular examination of NET mRNA and protein amount. One possibility is that NET mRNA and/or protein is downregulated in hypertension, possibly by reduced NGF in the heart,

causing reduced NE uptake. We examined regional differences in NET mRNA and protein in the right versus left stellate ganglia that provide sympathetic innervation to the heart and in heart chambers in hypertension. The purpose of this study was to: 1) determine if reduced cardiac NET mRNA and protein in the stellate ganglia and heart chambers is the cause of reduced NE reuptake that occurs in the hypertensive heart, 2) identify if a reduction in cardiac NGF occurs in hypertension to cause NET downregulation, and 3) determine if NET mRNA and protein are regionally altered in hypertension.

Materials and Methods

Animals

Adult male Sprague Dawley rats (250-300 g; Charles River Laboratories, Inc., Portage, MI) were used. Normal rats were used in control studies (C). The hypertensive group underwent uninephrectomy and subcutaneous implantation of deoxycorticosterone acetate salt (DOCA, 200 mg kg^{-1}) under isoflurane anesthesia. Post-operatively, the rats were given drinking water containing 1% NaCl and 0.2%KCl (herein, the DOCA-salt treated group is referred to as hypertensive (HT)). Normotensive (NT) controls to the HT rats were uninephrectomized but were not given DOCA implantation or salt drink. Four weeks after surgery, the arterial blood pressure was measured using the tail cuff method. Rats with a mean systolic arterial pressure of > 150 mmHg were considered hypertensive. All animal experiments were performed in accordance with the "Guide for the Care and Usage of Laboratory Animals" (National

Research Council) and were approved by the Animal Use and Care Committee of Michigan State University. Animals were housed two per cage in temperature and humidity-controlled rooms with a 12 hour/12 hour light-dark cycle. Standard pellet rat chow and water were given *ad libitum*.

Tissue Collection

Rats were anesthetized with sodium pentobarbital (Sigma-Aldrich Corp, St. Louis, MO, 65 mg/kg, i.p.) followed by thoracotomy. Freshly dissected hearts were removed quickly from anesthetized rats and immediately placed into chilled (4 °C) phosphate buffered saline (PBS, 137 mM sodium chloride, 2.7 mM potassium chloride, 4.3 mM sodium phosphate dibasic and 1.4 mM potassium phosphate monobasic) for rinsing and separation of chambers. While in buffer, the chambers were quickly separated in the following order: right atrium, left atrium, right ventricle outer wall, ventricular septal wall, and left ventricle outer wall. The freshly dissected heart chambers were immediately placed into Trizol (2ml for atria and 4 ml for ventricles) then processed using a variable speed Omni TH-115 homogenizer with 7mm saw tooth generator probe (Omni International Inc., Warrenton, VA) for ~30 seconds at high speed and allowed to stand on ice for ~10 minutes. Total RNA was isolated immediately or from Trizol homogenates stored less than 1 week at -80°C. Right and left stellate were removed and fixed as described below or placed immediately into Trizol reagent for RNA isolation (300uL for ganglia) and allowed to stand on ice for ~20 minutes to ensure penetration of Trizol into the tissue, then stored at -80°C for less than

one week until RNA isolation. For preparation of tissue for NE analyses see below.

Stellate Immunohistochemistry

Stellate ganglia were fixed in 10% neutral buffered formalin for 2 hours then transferred to 70% ethanol, routinely processed, embedded in paraffin and sectioned on a rotary microtome at 5μM. Sections were placed on slides coated with 2% 3-Aminopropyltriethoxysilane, dried at 56°C overnight then deparaffinized in Xylene and hydrated through descending grades of ethyl alcohol to distilled water. After incubation in Tris buffered saline (TBS, pH 7.4) for 5 minutes, slides were antigen retrieved utilizing citrate buffer pH 6.0 (Biogenex, San Ramon CA) in a vegetable steamer (Oster, Boca Raton FL) for 30 minutes at 100°C, allowed to cool on the counter at room temperature for 10 minutes and rinsed in several changes of distilled water. Endogenous peroxidase was blocked utilizing 3% hydrogen peroxide for 30 minutes followed by running tap and distilled water rinses. Standard avidin-biotin complex staining steps were performed at room temperature on the DAKO Autostainer. After blocking with normal goat serum for 30 minutes, slides were incubated 15 minutes each in avidin D (Vector, Burlingame CA) and d-biotin (Sigma, St. Louis MO) to block endogenous avidin and biotin. Slides were then rinsed in several changes of TBS + Tween 20 (TBS-T), incubated for 60 minutes at room temperature with the polyclonal primary antibody NET 48411 (1:250 in Scytek normal antibody diluent (Scytek, Logan, UT)). Slides were then rinsed in several

changes of TBS-T then incubated in biotinylated goat anti-rabbit IgG H+L (Vector, Burlingame CA) in normal antibody diluent 1:200 for 30 minutes. Slides were rinsed in TBS-T followed by the application of Vectastain® Elite ABC Reagent (Vector, Burlingame CA) for 30 minutes. The slides were rinsed with TBS-T and developed using Nova Red Peroxidase substrate kit (Vector, Burlingame CA) for 15 minutes. Slides were rinsed in distilled water, counterstained using Lerner 2 hematoxylin for 1 minute, differentiated in 1% aqueous glacial acetic acid, and rinsed in running tap water then dehydrated through ascending grades of ethyl alcohol, cleared through several changes of xylene and cover slipped using Flotex (Lerner, Pittsburgh PA) permanent mounting media.

Sections of right and left stellate ganglia from an animal were mounted on the same slide for a direct comparison under the same experimental conditions. Images were viewed using standard brightfield microscopy (Olympus BX60, Center Valley, PA). NET staining in ganglia was quantified by assessing all individual neuron cell bodies in a single section of stellate ganglia using NIH Image J Version 1.37 software. The nucleus did not stain positive for NET and was not included in the determination of staining intensity. The arbitrary intensity of NET staining was determined by using the straight line measurement tool and drawing a line in a region defined by the user to contain cytoplasmic NET staining in every cell in a section from each ganglion. The mean intensity values in arbitrary units for individual neurons were then averaged to determine total

NET staining intensity per ganglia. Staining intensity of right stellate ganglia was compared to left stellate ganglia using a paired t-test.

RNA isolation and real time PCR

Frozen ganglia and adrenal gland in Trizol were thawed on ice then were homogenized in Trizol using an RNase-free Kontes Pellet Pestle® with hand-held motor in a compatible RNase-free Kontes mircocentrifuge tube (Fisher Scientific, Hanover Park, IL). Homogenized heart tissue in Trizol was thawed on ice. Total RNA was isolated from all tissues using the standard TRIzol® procedure (GIBCO Life Technologies, Carlsbad, CA) with the use of glycogen as an RNA carrier for ganglia. The RNA pellet was dried for 5 minutes, resuspended in an appropriate volume of TE Buffer (pH 7.0, Ambion, Austin, TX) and stored at -80°C. The concentration and purity/integrity of RNA was ascertained spectrophotometrically (A260/A280 and A260/A230) using a Nanodrop ND-1000 Spectrophotometer (Nanodrop, Wilmington, DE). To eliminate residual genomic DNA in the preparation, total RNA samples were treated with diluted RNase-free DNase I (10U/μl, Roche Diagnostics, Nutley, NJ) for 30 minutes at 37°C; DNase I was inactivated by heating for 10 minutes at 75°C.

NET primers were derived from the Rattus Norvegicus NET gene (Ascension # Y13223, National Center for Biotechnology Information GenBank). Primers were developed using Primer3 software (http://frodo.wi.mit.edu/, Massachusetts Institute of Technology). A NCBI basic local alignment search tool (BLAST)

search ensured the specificity of primer sequences for rat NET and the primers were synthesized at the Macromolecular Structure, Sequencing and Synthesis Facility at Michigan State University. Predicted sequences of PCR amplification products were aligned with other rat sequences in GenBank to examine the stringency. Primers were tested to determine efficiency and this value used in calculations of fold-change. NET forward primer: 5'-GCC TGA TGG TCG TTA TCG TT-3', NET reverse primer: 5'-CAT GAA CCA GGA GCA CAA AG-3', GAPDH forward primer: 5'-ATC ACT GCC ACT CAG AAG-3', GAPDH reverse primer: 5'-AAG TCA CAG GAG ACA ACC -3'.

All samples to be compared were run on a single 96 well plate when possible to allow for accurate comparisons. A two-step RT–PCR was performed. The first strand complementary DNA (cDNA) was synthesized from a starting amount of 70 ng total DNase treated RNA for real time PCR by adding the following components into a nuclease-free microcentrifuge tube (20 μl reaction volume): Oligo(dT) (500 μg/ml) (Invitrogen, Carlsbad, CA), 10mM dNTP mix (Invitrogen, Carlsbad, CA), 5X first strand buffer, 0.1 M DTT (dithiothreitol), RNase inhibitor (Roche Diagnostics, Indianapolis, IN), and Superscript II RNase H- reverse transcriptase (Invitrogen, Carlsbad, CA). Samples were mixed, incubated at 42°C for 60 minutes, and Superscript II was inactivated by heating at 70°C for 15 minutes. Additional samples were run without reverse transcriptase enzyme (no RT) to rule out contamination and a negative control was run in which no cDNA template was added to the PCR reaction (No Template Control). For real time

PCR, a 25 μl PCR reaction volume was prepared with cDNA (70ng/μl) from the first-strand reaction, forward primer (20mM), reverse primer (20 mM), SYBR Green Supermix (Applied Biosystems, Bedford, MA) and DEPC-treated distilled water (Ambion, Austin, TX). Real time PCR thermal profile was set up according to manufacturers instructions for SYBR green and run for 60 cycles to achieve full amplification of NET in the heart. A dissociation protocol (60-95 °C melt) was done at each end of the experiment to verify that only one amplicon was formed during the process of amplification. Relative quantification of mRNA was measured against the internal control, GAPDH. End point, used in qPCR quantification and Ct value, is defined as the PCR cycle number that crosses an arbitrarily placed signal threshold. Relative expression value calculation and statistical analysis was performed by Pair Wise Fixed Reallocation Randomization Test© (http://www.gene-quantification.info) using Relative Expression Software Tool (REST) (48)

^{3}H-nisoxetine binding

Preparation of Total Cardiac Membranes: Frozen heart chambers were pulverized on dry ice and then transferred to a mortar and pestle that had been pre-chilled with liquid nitrogen. Tissue was further processed by grinding and then suspended in the appropriate amount of homogenization buffer without detergent to keep membranes intact (50 mM Tris pH 7.4, 120 mM NaCl, 5 mM KCl). The suspended tissue in solution was transferred to an ice cold 10 ml glass hand-held homogenizer for 10 strokes of further gentle processing in ice.

For ventricular tissue, the homogenate was centrifuged (Sorvall RC 5B Plus) at 700 xg for 10 min at 4°C to remove nuclei and cellular debris, and atrial membranes were used without centrifugation. Samples were spun at 40,000 xg for 30 minutes after which the supernatant was discarded and the pellet resuspended in an additional 4 ml of buffer. A second identical spin was performed, the supernatant discarded, and the pellet stored at -80°C until use.

Binding Assay: Differences in NET protein expression in cardiac membranes from individual heart chambers from NT and HT animals was determined by assessing [^{3}H]-Nisoxetine (Perkin-Elmer, Waltham, MA) binding in a manner similar to that described previously (42; 64). Frozen membrane pellets were resuspended in ice cold incubation buffer (50mM Tris pH 7.4, 300mM NaCl, 5 mM KCl) on ice just prior to use. The resuspended membranes were loaded in quadruplicate into 96-well reaction plates and aliquots were used in parallel for a Bradford protein assay to determine protein concentration. Samples were assessed for total and background binding. Cardiac membranes from both groups were incubated with 15 nM [^{3}H]-Nisoxetine in duplicate with additional duplicate wells used to determine non-specific binding with 1.5 mM desipramine. Samples were incubated on a shaker for a minimum of 4 hours at 0° C then filtered through glass fiber filters presoaked in 0.5% polyethylenimine using a 96-well Filtermate cell harvester (Packard Biosciences, Shelton, CT, USA). Standard scintillation counting was performed using Ecolite scintillation fluid (ICN Biomedicals, Irvine CA, USA).

Western Blotting

Frozen heart chambers were pulverized on dry ice and then transferred to a mortar and pestle that had been pre-chilled with liquid nitrogen. Tissue was further processed by grinding, then suspended in the appropriate amount of homogenization buffer (10mM HEPES (Sigma, St. Louis, MO), 0.15M NaCl (VWR, West Chester, PA), 1mM EDTA (Sigma, St. Louis, MO), 1mM phenol methane sulfanyl fluoride (PMSF, Roche, Indianapolis, IN), 1μg/ml leupeptin (Roche, Indianapolis, IN), and 1μg/ml aprotinin (Roche, Indianapolis, IN), amount per tissue). The suspended tissue was then homogenized using a variable speed Omni TH-115 homogenizer with 5mm saw tooth generator probe (Omni International Inc., Warrenton, VA) for ~30 seconds at high speed. Finally, the processed tissue in solution was transferred to a 10 ml glass hand-held homogenizer for 10 strokes of further processing. The homogenate was centrifuged (Sorvall RC 5B Plus) at 700xg for 10 min at 4°C to remove nuclei and cellular debris, assessed in triplicate for protein concentration using a modified Bradford protein assay (Bio-Rad, Hercules, CA), and the supernatant containing total protein was frozen until use at -80°C.

Standard Western blotting was performed. Samples containing 50μg protein were prepared, loaded into 4% stacking gel/10% resolving gels and run at 100 V for ~90 minutes until the leading edge of samples traveled to the bottom of gel. All heart chambers from an animal were run on the same gel to ensure accurate

comparison across chambers. Transfer to polyvinylidene fluoride (PVDF) membranes (Bio-Rad, Hercules, CA) was performed at a constant voltage of 100 V at 4°C for 60 minutes. The membranes were blocked with 4% non-fat dry milk in PBS containing 0.1% Tween-20 for one hour with shaking at room temperature. Membranes were then incubated overnight at 4°C with rabbit anti-rat NET 11-A primary antibody (Alpha Diagnostics Intl Inc, San Antonio, TX) diluted 1:250 in 4% milk solution. The primary antibody was prepared fresh and was not reused. The membranes were rinsed with PBS containing 0.1% Tween-20 and incubated for one hour at 4°C with anti-rabbit IgG horseradish peroxidase (HRP) secondary antibody (Santa Cruz Biotech, Santa Cruz, CA) diluted 1:2000 in 4% milk solution. Immunoreactivity was detected using Femto® chemiluminescence kit (Pierce Chemical, Rockford, IL) to visualize bands. The membrane was imaged using Syngene ChemiGenius Gel Documentation System with GeneSnap software and was quantified using GeneTools software (Syngene, Frederick, MD). All membranes were counter-stained with Coomassie Blue (Invitrogen, Carlsbad, CA) to verify equal protein loading. Data were normalized for protein loading using Coomassie Blue staining. Data are expressed as arbitrary density units normalized for protein loading. Total NET was calculated as the sum of the normalized densities of all three molecular weight variants per chamber.

Norepinephrine measurements

Heart chambers were homogenized in ice-cold 0.1 M perchloric acid. The homogenate was then centrifuged at 10,000 rpm for 15 min at 4°C and the supernatant was further processed by solid phase extraction using Oasis MCX cartridges, 30 mg / 1cc (Waters, Milford, MA, USA) as previously described (44). The eluate was analyzed by capillary electrophoresis with electrochemical detection (CE-EC). CE-EC using boron-doped diamond electrode was employed for NE determination in the heart chambers. The CE-EC system, electrochemical detection cell and electrode fabrication was described elsewhere (12). The separation and detection was performed using following conditions: 76 cm long, 362 μm o.d., 29 μm i.d. capillary, 250 mM boric acid - 1 M potassium hydroxide run buffer of pH 8.8, separation voltage 24 kV, detection potential +0.86 V vs Ag/AgCl and electrokinetic injection at 18 kV for 8 s.

Results

Blood pressure

Systolic blood pressure was significantly elevated following 4-weeks of DOCA-salt treatment compared to uninephrectomized control rats (Figure1, $p<0.001$). Hypertensive (HT) rats has a mean systolic blood pressure of 185.2 ± 6.97 mmHg (n=19) while normotensive control (NT) had a mean systolic blood pressure of 142.6 ± 4.03 mmHg (n=23).

NET mRNA expression in stellate ganglion

NET mRNA was expressed in right and left stellate ganglia in both HT and NT groups. NET mRNA was significantly higher in the right versus the left stellate ganglion in NT rats (data not shown). NET expression in NT animals from both right and left stellate ganglia was normalized to 1 so that a relative expression ratio of NT to HT could be calculated. There was no difference in expression of NET mRNA in NT versus HT in either the left (Figure 2A, left panel; 1.00 vs 1.08 ± 0.45 relative expression ratio, $p>0.05$, $n=5$) or right (Figure 2A, right panel; 1.00 vs 1.47 ± 0.84 relative expression ratio, $p>0.05$, $n=7$) stellate ganglia. These results are also apparent from the mean cycle threshold (Ct) values for each tissue (Figure 2B).

NET immunoreactivity in stellate ganglion

NET protein expression was not different between left and right stellate ganglion in NT animals (Figure 3; $p>0.05$, $n=4$). There was a significant increase in NET protein in the left stellate of HT animals compared to control ($p<0.05$, $n=4$), but there was no difference in NET protein in the right stellate ganglion from HT animals (Figure 3; $p>0.05$, $n=4$).

Chamber NE content

Assessment of chamber NE content was performed in normal control animals (C), NT, and HT rats (Figure 4). In the RA, there was a significant reduction in NE in NT (2.39 ± 0.31 µg NE/g tissue, $p<0.05$, $n=6$) and HT (1.04 ± 0.11 µg NE/g tissue, $p<0.05$, $n=5$) compared to C (0.52 ± 0.08 µg NE/g tissue, $n=3$) and there

was also a significant reduction in NT compared to HT ($p<0.05$). This was the only chamber in which there was reduction in tissue NE levels between NT and HT groups. In the LA and the VS, both NT (n=6) and HT (n=5) groups had significantly lower NE than C animals (n=3) but NT and HT were not different ($p>0.05$) from each other (LA-C 1.60 ± 0.18, LA-NT 0.86 ± 0.10, LA-HT 0.72 ± 0.052; VS-C 0.52 ± 0.04, VS-NT 0.35 ± 0.05, VS-HT 0.23 ± 0.03). In the RV and LV there was no change in tissue NE levels in any group.

Nerve Growth Factor

NGF protein was measured in all heart chambers from NT and HT rats. There was no difference in the amount of NGF protein expressed in NT versus HT rats in any chamber (Figure 5, $p>0.05$, n=4).

NET mRNA expression in heart chambers

NET mRNA was found in extracts from all heart chambers and was expressed at higher levels in the atria than the ventricles from NT animals (data not shown). NET expression in NT animals from each chamber was normalized to 1 so that a relative expression ratio of NT to HT could be calculated. In HT animals there was a regional difference in NET mRNA changes with elevated blood pressure (Figure 6A). NET mRNA in the RA was unchanged (1.00 vs 1.01 ± 0.37) relative expression ratio $p>0.05$, n=6). The LA was the only chamber in which NET mRNA displayed a significant reduction in expression in HT animals 1.00 vs 0.34 ± 0.12 relative expression ratio, $p<0.05$, n=6). In both ventricles there was a

significant elevation in NET mRNA expression in HT animals. NET mRNA expression in the RV from HT animals was increased compared to NT (1.69 ± 0.41; $p<0.05$, n=4). Similarly, NET mRNA from the HT LV was increased from NT (3.69 ± 0.93; $p<0.05$, n=7). These differences are also apparent from the mean cycle threshold (Ct) values for each tissue (Figure 6B).

NET protein expression in heart chambers

Chamber NET protein level between NT and HT animals was compared using single concentration ^{3}H-nisoxetine binding in cardiac membranes. In the RA from HT animals, there was a significant increase in NET protein compared to NT (Figure 7A: 81.49 ± 0.49 vs 306.8 ± 42.63 fmol/mg, $p<0.05$, n=7-8). There was a significant reduction in LA NET protein from HT animals (Figure 7B: 160 ± 30.89 vs 79.21 ± 17.97 fmol/mg, $p<0.05$, n=5-7). There was no difference between NT and HT NET protein in the LV (Figure 7C: 121.4 ± 15.84 vs 115.6 ± 17.68 fmol/mg, $p<0.05$, n=8).

Discussion

In many cases of hypertension, there is evidence of sympathetic nervous system activation and reduced catecholamine clearance by the heart. The underlying cause of reduction of NE accumulation by the heart is not fully understood. This study aimed to determine if the well established reduction in cardiac NE reuptake in the hypertensive heart was due to a decrease in expression of NET mRNA and/or protein in either the stellate ganglia or the individual heart chambers.

Using the DOCA-salt rat model we determined that there was no evidence for NET mRNA or protein downregulation in the either the right or the left stellate ganglia from hypertensive rats. In fact, there was an increase in the amount of NET protein in the left stellate ganglion. In the heart chambers, there was a regional reduction of NET mRNA and protein in the LA only, while other heart chambers had unchanged or increased NET expression. Therefore, the functional reduction in whole heart reuptake in hypertension is not due to a global reduction in NET mRNA or protein in the stellate ganglion and heart.

Stellate ganglion response to hypertension

Generally, it is accepted that synthesis of mRNA and protein for the cardiac sympathetic innervation occurs in the stellate ganglion with protein shipped to the nerve terminals via axonal transport. Therefore, it was assumed that the study of NET mRNA in the stellate would reflect changes in NET protein/function observed in the heart. The NET promoter contains CpG islands which can be methylated to repress transcription. Hypermethylation of the NET promoter has been noted in buffy coat lymphocytes from hypertensive patients (25). This is often associated with increased binding of MeCP2, a transcription factor that binds methylated DNA and represses transcription, as is observed in panic disorder patients (16). Methylation studies not been confirmed by assessment NET mRNA levels though; presumably, in these studies there would be evidence of NET mRNA reduction. With the interest in transcriptional suppression by methylation of the NET gene, we expected that there would be a reduction in

NET mRNA in the stellate ganglion to correspond to the reduced NE uptake in the heart. However, we show no evidence of NET mRNA reduction in stellate ganglia from the hypertensive rat. Assuming that there is no change in RNA stability in hypertension, this rules out the role of transcriptional repression by DNA methylation as a regulatory mechanism for NET mRNA in the stellate ganglia in hypertension.

NET mRNA expression in the stellate ganglion is not reflective of NET protein expression in either the stellates themselves or in the heart. This could occur because there are alternative post-transcriptional mechanisms of NET regulation. There is evidence for post-transcriptional modification in NET. Studies in heart failure and myocardial infarction demonstrate that NET mRNA in the stellate ganglion is unchanged in the face of reduced cardiac NET function suggesting that the reduction in NET protein is not due to a decreased in NET mRNA but rather is a post-transcriptional change (2; 38).

While there was no difference in NET mRNA in either stellate ganglion in hypertension, the left stellate ganglion exhibited an increase in NET protein suggesting a post-transcriptional upregulation of protein. NET mediated reuptake of NE increases when elevated nerve firing releases more NE into the synapse (15). Since there is elevated sympathetic drive to the heart in hypertension (23; 32; 57), it is feasible that there would be a corresponding elevation in NET protein in the stellate ganglia. Given that, it may be that the left

stellate receives preferential sympathetic drive from the central nervous system resulting in elevated NET protein in only the left ganglia.

There is substantial cross innervation from both stellate ganglia to all heart chambers (47) so making any determination of functional changes in the heart following unilateral ganglion change are difficult. However, it is known that the left stellate is functionally important in augmenting contractility and increasing coronary artery blood flow moreso that rate of contraction (30). Left stellate blockade does not alter heart rate variability or have a role in SA node innervation (18). If the increase expression of NET protein in the left stellate ganglia resulted in an increase in NET protein in the nerve terminals of these same cells, there would be an increased reuptake capacity and a reduction in the post-junctional effects of NE; this is contrary to the findings of enhanced inotropic response in the hypertensive heart associated with a reduction in NE uptake (40). This is further evidence that the stellate ganglion expression of NET does not reflect the function of NET in the heart.

We assessed the entire stellate ganglion rather that putative cardiac neurons alone. Not all cell bodies in the stellate ganglion project axons to the heart and therefore we measured NET mRNA and protein in both cardiac and non-cardiac neurons. Cardiac neurons exist in a zone near the exit of the cardiac nerve in the medial ganglia (59). While these nerves do not exhibit any significant differences in morphology compared to other stellate neurons (59), their function and

response to hypertension may be different. Ideally, a measurement of NET changes in only in the cardiac projecting neurons that exit the stellate ganglion via the cardiac nerve could be measured. This type of study is feasible using retrograde tracer in neurons that exit via the cardiac nerve (59) or by injecting tracer in the heart wall (52; 59). This is based on the idea that there are functional specific pathways in autonomic ganglia (31). There is evidence that individual neurons can project selectively to a single organ or part of the organ such as the vasculature (8; 19; 20).

Heart chamber response to hypertension: NE, NGF, and NET

NE content:

We analyzed the heart by chamber to determine regional difference in the NE content with hypertension. There is only a decrease in the NE content of the RA while the other chambers are unchanged. This is in contrast to the reports indicating a reduction in whole heart NE content in hypertension using the uninephrectomized normotensive control and the uninephrectomized DOCA-salt rat as used in our study (33) (14; 37). This regional difference in NE content could have been missed in an examination of whole heart NE. We conclude that the reduction of NE content in the hypertensive heart is regional and therefore the uptake of NE in hypertension may also show chamber differences. In fact, there is evidence of both inter- and intra-chamber differences in NE uptake capacity (3; 10; 27; 49). It is also quite interesting that the most obvious reduction in NE content in the heart chambers is not related to hypertension but

rather to uninephrectomy. We show that there is a significant reduction in NE content in the atria due to uninephrectomy alone, while the ventricular NE content is unchanged.

NGF:

NGF overexpressing mice have a greater heart NE content, an increased in presence of neuronal NE metabolites in the plasma, and great neuronal uptake of NE in LV tissue strips (35). There is reduction in NGF protein in heart, but not NGF mRNA, that occurs prior to the reduction of NE uptake seen in heart failure suggesting that NGF reduction might be the initial event leading to NE uptake reduction (38). In another model of heart failure, the reduction in NE uptake and tissue NE levels with disease is recovered by injection of NGF into the stellate ganglion (39). Therefore, we examined if changes in NGF are related to the reduced NE uptake in the hypertensive heart. There were no differences in NGF in any chamber in the DOCA-salt heart indicating that it is not NGF reduction that mediates the reduction in NE reuptake capacity.

NET:

Until recently, cardiac NET mRNA was thought to be found only in the stellate ganglion and not in the heart (41; 51; 58). We have recently demonstrated that NET mRNA is present in heart extracts and therefore may play a yet unknown role in expression of cardiac NET protein (61). The precise cellular location of this mRNA has not been determined but since sympathetic denervation did not

deplete NET mRNA from heart extract, the source is not sympathetic nerve fibers in the heart. We suggest that it is from intrinsic cardiac neurons and intrinsic cardiac adrenergic cells. Assessment of NET mRNA without knowledge of the cell type from which it is expressed makes conclusions on the functional relevance difficult.

NET mRNA exists in the heart in a chamber specific pattern with the atria expressing more than the ventricles (61). We show that NET mRNA in the heart chambers in regionally altered in DOCA-salt hypertension. NET mRNA expression is elevated in both ventricles, reduced in the LA and unchanged in the RA. Only in the LA is the reduction of cardiac NET mRNA expression mirrored by a reduction in NET protein amount in a chamber suggesting that the NET mRNA is coupled to protein expression in the LA while in other chambers this is not the case. It could be that the source of NET mRNA in the LA does indeed have a transcriptional regulatory mechanism in place to alter levels of NET protein in this region of the heart. We recently demonstrated that NET mRNA in the LA increased after sympathetic denervation (a reduction in sympathetic activity to the LA) (60) thus it follows that an increase in sympathetic activity with hypertension would have the opposite effect and decrease. Together, NET mRNA in the LA is regulated by sympathetic input to the heart.

We report that changes in NET protein vary by chamber in hypertension. While there is an overall reduction in NE uptake in the heart that we predicted would be

related to a reduction in NET protein amount, there is only a reduction in NET protein in the LA. Surprisingly, there is no change, or even an increase, in the other chambers. Thus, the reduction of heart NE reuptake is not due to a global reduction in NET protein expression. Importantly we report NET binding in cardiac membrane preparations that should only contain NET that it functionally inserted in the membrane therefore would reflect functional uptake capacity of each chamber. We recently reported that there is a low amount if NET in the atria compared to the ventricles (62) so it is unlikely that a reduction in LA NET protein with hypertension would be enough to result in a reduction in whole heart uptake.

Having ruled out a loss of NET protein in the heart as a cause for reduced reuptake, other factors that could cause a decrease in NE uptake must be considered. Perturbations in NE release, NE storage in vesicles, and/or altered regulation of NET function or trafficking could also play a role. NET has long, intracellular N-terminal and C-terminal tails with consensus sequences for phosphorylation indicating that NET transport function and subcellular distribution are regulated by phosphorylation. Acutely, NET is regulated by membrane potential, substrate exposure, pre-synaptic receptor manipulation, altered electrochemical gradients that drive substrate transport, and second messenger systems such as protein kinase C (5; 63). The acute regulation occurs quickly with a subcellular redistribution of transporter from insertion in the plasma membrane to intracellular sites, or by changing the transport efficiency while

inserted in the membrane (63). Other modulators of NET function include: reduction in NE reuptake in the heart by endothelin-1 (1) and aldosterone (9), and oxidative stress in PC12 cells (43). Enhanced NE uptake was cause by B- and C-type natriuetic peptides and angiotensin II (5).

Perspectives: NE reuptake and NET in hypertension

While the literature presents a strong case for reduced NE uptake in the hypertensive heart, there are some substantial conflicts with the historical literature relating to NE handling and hypertension. This first studies on catecholamine handling in the hypertensive heart indicated that there was a reduction in whole heart NE content (14). This was associated with a reduced accumulation of [^{3}H] NE in vivo yet no difference in initial NE uptake via uptake-1 in isolated DOCA hearts. Thus, the decreased endogenous NE content and decreased accumlation of exogeneous [^{3}H] NE was concluded to be due to a reduction of NE storage into vesicles and not to initial binding and uptake via the neuronal membrane transporter (14). Furthermore, since more [^{3}H] NE is not packaged into vesicles it remains in the cytoplasm and is more accessible for both intraneuronal metabolism via deamination by monamine oxidase as well as for release and subsequent metabolism by the extraneuronal pathway. There was an increase in both the intraneuronal metabolite,DHPG, and the extracellular metabolite in hypertension to support this idea (37). However, this is controversial since later studies indicated that NE uptake via NET was indeed

impaired and indicate a decrease in release of the intraneuronal metabolite DHPG (17; 21; 22; 53-55).

DOCA-salt treatment is related to a reduction in [^{3}H] NE accumulation by the heart in vivo that is inversely related to blood pressure (14; 33) with higher blood pressure corresponding to reduced accumulation NE. This supports a relationship between reduced NE uptake and elevated blood pressure. To the contrary, [^{3}H] NE uptake in ventricular heart slices it is not dependent upon blood pressure since both hypertension prone and hypertension resistant animals on DOCA-salt have reduced NE uptake even with significantly different blood pressures (36).

It may be that reduction in reuptake of NE is not the primary mechanism for hypertension development such that the cardiac neurogenic component may require other abnormalities such as baroreflex dysfunction or increased sympathetic tone (36) in order to develop hypertension. Under normal conditions there is a central sympatholytic mechanism that counteracts the pressor response to elevated junctional NE. Central sympathetic inhibition may explain why blood pressure is only modestly, albeit significantly, increased in NET knockout mice and why these mice do not have a strong hypertensive phenotype (34). In other words, an intact baroreflex pathway is vital in the prevention of hypertension in the face of NET blockade or dysfunction. Moreover, NET inhibition causes hypertension in patients with central autonomic failure (56). In

patients with multiple system atrophy with central autonomic failure, even an extremely low dose of NET inhibitor causes substantial blood pressure elevation (56) supporting the idea that NET dysfunction alone does not cause hypertension.

Conflicts on the role of the heart in hypertension

With a reduction in cardiac NET function in hypertension, there would be increased junctional NE and NE spillover. This would be associated with increased adrenergic signaling associated with elevated heart rate, contractility, and cardiac output. However, there is not a consensus as to the role of increased heart rate and contractility in DOCA-salt hypertension. Brown et al demonstrated that cardiac contractility is not increased in DOCA (7), while LeLorier et al reports an elevation in inotropism in the same model (40). Stroke volume and cardiac output are unchanged or reduced in a DOCA-salt model suggesting that the heart does not drive the elevation in blood pressure (46). Some rats administered the DOCA-salt regimen have elevated heart rate that corresponds to hypertension (6; 45) yet in other studies the opposite was found (29).

Hypertension development in some DOCA-salt animals is dependent upon an intact cardiac sympathetic nervous system, lending credence to the importance of the heart in hypertension and to a strong neurogenic component to the disease. The development of hypertension can be prevented in DOCA-salt

treated animals by removal of cardiac sympathetic nerves by stellate ganglionectomy, destruction of the sympathetic nervous system at birth with treatment with guanethadine, or inhibition of cardiac beta-adrenergic receptors (4). Furthermore, bilateral sympathetic block at T3 (stellate ganglion) in humans was successful in reducing heart rate, systolic blood pressure and diastolic blood pressure in hypertensive patients while had no effect on blood pressure in normotensive patients that underwent this procedure (11). It is likely that in these instances, there is a role of elevated heart rate and cardiac output in the hypertension. It is possible that in cases where heart rate is reduced with the disease that these treatments would not be effective.

Summary

We examined the mechanisms underlying the reported decrease in NE uptake in the hypertensive heart. Using the DOCA-salt rat model we determined that there was no evidence for NET mRNA or protein downregulation in either the right or the left stellate ganglia from hypertensive rats. In fact, there was an increase in NET protein in the left stellate ganglion. In the heart chambers, there was a regional reduction of NET mRNA and protein in the LA only, while other heart chambers had unchanged or increased NET expression. These changes were unrelated to NGF in the heart. Therefore, the functional reduction in whole heart reuptake in hypertension is not due to a global reduction in NET mRNA or protein in the stellate ganglion and heart.

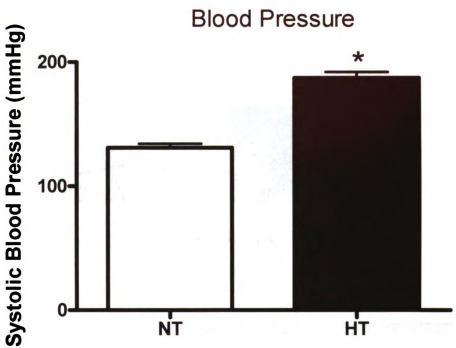

Figure 6.1: Blood pressure is elevated following 4-weeks of DOCA-salt treatment. Blood pressure was measured using tail cuff plethysmography and systolic blood pressure is reported as mmHg. Normotensive animals were uninephrectomized. Hypertensive animals were uninephrectomized, received an implant of DOCA, and were given saline in the drinking water to induce hypertension. (n=19-23, * indicates significance of $p<0.05$).

A.

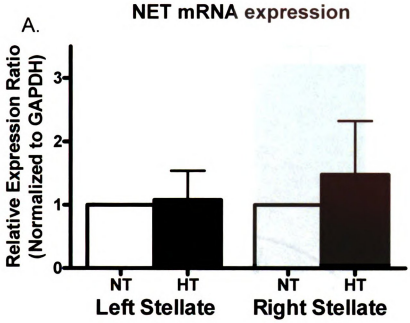

B.

Tissue	Average NET Ct	NET Ct St Err	Average GAPDH Ct	GAPDH Ct St Err	N
Right Stellate NT	23.27	0.61	17.64	0.32	6
Right Stellate HT	22.83	0.38	17.77	0.26	7
Left Stellate NT	21.93	0.49	17.09	0.17	5
Left Stellate HT	22.78	0.24	18.07	0.24	5

Figure 6.2: NET mRNA expression is unchanged in the bilateral stellate ganglia with DOCA-salt hypertension. A) RNA was isolated from stellate ganglia from normotensive (NT, white bar) and DOCA-salt hypertensive (HT, black bar) rats and analyzed for expression of NET mRNA. Data are shown as relative expression ratio using GAPDH as a control gene. For each ganglion, expression in NT ganglia is set to one and the HT is analyzed relative to control. Calculations of fold change and significance were run separately for each ganglion using pair-wise randomization on REST® 384 software. To eliminate intra-run error, NT and HT samples from each ganglion were run together on the same qPCR plate. B) Descriptive statistics from REST® 384 analysis of NET mRNA.

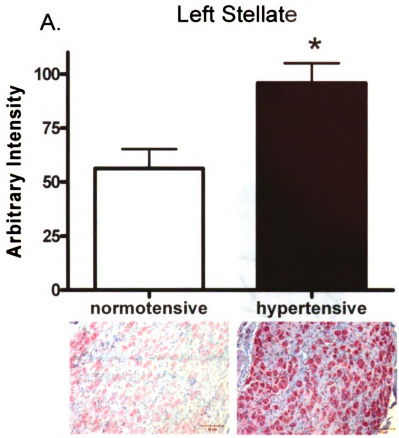

Figure 6.3: NET protein expression is elevated in left but not right stellate ganglia from DOCA-salt hypertensive rats. A) Left stellate ganglion and B) Right stellate ganglion from normotensive (white bars) and hypertensive (black bars) were fixed, sectioned, and analyzed for NET immunoreactivity (IR) using NIH Image J software as described in the methods section. A representative section (scale bar=10μM) is shown below each bar with NET IR shown in red. NET IR was determined in all neurons in a section and then averaged per ganglia. (n=4, * indicates significance $p<0.05$).

Figure 6.3 continued

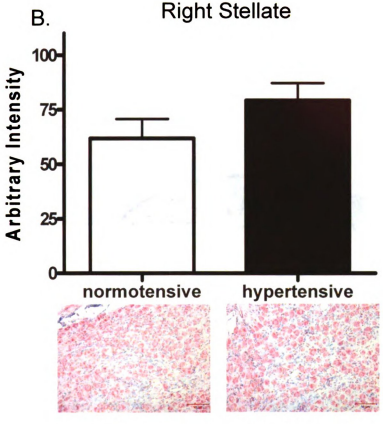

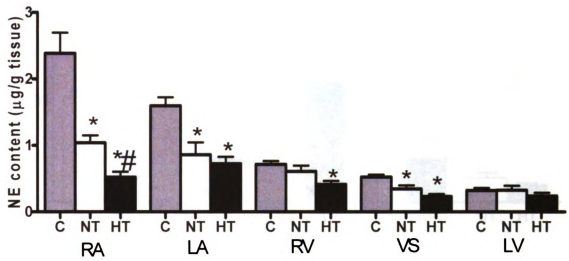

Figure 6.4: Chamber norepinephrine (NE) content was regionally decreased with uninephrectomy and DOCA-salt hypertension. NE content per chamber was determined by capillary electrophoresis with electrochemical detection in control (C), uninephrectomized normotensive (NT), and DOCA-salt hypertensive (HT) rats. * indicates significance $p<0.05$ C versus NT, # indicates significance NT versus HT.

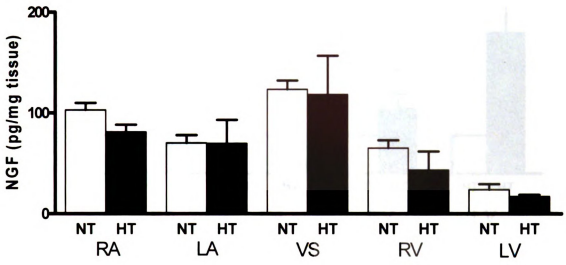

Figure 6.5: NGF protein is unchanged in the heart chambers of DOCA-salt hypertensive rats. NGF (pg/mg) was measured using enzyme linked immunosorbant assay (ELISA) in heart homogenates of all chambers from normotensive (NT, white bars) and DOCA-salt hypertensive rats (HT, black bars).

A.

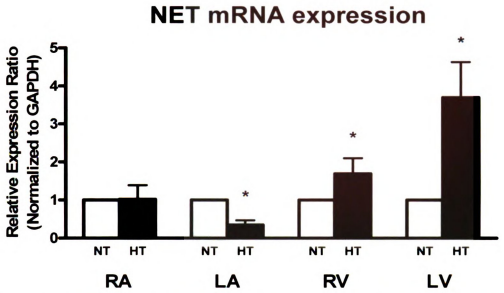

B.

Tissue	Average NET Ct	NET Ct St Err	Average GAPDH Ct	GAPDH Ct St Err	N
RA Normotensive	36.02	0.44	16.47	0.13	6
RA Hypertensive	36.35	0.27	16.82	0.07	6
LA Normotensive	35.03	0.37	18.33	0.25	5
LA Hypertensive	35.82	0.27	17.57	0.12	6
RV Normotensive	36.08	0.15	16.35	0.24	5
RV Hypertensive	35.97	0.20	17.00	0.08	6
LV Normotensive	34.26	0.21	14.31	0.14	7
LV Hypertensive	34.61	0.20	16.58	0.18	7

Figure 6.6: NET mRNA from the heart is regionally regulated in DOCA-salt hypertension. A) RNA was isolated from heart chambers of normotensive (NT, white bar) and DOCA-salt hypertensive (HT, black bar) rats and analyzed for expression of NET mRNA. Data are shown as relative expression ratio using GAPDH as a control gene. For each chamber, expression in NT ganglia is set to one and the HT is analyzed relative to control. Calculations of fold change and significance were run separately for each ganglion using pair-wise randomization on REST® 384 software. NT and HT samples from each chamber were run together on the same qPCR plate. B) Descriptive statistics from REST® 384 analysis of NET mRNA. * indicates significance $p<0.05$.

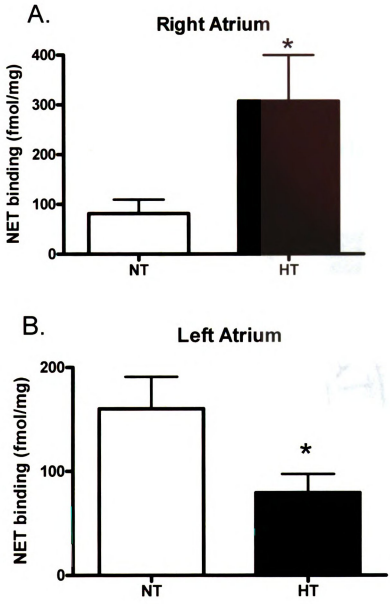

Figure 6.7: NET protein in cardiac membranes is regionally regulated in different heart chambers in DOCA-salt hypertensive rats. NET protein (fmol/mg) was assessed by [^{3}H]-nisoxetine binding in cardiac membranes from heart chambers of normotensive (NT, white bars) and DOCA-salt hypertensive (HT, black bars). A) right atrium, B) left atrium, and C) left ventricle. (n=7-8, * indicates significance $p<0.05$).

Figure 6.7 continued

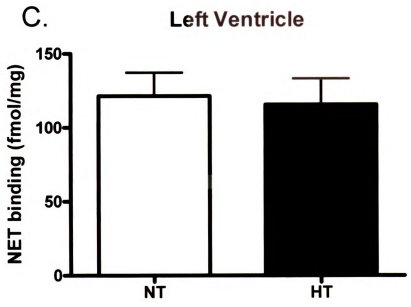

Reference List

1. **Backs J, Bresch E, Lutz M, Kristen AV and Haass M**. Endothelin-1 inhibits the neuronal norepinephrine transporter in hearts of male rats. *Cardiovasc Res* 67: 283-290, 2005.

2. **Backs J, Haunstetter A, Gerber SH, Metz J, Borst MM, Strasser RH, Kubler W and Haass M**. The neuronal norepinephrine transporter in experimental heart failure: evidence for a posttranscriptional downregulation. *J Mol Cell Cardiol* 33: 461-472, 2001.

3. **Beau SL and Saffitz JE**. Transmural heterogeneity of norepinephrine uptake in failing human hearts. *J Am Coll Cardiol* 23: 579-585, 1994.

4. **Bell C and McLachlan EM**. Dependence of deoxycorticosterone/salt hypertension in the rat on the activity of adrenergic cardiac nerves. *Clin Sci (Lond)* 57: 203-210, 1979.

5. **Bonisch H and Bruss M**. The norepinephrine transporter in physiology and disease. *Handb Exp Pharmacol* 485-524, 2006.

6. **Brooks VL, Freeman KL and Qi Y**. Time course of synergistic interaction between DOCA and salt on blood pressure: roles of vasopressin and hepatic osmoreceptors. *Am J Physiol Regul Integr Comp Physiol* 291: R1825-R1834, 2006.

7. **Brown L, Ooi SY, Lau K and Sernia C**. Cardiac and vascular responses in deoxycorticosterone acetate-salt hypertensive rats. *Clin Exp Pharmacol Physiol* 27: 263-269, 2000.

8. **Browning KN, Zheng ZL, Kreulen DL and Travagli RA**. Two populations of sympathetic neurons project selectively to mesenteric artery or vein. *Am J Physiol* 276: H1263-H1272, 1999.

9. **Buss SJ, Backs J, Kreusser MM, Hardt SE, Maser-Gluth C, Katus HA and Haass M**. Spironolactone preserves cardiac norepinephrine reuptake in salt-sensitive Dahl rats. *Endocrinology* 147: 2526-2534, 2006.

10. **Chilian WM, Boatwright RB, Shoji T and Griggs DM, Jr.** Regional uptake of [3H]norepinephrine by the canine left ventricle (41491). *Proc Soc Exp Biol Med* 171: 158-163, 1982.

11. **Chou SH, Kao EL, Lin CC, Chuang HY and Huang MF**. Sympathetic hypertensive syndrome: a possible surgically curable type of hypertension. *Hypertens Res* 28: 409-414, 2005.

12. **Cvacka J, Quaiserova V, Park J, Show Y, Muck A, Jr. and Swain GM**. Boron-doped diamond microelectrodes for use in capillary electrophoresis with electrochemical detection. *Anal Chem* 75: 2678-2687, 2003.

13. **de Champlain J, Krakoff LR and Axelrod J**. A reduction in the accumulation of H3-norepinephrine in experimental hypertension. *Life Sci* 5: 2283-2291, 1966.

14. **de Champlain J, Krakoff LR and Axelrod J**. Catecholamine metabolism in experimental hypertension in the rat. *Circ Res* 20: 136-145, 1967.

15. **Eisenhofer G, Cox HS and Esler MD**. Parallel increases in noradrenaline reuptake and release into plasma during activation of the sympathetic nervous system in rabbits. *Naunyn Schmiedebergs Arch Pharmacol* 342: 328-335, 1990.

16. **El-Osta A and Wolffe AP**. DNA methylation and histone deacetylation in the control of gene expression: basic biochemistry to human development and disease. *Gene Expr* 9: 63-75, 2000.

17. **Esler MD, Rumantir M, Kaye DM, Jennings G, Hastings J, Socratous F and Lambert G**. Sympathetic nerve biology in essential hypertension. *Clin Exp Pharmacol Physiol* 28: 986-989, 2001.

18. **Fujiki A, Masuda A and Inoue H**. Effects of unilateral stellate ganglion block on the spectral characteristics of heart rate variability. *Jpn Circ J* 63: 854-858, 1999.

19. **Gibbins IL, Hoffmann B and Morris JL**. Peripheral fields of sympathetic vasoconstrictor neurons in guinea pigs. *Neurosci Lett* 248: 89-92, 1998.

20. **Gibbins IL, Morris JL, Furness JB and Costa M**. Innervation of Systemic Blood Vessels. In: Nonadrenergic Innervation of Blood Vessels, edited by Burnstock G and Griffith SG. Boca Raton: CRC Press, 1988, p. 1-36.

21. **Goldstein DS, Robertson DM, Esler MD, Straus SE and Eisenhofer G**. Dysautonomias: clinical disorders of the autonomic nervous system. *Ann Intern Med* 137: 753-763, 2002.

22. **Grassi G and Esler MD**. How to assess sympathetic activity in humans. *J Hypertens* 17: 719-734, 1999.

23. **Grassi G and Mancia G**. Neurogenic hypertension: is the enigma of its origin near the solution? *Hypertension* 43: 154-155, 2004.

24. **Gudeska S, Glavas E, Stojanova D, Petrov S, Trajkov T and Nikodijevic B**. Alteration in the uptake and storage of cardiac noradrenaline in spontaneously hypertensive rats. *Biomedicine* 25: 157-159, 1976.

25. Guo, L., Schlaich, M. P., Esler, M., Lambert, E., Lambert, G., and El-Osta, A. An epigenetic mechanism for the phenotype of faulty neuronal noradrenaline reuptake in essential hypertension. Clin.Exp.Pharmacol.Physiol Abstract 32. 2005.
Ref Type: Abstract

26. **Hertting G and Axelrod J**. Fate of tritiated noradrenaline at the sympathetic nerve-endings. *Nature* 192: 172-173, 1961.

27. **Ieda M, Kanazawa H, Kimura K, Hattori F, Ieda Y, Taniguchi M, Lee JK, Matsumura K, Tomita Y, Miyoshi S, Shimoda K, Makino S, Sano M, Kodama I, Ogawa S and Fukuda K**. Sema3a maintains normal heart rhythm through sympathetic innervation patterning. *Nat Med* 13: 604-612, 2007.

28. **Iversen LL**. The uptake of noradrenaline by isolated perfused rat heart. *Br J Pharmacol* 21: 523-537, 1963.

29. **Jacob F, Clark LA, Guzman PA and Osborn JW**. Role of renal nerves in development of hypertension in DOCA-salt model in rats: a telemetric approach. *Am J Physiol Heart Circ Physiol* 289: H1519-H1529, 2005.

30. **Janes RD, Johnstone DE and Armour JA**. Chronotropic, inotropic, and coronary artery blood flow responses to stimulation of specific canine sympathetic nerves and ganglia. *Can J Physiol Pharmacol* 62: 1374-1381, 1984.

31. **Janig W and McLachlan EM**. Characteristics of function-specific pathways in the sympathetic nervous system. *TINS* 15: 475-481, 1992.

32. **Julius S and Majahalme S**. The changing face of sympathetic overactivity in hypertension. *Ann Med* 32: 365-370, 2000.

33. **Kazda S, Pohlova I, Bibr B and Kockova J**. Norepinephrine content of tissues in Doca-hypertensive rats. *Am J Physiol* 216: 1472-1475, 1969.

34. **Keller NR, Diedrich A, Appalsamy M, Tuntrakool S, Lonce S, Finney C, Caron MG and Robertson DM**. Norepinephrine transporter-deficient mice exhibit excessive tachycardia and elevated blood pressure with wakefulness and activity. *Circulation* 110: 1191-1196, 2004.

35. **Kiriazis H, Du XJ, Feng X, Hotchkin E, Marshall T, Finch S, Gao XM, Lambert G, Choate JK and Kaye DM**. Preserved left ventricular structure and function in mice with cardiac sympathetic hyperinnervation. *Am J Physiol Heart Circ Physiol* 289: H1359-H1365, 2005.

36. **Krakoff LR, Ben Ishay D and Mekler J**. Reduced sympathetic neuronal uptake (uptake1) in a genetic model of desoxycorticosterone-NaCl hypertension. *Proc Soc Exp Biol Med* 178: 240-245, 1985.

37. **Krakoff LR, de Champlain J and Axelrod J**. Abnormal storage of norepinephrine in experimental hypertension in the rat. *Circ Res* 21: 583-591, 1967.

38. **Kreusser MM, Buss SJ, Krebs J, Kinscherf R, Metz J, Katus HA, Haass M and Backs J**. Differential expression of cardiac neurotrophic factors and sympathetic nerve ending abnormalities within the failing heart. *J Mol Cell Cardiol* 44: 380-387, 2008.

39. **Kreusser MM, Haass M, Buss SJ, Hardt SE, Gerber SH, Kinscherf R, Katus HA and Backs J**. Injection of nerve growth factor into stellate ganglia

improves norepinephrine reuptake into failing hearts. *Hypertension* 47: 209-215, 2006.

40. **LeLorier J, Hedtke JL and Shideman FE**. Uptake of and response to norepinephrine by certain tissues of hypertensive rats. *Am J Physiol* 230: 1545-1549, 1976.

41. **Li H, Ma SK, Hu XP, Zhang GY and Fei J**. Norepinephrine transporter (NET) is expressed in cardiac sympathetic ganglia of adult rat. *Cell Res* 11: 317-320, 2001.

42. **Li W, Knowlton D, Van Winkle DM and Habecker BA**. Infarction alters both the distribution and noradrenergic properties of cardiac sympathetic neurons. *Am J Physiol Heart Circ Physiol* 286: H2229-H2236, 2004.

43. **Mao W, Qin F, Iwai C, Vulapalli R, Keng PC and Liang CS**. Extracellular norepinephrine reduces neuronal uptake of norepinephrine by oxidative stress in PC12 cells. *Am J Physiol Heart Circ Physiol* 287: H29-H39, 2004.

44. **Muna GW, Quaiserova-Mocko V and Swain GM**. Chlorinated phenol analysis using off-line solid-phase extraction and capillary electrophoresis coupled with amperometric detection and a boron-doped diamond microelectrode. *Anal Chem* 77: 6542-6548, 2005.

45. **O'Donaughy TL and Brooks VL**. Deoxycorticosterone acetate-salt rats: hypertension and sympathoexcitation driven by increased NaCl levels. *Hypertension* 47: 680-685, 2006.

46. **Obst M, Gross V and Luft FC**. Systemic hemodynamics in non-anesthetized L-. *J Hypertens* 22: 1889-1894, 2004.

47. **Pardini BJ, Lund DD and Schmid PG**. Organization of the sympathetic postganglionic innervation of the rat heart. *J Auton Nerv Syst* 28: 193-201, 1989.

48. **Pfaffl MW, Horgan GW and Dempfle L**. Relative expression software tool (REST) for group-wise comparison and statistical analysis of relative expression results in real-time PCR. *Nucleic Acids Res* 30: e36, 2002.

49. **Pierpont GL, DeMaster EG and Cohn JN**. Regional differences in adrenergic function within the left ventricle. *Am J Physiol* 246: H824-H829, 1984.

50. **Rascher W, Schomig A, Dietz R, Weber J and Gross F**. Plasma catecholamines, noradrenaline metabolism and vascular response in desoxycorticosterone acetate hypertension of rats. *Eur J Pharmacol* 75: 255-263, 1981.

51. **Reja V, Goodchild AK and Pilowsky PM**. Catecholamine-related gene expression correlates with blood pressures in SHR. *Hypertension* 40: 342-347, 2002.

52. **Richardson RJ, Grkovic I, Allen AM and Anderson CR**. Separate neurochemical classes of sympathetic postganglionic neurons project to the left ventricle of the rat heart. *Cell Tissue Res* 324: 9-16, 2006.

53. **Rumantir MS, Kaye DM, Jennings GL, Vaz M, Hastings JA and Esler MD**. Phenotypic evidence of faulty neuronal norepinephrine reuptake in essential hypertension. *Hypertension* 36: 824-829, 2000.

54. **Schlaich MP, Lambert E, Kaye DM, Krozowski Z, Campbell DJ, Lambert G, Hastings J, Aggarwal A and Esler MD**. Sympathetic augmentation in hypertension: role of nerve firing, norepinephrine reuptake, and Angiotensin neuromodulation. *Hypertension* 43: 169-175, 2004.

55. **Shannon JR, Flattem NL, Jordan J, Jacob G, Black BK, Biaggioni I, Blakely RD and Robertson DM**. Orthostatic intolerance and tachycardia associated with norepinephrine- transporter deficiency. *N Engl J Med* 342: 541-549, 2000.

56. **Shibao C, Raj SR, Gamboa A, Diedrich A, Choi L, Black BK, Robertson D and Biaggioni I**. Norepinephrine transporter blockade with atomoxetine induces hypertension in patients with impaired autonomic function. *Hypertension* 50: 47-53, 2007.

57. **Smith PA, Graham LN, Mackintosh AF, Stoker JB and Mary DA**. Sympathetic neural mechanisms in white-coat hypertension. *J Am Coll Cardiol* 40: 126-132, 2002.

58. **Ungerer M, Chlistalla A and Richardt G**. Upregulation of cardiac uptake 1 carrier in ischemic and nonischemic rat heart. *Circ Res* 78: 1037-1043, 1996.

59. **Wallis D, Watson AH and Mo N**. Cardiac neurones of autonomic ganglia. *Microsc Res Tech* 35: 69-79, 1996.

60. Wehrwein, E. A., Esfahanian, M, Novotny, M., Quaiserova-Mocko, V., Swain, G. M., Yoshimoto, M, Osborn, J. W., and Kreulen, D. L. NOREPINEPHRINE TRANSPORTER mRNA IS PRESENT IN THE HEART BEFORE AND AFTER SYMPATHETIC DENERVATION. 2008.
Ref Type: Unpublished Work

61. Wehrwein, E. A., Fink, G. D., and Kreulen, D. L. Norepinephrine transporter mRNA is present in the heart and stellate ganglion, and is differentially regulated in hypertension. American Heart Association, Council for High Blood Pressure Research Abstract . 2006.
Ref Type: Abstract

62. Wehrwein, E. A., Parker, L. M., Wright, A. A., Spitsbergen, J. M., Novotny, M., Babankova, D, Swain, G. M., Habecker, B. A., and Kreulen, D. L. Cardiac norepinephrine transporter (NET) protein expression is inversely correlated to chamber norepinephrine content. 2008.
Ref Type: Unpublished Work

63. **Zahniser NR and Doolen S**. Chronic and acute regulation of Na+/Cl- -dependent neurotransmitter transporters: drugs, substrates, presynaptic receptors, and signaling systems. *Pharmacol Ther* 92: 21-55, 2001.

64. **Zhu MY and Ordway GA**. Down-regulation of norepinephrine transporters on PC12 cells by transporter inhibitors. *J Neurochem* 68: 134-141, 1997.

CHAPTER 7: SUMMARY, CONCLUSION, AND PERSPECTIVES

I. Complexity of cardiac innervation

The innervation of the heart is described in textbooks as a simple two input system with an "accelerator" and "brake" of the sympathetic and parasympathetic nervous systems, respectively. These two branches of the autonomic nervous system are touted as the ultimate control systems for cardiac function. The sympathetic nervous system functions to increase heart rate and contractility, while the parasympathetic nervous system reduces heart rate and contractility. Each system is described as having a classic neurotransmitter associated with it: norepinephrine in sympathetic nerves and acetylcholine in parasympathetic nerves. The sensory innervation of the heart is often neglected in discussion of neural control of the heart yet is a vital component that senses the mechanical and chemical environment then transduces these afferent signals to modulate autonomic input accordingly. The sensory nerve endings can also serve efferent function by releasing CGRP onto the heart thus are described as "sensory-motor" nerve fibers (i.e., they have both afferent and efferent properties). Even considering the sensory nerves as part of the nervous system of the heart, the above description of cardiac innervation is an oversimplification.

Cardiac innervation is highly complex and redundant with roles for both extrinsic innervation as described above and intrinsic innervation associated with the "little brain of the heart" (1). It is the case that sympathetic, parasympathetic, sensory

and intrinsic systems are interconnected, highly integrated, and redundant. Not unlike the gut, the heart has its own intrinsic nervous system in intrinsic cardiac ganglia. Contrary to the widely held notion that the intrinsic neurons are solely parasympathetic postganglionic efferent somata, the intrinsic cardiac ganglia or "little brain of the heart" consists of sensory afferent, interconnecting local circuit, and motor (parasympathetic/cholinergic and sympathetic/adrenergic) neurons (2). It has been described as displaying "stochastic" (i.e., being or having a random variable) and "emergent" properties (i.e., rising or occurring unexpectedly) suggesting that the intrinsic innervation is not a relay station but can and does modulate inputs and function independently (2). As well, it is capable of mediating local reflexes without the need for central nervous system involvement.

There are four primary sites of intrinsic cardiac neurons clustered into ganglia in the atria (31). These intrinsic neurons are anatomically classified as part of the parasympathetic nervous system (i.e., ganglia in or near the tissue innervated) and are cholinergic (i.e., synthesize and release acetylcholine); however, it is now known that some of these neurons have catecholaminergic properties (4; 27; 34) that would then blur the definition of which branch of the nervous system these cells belong since the catecholaminergic properties makes them functionally part of the sympathetic innervation to the heart.

In addition, there are intrinsic cardiac adrenergic (ICA) cells throughout the heart that contain NE, have NE uptake capabilities, and function to provide sympathetic input in the fetal heart before the sympathetic innervation is developed and may also be important in maintaining sympathetic control in the denervated or transplanted heart (15; 16). These cells are non-neuronal yet also express catecholaminergic features.

II. Regulation and localization of NET in the stellate ganglion and heart

NET is undeniably in cardiac sympathetic fibers where it plays a key role in the attenuation of NE signaling. There is a reduction in NE uptake in the sympathetically denervated heart thus it was assumed that these nerve fibers were the source of NET in the heart (14). Likewise, NET mRNA has been reported many times to exist in the sympathetic stellate ganglion which provides innervation to the heart (3; 13; 23; 37; 38). NET mRNA was examined in the heart previously and was reported to be absent (22; 30; 35). Thus, the current opinion is that NET mRNA is in the stellate ganglion and NET protein is in the stellate ganglion and heart in sympathetic neurons. This view of NET mRNA and protein expression, while accurate, is an oversimplification. Given the recently discovered complexities and redundancies of the cardiac innervation, it is not as surprising that this thesis reports novel sites of NET in the heart.

NET mRNA:

My studies offer the insight into the complexity of NET expression in the heart by demonstrating that NET mRNA is found in the heart itself identified in extracts of all chambers. NET mRNA in the heart is labile and found in low so it is feasible that it was not detected in previous studies. My studies using cardiac sympathetic denervation did not result in a depletion of NET mRNA in the heart so NET mRNA is not contained in sympathetic nerve fibers. The cellular source of this NET mRNA has not been conclusively determined, but is most likely from the intrinsic innervation of the heart (i.e., intrinsic cardiac neurons) and ICA cells. NET protein is present in both intrinsic cardiac neurons as reported in this thesis and in ICA cells (15; 16), it is quite clear that as independent cells in the heart they must also contain NET mRNA. Intrinsic cardiac neurons have cell bodies clustered in the atria (2; 4; 27) and not only should contain NET mRNA, contributing to the NET mRNA signal, but also would offer an explanation for the high levels of expression in the atria compared to the ventricles. ICA cells are found throughout the myocardium (15; 16) and would explain the presence of NET mRNA in all chambers.

NET protein:

The notion of alternative sources of NET mRNA, and hence NET protein, in the heart were supported by my studies demonstrating that there was substantial NET mRNA and protein in the sympathetically denervated heart. It was reported previously that NET protein is present in ICA cells and this provided the first evidence of cardiac NET outside of sympathetic neurons (16). The current

studies further determined that NET was also present in intrinsic cardiac neurons colocalized with makers of both cholinergic and catecholaminergic neurons. However, there was no evidence of NET in sensory nerve fibers or in cardiac muscle. Interestingly, there was NET in sensory dorsal root ganglia at all spinal levels; these NET-containing cell bodies either do not ship NET to axons or the axons that contain NET project to other organs besides the heart. These sites of NET mRNA and protein are novel sites of regulation of this key protein and play a yet undetermined role in the regulation of cardiac function in health and disease.

Since my work has established that NET is present in other cell types in the heart, it may not be as surprising to learn that NET protein is inversely correlated to sympathetic innervation density of the heart chambers. The fact that high amounts of NET protein are found in areas of low NE content seems counterintuitive since NET functions to clear NE; however, it must be considered that there are sources of NET outside of sympathetic fibers that innervate the myocardium.

Perhaps, NET plays a wider role in the heart than simply the reuptake of released NE from the neuroeffector junction. NET can also take up NE and epinephrine from the circulation, which is important in instances of high stress and during heart failure where plasma catecholamines are circulating at high levels. Dopamine and serotonin are also substrates for NET (6) and therefore

NET in sites outside the sympathetic nervous system could function to regulate these neurotransmitters as well. This notion should be heavily considered since there dopaminergic and seratonergic cells in the heart (34) and these transmitters are present in all chambers. Dopamine increases myocardial contractility and cardiac output (36). Serotonin causes tachycardia, increased atrial contractility, atrial arrhythmias, as well as inotropic and arrhythmic effects ventricle (18). Moreover, the amount of these transmitters is regulated by sympathetic innervation and NE so NET could play undetermined role in modulating the levels of other neurotransmitters in the heart.

III. Regulation of NET in hypertension

The hypertensive heart demonstrates a decrease in NE clearance, reduction of neuronal metabolites if NE, and an increased spillover of NE from the neuroeffector junction to the plasma (10). This evidence strongly suggests that a reduction in NET in the heart occurs in hypertension. By examining NET mRNA and protein in the stellate ganglia, there is no evidence of reduced NET expression in hypertension. In the heart, there is regional downregulation of NET that occurs in the LA only while other chambers are unchanged or increased. Therefore, a global downregulation of cardiac NET does not occur in hypertension and that the downregulation of NET in the LA is not due to a decrease in NET in the stellate ganglion, rather appears to be related to a reduced NET mRNA expression in the LA itself.

It is appropriate to comment at this point on the fact that this thesis presents a situation in which there is local regulation of NET in the target tissue, for example a downregulation in the LA in hypertension, when the cell bodies of sympathetic neuron in the stellate ganglion do not have a corresponding change. It makes sense that the regulation of this key nerve terminal protein would be regulated on a short time scale by acute local regulation in the tissue as opposed to a long term regulatory change dictated by the stellate ganglion at considerable distance from the heart. Certainly the stellate ganglion does play a role in regulation of the sympathetic axons and nerve terminals in the heart; however, it is now clear that this is by no means the only regulatory mechanism for NE handling in the heart.

There is much speculation of a causative role for reduced NE uptake in hypertension. However, a detailed review of the literature in human and animal models of hypertension supports that a reduced NE clearance in the heart does not cause hypertension if that is the only perturbation (19; 33). Reduced NET function and the resulting elevation of NE drive to the heart causes a baroreflex response that blunts sympathetic outflow to compensate. This is evident in the NET KO mouse model which only has a modest elevation of blood pressure despite elevated plasma NE levels and tachycardia (19). Only in the case of a combined aberrant baroreflex function or central autonomic failure with NET dysfunction cause sustained hypertension. This was nicely demonstrated when NET inhibitors were administered to patients with central autonomic failure

resulting in hypertension, while this did not occur in non-diseased patients (33). As to a direct causative role of NET functional changes in hypertension, it is not the case; however, NET is a critical player that under the right circumstances contributes to the hypertensive state.

Hypertension is a multifactorial/multigenic disease that is not likely to have one root cause. It is then not surprising that many hypertensive patients are on multiple medications and have poorly controlled blood pressure. That being the case, it is not surprising that a NET KO mouse is not a good model of hypertension. NET dysfunction has to occur in concert with other changes and the candidates are myriad. Even though there 5 identified missence mutations of NET found in genetic screening of the general population, similar studies on human hypertensive patients so far have not identified any NET mutations associated with the disease (11). The one NET mutation that results in a complete loss of NET function was identified and that patient had postural tachycardia syndrome without hypertension (32).

NET dysfunction or NET blockade results in excess junctional NE and NE spillover which would increase heart rate and cardiac output. In order to determine if NET plays a role in hypertension in a particular animal or patient, it makes sense to analyze hemodynamics to see if cardiac output and heart rate are increased with the disease. This would suggest enhanced sympathetic drive to the heart and a cardiogenic role in disease. It is interesting that only some

cases have increased cardiac output and heart rate, while in others the opposite is true. I propose that the cases with elevated heart rate and blood pressure are candidates for a role of NET dysfunction and a cardiac specific sympathetic input that dictates the elevation in blood pressure. The other cases may be more related to increased total peripheral resistance mediated by a vascular mechanism. In the case of a cardiogenic component, stellate ganglionectomy or equivalent surgical treatment would be effective to prevent or treat high blood pressure; however, in other instances this type of treatment would not influence blood pressure because the primary cause is non-cardiac.

IV. Bridging the gap: historical studies on NE uptake in heart to NET overexpression in transfected cells

The studies presented in this thesis attempt to bridge the gap between recent molecular breakthroughs in NET function and regulation obtained by using cellular expression systems and functional studies of NE uptake in health and disease. There has been little work done to apply the cell culture and molecular techniques to integrative physiology of reuptake in the heart. Unfortunately, this type of assessment is extremely difficult given the complex nature of the heart and its innervation; however, it is the necessary next step to use the detailed understanding of NET regulation *in vitro* to understand physiological systems such as the whole heart. There is a wealth of information of both the basic nature of NE handling in the heart and the detailed regulation of NET *in vitro* ref (6), but yet the connection of these two bodies of literature is lacking.

It is time that the current tool and techniques for examining NET be used to clarify and further the initial observations of NE uptake starting from the early 1960's. The studies reported here made an attempt to use the antibodies and primers used in molecular studies and apply these to the heart in order to better understand the nature of NET in the normal and diseased heart, both of which have importance in cardiac function. Applying new techniques to old questions it was determined that NET expression and localization occur in more cell types than previously known. These studies lay the groundwork for further examination of NET function.

V. Unresolved issues in NET regulation and the role of the heart and NET in hypertension

It should be noted that there are controversies in the literature and uncertainty in several key areas: 1) what role does the heart and its innervation play in the etiology of hypertension?, 2) Is the reduction in tissue NE and NE storage in the hypertensive heart due to a reduction in NET function or otherwise?, 3) Does the study of whole heart reuptake really give a good understanding of the subtleties of NET function and the regional nature of NET regulation?, and 4) Are the antibodies and tools available to study NET specific?

First, there are conflicting reports as to the role of the heart and its innervation (including NET dysfunction) as a causal factor in hypertension. A variety of

methods including surgical, chemical, and immuno-sympathetctomy demonstrated a blunting of the blood pressure response or maintenance of normotension under stimuli to induce high blood pressure (5). This suggests that there is a role of sympathetic activation of heart rate and contractility in the developmental and maintenance phases of hypertension and some cases of hypertension are associated with elevated heart rate (7; 29) and contractility (21). However, in other hypertensive models there is reduction in cardiac output and heart rate (17) presumably as a baroreceptor-mediated compensation for the elevation in total peripheral resistance. Therefore, the heart and its innervation are clearly involved in some cases of hypertension, but hypertension in animals and humans has many different causes.

Second, there are conflicting reports as to the nature of NE metabolites in the hypertensive heart. The use of [^{3}H]-NE infusion into the heart and measurement of [^{3}H]-metabolites is a common technique to estimate the amount of neuronal uptake of NE by NET (12). The idea is that once [^{3}H]-NE is taken up by the nerve it is accessible to the intraneuronal enzyme monoamine oxidase (MAO) and is converted to [^{3}H]-DHPG. [^{3}H]-DHPG is then released in to the plasma where it can be measured. There is evidence of both increased (20) and decreased (9) DHPG production in the hypertensive heart indicating that there are some cases where neuronal metabolism is increased while in others it is decreased. This may or may not be directly related to NET mediated uptake into the nerve. Accessibility to MAO in the cytoplasm could also be regulated by the

uptake and storage of NE into vesicles rather than simply by uptake via NET alone.

Third, most of the studies on NET function have been done *in vivo* or in isolated perfused hearts. However, this thesis and other studies have reported that there are substantial regional differences in NE content (28), NE uptake capacity (8; 14), and NET expression in the heart (39). While the whole organ studies are vital in understanding NET function in a physiological setting, it is unknown how regional differences in NE handling or subtle local changes a particular junctional site may impact the overall function of the heart. It is unclear how infusing [^{3}H]-NE into the heart and measuring whole heart NE uptake or metabolism particularly reflects function of NET in any of the innervated sites such as coronary vasculature, cardiac muscle, nodal tissue, conduction system, or cardiac intrinsic neurons. Certainly, this type of study does not differentiate NE uptake at a particular site of innervation. It is difficult to construct an integrative explanation of the functional findings (i.e., reduced uptake of [^{3}H]-NE, increased release of [^{3}H]-DHPG) when my studies of the regional components of the innervation of the heart do not offer insight into the original functional results. The functional studies suggest NET would be globally downregulated in the heart resulting in reduced neuronal reuptake of NE, yet that explanation that breaks down when we examine the individual components of the systems using cellular and molecular techniques. Considering that there are vast regional differences in uptake function both inter- and intra-chamber it is time that studies move in the

direction of regional analysis and discrete sites of regulation to understand the individual components of the system.

Fourth, it is worth discussing a technical issue related to the study of NET. While there are numerous antibodies for NET that have been synthesized by individual laboratories and commercially, there has yet to be a clear demonstration of antibody specificity for NET in western blotting. This is true even though there are numerous reports in the literature based on these antibodies (13; 24-26). The specificity of a popular NET antibody was examined in these studies and there was no evidence for NET detected using this antibody. Therefore, caution must be used when interpreting data using NET antibodies unless the protein was assessed in another way to verify findings.

VI. Overall conclusion

This thesis challenges the current opinion that cardiac-associated NET mRNA is only in the stellate ganglia and NET protein is found only in sympathetic nerve fibers and ICA cells in the heart. NET mRNA was also found in the heart, likely in intrinsic cardiac neurons and ICA cells. NET protein was found in a variety of cardiac cells types including sympathetic nerve fibers, intrinsic cardiac neurons, and ICA cells. Neither NET mRNA expression in the heart nor NET protein in intrinsic cardiac neurons has been previously reported and offers a new area of study into the function and regulation of NET in health and disease. Furthermore, as to the role of NET in hypertension, there is no downregulation of

NET mRNA or protein in the stellate ganglia and only a regional downregulation in the heart suggesting that the previously reported reduction in NE uptake function is not due to a global reduction of cardiac NET. This, coupled with recent reports in human and animal models indicating that NET blockade, protein mutation, or genetic knockout is not a causal factor in hypertension, leads to the conclusion that while a reduction in NET function may be a contributing factor, it is not a cause of hypertension.

Reference List

1. **Armour JA**. The little brain on the heart. *Cleve Clin J Med* 74 Suppl 1: S48-S51, 2007.

2. **Armour JA**. Potential clinical relevance of the 'little brain' on the mammalian heart. *Exp Physiol* 93: 165-176, 2008.

3. **Backs J, Haunstetter A, Gerber SH, Metz J, Borst MM, Strasser RH, Kubler W and Haass M**. The neuronal norepinephrine transporter in experimental heart failure: evidence for a posttranscriptional downregulation. *J Mol Cell Cardiol* 33: 461-472, 2001.

4. **Baluk P and Gabella G**. Some parasympathetic neurons in the guinea-pig heart express aspects of the catecholaminergic phenotype in vivo. *Cell Tissue Res* 261: 275-285, 1990.

5. **Bell C and McLachlan EM**. Dependence of deoxycorticosterone/salt hypertension in the rat on the activity of adrenergic cardiac nerves. *Clin Sci (Lond)* 57: 203-210, 1979.

6. **Bonisch H and Bruss M**. The norepinephrine transporter in physiology and disease. *Handb Exp Pharmacol* 485-524, 2006.

7. **Brooks VL, Freeman KL and Qi Y**. Time course of synergistic interaction between DOCA and salt on blood pressure: roles of vasopressin and hepatic osmoreceptors. *Am J Physiol Regul Integr Comp Physiol* 291: R1825-R1834, 2006.

8. **Chilian WM, Boatwright RB, Shoji T and Griggs DM, Jr.** Regional uptake of [3H]norepinephrine by the canine left ventricle (41491). *Proc Soc Exp Biol Med* 171: 158-163, 1982.

9. **Esler MD**. The sympathetic system in essential hypertension. *Rev Port Cardiol* 19 Suppl 2: II9-14, 2000.

10. **Esler MD, Lambert G, Brunner-La Rocca HP, Vaddadi G and Kaye DM**. Sympathetic nerve activity and neurotransmitter release in humans:

translation from pathophysiology into clinical practice. *Acta Physiol Scand* 177: 275-284, 2003.

11. **Esler MD, Rumantir M, Kaye DM, Jennings G, Hastings J, Socratous F and Lambert G**. Sympathetic nerve biology in essential hypertension. *Clin Exp Pharmacol Physiol* 28: 986-989, 2001.

12. **Grassi G and Esler MD**. How to assess sympathetic activity in humans. *J Hypertens* 17: 719-734, 1999.

13. **Habecker BA, Grygielko ET, Huhtala TA, Foote B and Brooks VL**. Ganglionic tyrosine hydroxylase and norepinephrine transporter are decreased by increased sodium chloride in vivo and in vitro. *Auton Neurosci* 107: 85-98, 2003.

14. **Hertting G and Schiefthaler T**. The effect of stellate ganglion excision on the catecholamine content and the uptake of H3-norepinephrine in the heart of the cat. *Int J Neuropharmacol* 3: 65-69, 1964.

15. **Huang MH, Bahl JJ, Wu Y, Hu F, Larson DF, Roeske WR and Ewy GA**. Neuroendocrine properties of intrinsic cardiac adrenergic cells in fetal rat heart. *Am J Physiol Heart Circ Physiol* 288: H497-H503, 2005.

16. **Huang MH, Friend DS, Sunday ME, Singh K, Haley K, Austen KF, Kelly RA and Smith TW**. An intrinsic adrenergic system in mammalian heart. *J Clin Invest* 98: 1298-1303, 1996.

17. **Jacob F, Clark LA, Guzman PA and Osborn JW**. Role of renal nerves in development of hypertension in DOCA-salt model in rats: a telemetric approach. *Am J Physiol Heart Circ Physiol* 289: H1519-H1529, 2005.

18. **Kaumann AJ and Levy FO**. 5-hydroxytryptamine receptors in the human cardiovascular system. *Pharmacol Ther* 111: 674-706, 2006.

19. **Keller NR, Diedrich A, Appalsamy M, Tuntrakool S, Lonce S, Finney C, Caron MG and Robertson DM**. Norepinephrine transporter-deficient mice exhibit excessive tachycardia and elevated blood pressure with wakefulness and activity. *Circulation* 110: 1191-1196, 2004.

20. **Krakoff LR, de Champlain J and Axelrod J**. Abnormal storage of norepinephrine in experimental hypertension in the rat. *Circ Res* 21: 583-591, 1967.

21. **LeLorier J, Hedtke JL and Shideman FE**. Uptake of and response to norepinephrine by certain tissues of hypertensive rats. *Am J Physiol* 230: 1545-1549, 1976.

22. **Li H, Ma SK, Hu XP, Zhang GY and Fei J**. Norepinephrine transporter (NET) is expressed in cardiac sympathetic ganglia of adult rat. *Cell Res* 11: 317-320, 2001.

23. **Li W, Knowlton D, Van Winkle DM and Habecker BA**. Infarction alters both the distribution and noradrenergic properties of cardiac sympathetic neurons. *Am J Physiol Heart Circ Physiol* 286: H2229-H2236, 2004.

24. **Mao W, Iwai C, Qin F and Liang CS**. Norepinephrine induces endoplasmic reticulum stress and downregulation of norepinephrine transporter density in PC12 cells via oxidative stress. *Am J Physiol Heart Circ Physiol* 288: H2381-H2389, 2005.

25. **Melikian HE, McDonald JK, Gu H, Rudnick G, Moore KR and Blakely RD**. Human norepinephrine transporter. Biosynthetic studies using a site-directed polyclonal antibody. *J Biol Chem* 269: 12290-12297, 1994.

26. **Melikian HE, Ramamoorthy S, Tate CG and Blakely RD**. Inability to N-glycosylate the human norepinephrine transporter reduces protein stability, surface trafficking, and transport activity but not ligand recognition. *Mol Pharmacol* 50: 266-276, 1996.

27. **Murphy DA, O'Blenes S, Hanna BD and Armour JA**. Capacity of intrinsic cardiac neurons to modify the acutely autotransplanted mammalian heart. *J Heart Lung Transplant* 13: 847-856, 1994.

28. **Novotny M, Quaiserova-Mocko V, Wehrwein EA, Kreulen DL and Swain GM**. Determination of endogenous norepinephrine levels in different chambers of the rat heart by capillary electrophoresis coupled with amperometric detection. *J Neurosci Methods* 163: 52-59, 2007.

29. **O'Donaughy TL and Brooks VL**. Deoxycorticosterone acetate-salt rats: hypertension and sympathoexcitation driven by increased NaCl levels. *Hypertension* 47: 680-685, 2006.

30. **Reja V, Goodchild AK and Pilowsky PM**. Catecholamine-related gene expression correlates with blood pressures in SHR. *Hypertension* 40: 342-347, 2002.

31. **Richardson RJ, Grkovic I and Anderson CR**. Immunohistochemical analysis of intracardiac ganglia of the rat heart. *Cell Tissue Res* 314: 337-350, 2003.

32. **Shannon JR, Flattem NL, Jordan J, Jacob G, Black BK, Biaggioni I, Blakely RD and Robertson DM**. Orthostatic intolerance and tachycardia associated with norepinephrine- transporter deficiency. *N Engl J Med* 342: 541-549, 2000.

33. **Shibao C, Raj SR, Gamboa A, Diedrich A, Choi L, Black BK, Robertson D and Biaggioni I**. Norepinephrine transporter blockade with atomoxetine induces hypertension in patients with impaired autonomic function. *Hypertension* 50: 47-53, 2007.

34. **Slavikova J, Kuncova J, Reischig J and Dvorakova M**. Catecholaminergic neurons in the rat intrinsic cardiac nervous system. *Neurochem Res* 28: 593-598, 2003.

35. **Ungerer M, Chlistalla A and Richardt G**. Upregulation of cardiac uptake 1 carrier in ischemic and nonischemic rat heart. *Circ Res* 78: 1037-1043, 1996.

36. **Velasco M, Contreras F, Cabezas GA, Bolivar A, Fouillioux C and Hernandez R**. Dopaminergic receptors: a new antihypertensive mechanism. *J Hypertens Suppl* 20: S55-S58, 2002.

37. **Wehrwein, E. A., Esfahanian, M, Novotny, M., Quaiserova-Mocko, V., Swain, G. M., Yoshimoto, M, Osborn, J. W., and Kreulen, D. L.** NOREPINEPHRINE TRANSPORTER mRNA IS PRESENT IN THE HEART BEFORE AND AFTER SYMPATHETIC DENERVATION. 2008. Unpublished Work

38. **Wehrwein, E. A., Fink, G. D., and Kreulen, D. L**. Norepinephrine transporter mRNA is present in the heart and stellate ganglion, and is differentially regulated in hypertension. American Heart Association, Council for High Blood Pressure Research Abstract. 2006.

39. **Wehrwein, E. A., Parker, L. M., Wright, A. A., Spitsbergen, J. M., Novotny, M., Babankova, D, Swain, G. M., Habecker, B. A., and Kreulen, D. L.** Cardiac norepinephrine transporter (NET) protein expression is inversely correlated to chamber norepinephrine content. 2008. Unpublished Work